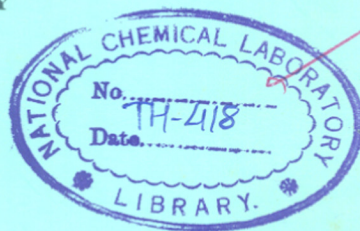


STUDIES ON MASS TRANSFER IN PACKED COLUMNS

A thesis submitted to the
UNIVERSITY OF POONA

for the Degree of
DOCTOR OF PHILOSOPHY
IN
CHEMISTRY



66.023:66.021.3(043)
SHR

by
VIDYADHAR R. SHROTRI, M. Sc.

Chemical Engineering Division
NATIONAL CHEMICAL LABORATORY
PUNE 411 008, INDIA.

April 1984



COMPUTERISED

DEDICATED
TO
MY
GRANDFATHER

FORM-A

CERTIFIED that the work incorporated in the thesis entitled '**Studies on Mass Transfer in Packed Columns**' submitted by Shri Vidyadhar R. Shrotri was carried out by the candidate under my supervision. Such material as has been obtained from other sources has been duly acknowledged in the thesis.



Dr. V.S. Patwardhan
(Supervisor)

AN APPRECIATION

The significance of great teachers is often overlooked, yet it is they who form the essential nucleus of any great centre of learning. It is they alone, who lead a student into a new world, who challenge his imagination, who sometimes seem to demand the impossible, yet unfold for him the path by which it can be attained. Such a teacher is my research guide


Dr. V.S. Patwardhan, Assistant Director, National Chemical Laboratory, Pune. Had it not been for his kind advice, keen interest and constant encouragement during the course of the present investigation, my whole pursuit would have been in vain. This is a small instalment of my life-long gratefulness to him.

I gratefully acknowledge the substantial help received from **Dr. R.V. Chaudhari**, Assistant Director, National Chemical Laboratory, Pune in my work on Flow Regimes. I also wish to record my deep sense of gratitude to **Dr. R.A. Mashelkar**, FNA, Deputy Director and Head of Chemical Engineering Department, and **Prof. L.K. Doraiswamy**, FNA, Director, National Chemical Laboratory for extending all the laboratory facilities and kind permission to submit this work in the form of thesis. My special thanks go to **Dr. B.D. Kulkarni**, Scientist, National Chemical Laboratory for his intellectual companionship in this endeavour.

To the lovable and memorable company of my friends, **Mr. D.S. Kolhe**, **A.M. Rajput**, **M.S. Gaikwad**, **P.A. Bhujang**, **A.S. Banerjee**, **H.M. Raheja** and **S.P. Bhalerao** is due my everlasting appreciation.

To my wife, **Nandini**, I owe to the fullest extent for inspiration and tremendous patience throughout the course of the present work. Finally, I wish to thank **Mr. K.G. Joshi** for his skillful typing of the thesis.

PUNE


VIDYADHAR RAMACHANDRA SHROTRI

CONTENTS

	P a g e
SUMMARY AND CONCLUSION	1
CHAPTER 1: MASS TRANSFER IN PACKED COLUMNS IN PRESENCE OF DEVELOPING WALL FLOW	6
1.1 Introduction	6
1.2 Liquid Distribution in Packed Columns	7
1.3 Development of Wall Flow	13
1.4 Mass Transfer in Packed Columns	17
1.5 Simplified Procedure	20
1.5.1 Uniform Distributor	20
1.5.2 Point Source Distributor	21
1.6 Comparison with Experimental Data	23
1.6.1 Estimation of Parameter Values	24
1.7 Conclusions	26
Tables	31
Figures	32
CHAPTER 2: DYNAMIC HOLD-UP FOR WETTABLE AND NON-WETTABLE PACKINGS	53
2.1 Introduction	53
2.2 Previous Work	53
2.3 Experimental	55
2.4 Results and Discussion	59
2.5 Conclusions	63
Tables	68
Figures	86

CHAPTER 3:	MASS TRANSFER BETWEEN STATIC AND DYNAMIC HOLD-UPS	95
3.1	Introduction	95
3.2	Previous Work	96
3.3	Theory	99
3.4	Experimental	102
3.3	Results and Discussion	104
3.6	Conclusions	107
	Tables	111
	Figures	124
CHAPTER 4:	FLOW REGIME STUDIES FOR TRICKLE-BED REACTORS USING INDUSTRIAL GAS-LIQUID SYSTEM	129
4.1	Introduction	129
4.2	Previous Work	130
4.3	Experimental	133
4.4	Results and Discussion	134
4.5	Conclusions	138
	Tables	144
	Figures	148
	LIST OF PUBLICATIONS	156



SUMMARY AND CONCLUSION

A packed column is one of the most widely used units which is industrially employed in several mass transfer operations like gas absorption and distillation. Packed trickle bed reactors are commonly employed in petrochemical industries for conducting chemical reactions between gas and a liquid using the packing as a catalyst. Considerable attention has therefore been focussed on understanding the fundamental mechanism involved in mass transfer and hydrodynamics. Such an understanding is important for designing packed columns and analysing their performance.

The present study was aimed at investigating several aspects connected with the hydrodynamics and mass transfer characteristics of packed columns and trickle bed reactors, both experimentally and theoretically. The thesis consists of four chapters each of which deals with a different aspect of packed columns as described in the following sections.

Chapter 1

Mass Transfer in Packed Columns in Presence of Developing Wall Flow

It is known that the presence of wall flow can reduce the overall mass transfer coefficient by as much as 30-40% when the column height is increased (1). The fraction of total liquid flow that flows over the wall of the column usually increases with column height till an equilibrium is reached between the wall flow and the central flow. In this study, a quantitative procedure was developed for calculating the effect of this wall flow on the overall mass transfer characteristics. For calculating the wall flow itself as a function of column height, the

liquid distribution model of Herskowitz and Smith (2) was used. This model was first expressed in a matrix form, so that the liquid distribution and the wall flow in long packed columns can be conveniently calculated. Using this procedure calculations were performed for a wide range of parameters (covering all possible practical situations) regarding the development of wall flow. Simple equations were developed to correlate the wall flow with column height and packing properties. A simple approximate procedure was proposed for predicting the effect of wall flow on overall mass transfer characteristics, using the equations mentioned above. The predictions based on this approximate procedure were shown to be in good agreement with both exact calculations and the experimental observations of Manqers and Ponter (1). Two types of distributors were considered in this study i.e. a point distributor and a uniform distributor.

Chapter 2

Dynamic hold-up for Wettable and Non-wettable Packings

In packed column, dynamic hold-up is one of the important parameters appearing in the design calculations. Conventionally, packed columns employ packings made from ceramics, which are completely wetted by water. Extensive information is available in the literature regarding the dynamic hold-up of such packings. However, packings made from polymeric materials like polypropylene can serve as good substitutes in many applications due to their corrosion resistance, low weight and low cost. Such materials are not wetted by water. The effect of this parameter, i.e. wettability of the packing surface, on

characteristics like the interfacial area and the equilibrium wall flow is known (3,4) but little data is available on its effect on the dynamic hold-up. In this study, the hold-up characteristics for non-wettable packings were investigated. In addition, wettable packings were also studied and the results were compared with those obtained with non-wettable packings. It was observed that within the range of physical properties of the irrigating liquid investigated in this study, the liquid viscosity and surface tension do not have a significant effect on the dynamic hold-up. It was found that the same form of correlation is applicable for both types of packings though the parameter values are different. The dynamic hold-up for non-wettable packings was found to be less than that for wettable packings. It was also found that a simplified correlation based on the Froude number is almost as accurate as the conventional correlation based on Reynolds and Gallileo numbers.

Chapter 3

Mass Transfer Between the Static and Dynamic Hold-ups

It is known that in the packed column, the stagnant pockets of liquid are not completely isolated from the main flow of the liquid, but there is a slow interchange of liquid between these stagnant pockets and the main liquid flow. This distribution of liquid into stagnant and moving parts with a slow interchange between the two is a phenomenon that has been used for explaining several experimental observations connected with packed columns. For example, several models have been proposed for the axial dispersion of liquid in packed

columns, and have been summarised by Gianetto et al. (5). The extended crossflow model by Patwardhan (6) explains the dependence of the effective interfacial area in packed columns on the chemical kinetics of the reaction conducted, in terms of this interchange, and leads to more accurate prediction of the effective interfacial area. Therefore, the interchange coefficient becomes an important parameter in estimating the overall performance of the packed column.

A tracer method was used for calculating the interchange rate between the static and dynamic hold-ups. This method involves a step decrease of tracer concentration at the column inlet, and measurement of the tracer concentration at the outlet. Experiments were conducted over wide ranges of operating conditions, which involved variations in liquid flow rates, liquid properties like viscosity and surface tension, packing size, shape and wettability of the packing surface. The results were correlated in terms of convenient dimensionless numbers. It was found that liquid surface tension has a significant effect on the interchange coefficient.

Chapter 4

Flow Regimes Studies for Trickle Bed Reactors Using Industrial Gas-Liquid Systems

Trickle bed reactors are commonly employed for hydrodesulfurization of petroleum fractions. They are also used for hydrogenation and oxidation reactions in organic processes and in waste water treatment. To design such trickle bed reactors having cocurrent two phase flow of liquid and gas through the catalyst bed, a knowledge of the flow

regime behaviour is essential. The importance of this factor in influencing the performance of the reactor has been shown recently by Horskwitz et al. (7).

In the present study, flow regimes in two phase flow were investigated using industrial catalyst particles and systems. The information obtained covers many important gas-liquid systems. Flow regime diagrams were obtained, based on experimental data obtained from several different packings and two phase systems. Comparison of the present data with literature correlations showed disagreement in certain ranges of parameter values. Considering the wide variety of systems studied in this work and the above observations, further work is necessary to evolve a generalized flow map of a trickle bed reactor.

References

1. Mangers R.J. and Ponter A.B.
Chem. Eng. Jl. 19, 139 (1980)
2. M. Herskwitz and J.M. Smith
AIChE Jl. 24, 439 (1978)
3. Mangers R.J. and Ponter A.B.
Chem. Eng. Jl., 19, 147 (1980)
4. Linek V., Stoy V., Machon V. and Krivsky Z.
Chem. Eng. Sci., 29, 1955 (1974)
5. Gianetto A., Baldi G., Specchia V. and Sicardi S.
AIChE Jl. 24, 1087 (1978)
6. Patwardhan, V.S.
Cand. Jl. Chem. Eng. 50, 56 (1978)
7. M. Herskwitz and J.M. Smith
AIChE Jl. 1, 1 (1983).



CHAPTER. 1

MASS TRANSFER IN PACKED COLUMNS IN
PRESENCE OF DEVELOPING WALL FLOW

1.1 INTRODUCTION

Packed columns are used very widely in chemical industry as gas-liquid contactors because of their low cost and ease of fabrication and operation. In many applications, the liquid is introduced at the top, either through a distributor or through a central inlet, and is allowed to trickle down under gravity, while the gas flow may be either cocurrent or counter-current. It is well established now that as the liquid trickles down the column, it gets redistributed radially, with a preferential flow at the column wall. Packed columns are often represented by models which do not account for the axial and radial maldistribution of liquid. Consequently, column dimensions can lead to unexpected effects on parameters calculated from such models. Gunn [1] has discussed, for example, the effect of this maldistribution on the overall axial dispersion coefficients. Stanek et al. [2] have presented calculations regarding the effect of liquid maldistribution on the performance of catalytic trickle bed reactors. Mangers and Ponter [3] investigated the effect of total packed height on the overall mass transfer coefficient between gas and liquid phases and found that increasing the height of a packed column from 25 cm to 75 cm could reduce the overall mass transfer coefficient by 35% or so. They attributed this to the existence of a wall flow which changes with height, but did not present any quantitative calculation. In this study we present a procedure whereby the effect of liquid maldistribution on the overall mass transfer characteristics can be calculated. First we consider the liquid maldistribution itself in some detail to arrive at

some useful generalisations, and then we apply these to describe the mass transfer characteristics.

1.2 LIQUID DISTRIBUTION IN PACKED COLUMNS

When a packed column is irrigated by a liquid, the liquid flows over the surface of the packing in the form of rivulets and films in a random manner. In many applications, a liquid flowing down the column contacts gas flowing up. The liquid is introduced at the top with a distributor to ensure a good distribution. If this distribution is improper, it can reduce the number of mass-transfer stages in a given depth of packing, as shown by Morris and Jackson [4]. The magnitude of this reduction varies with the degree of maldistribution and with the gas-liquid system under consideration. Thus, for predicting the performance of a packed column accurately, the liquid distribution in the column must be characterised properly. The initial distribution over the packing is not maintained as the liquid spreads laterally, and tends to flow preferentially over the wall. This wall flow increases with the depth of the packing and liquid flow in the bulk of packing is reduced. At certain depth of packing, the wall flow and main flow closely approach equilibrium. This is called the calming depth of the column. This calming bed depth depends upon the packing shape and size, column diameter, liquid flow rates and design of liquid distributor. This calming depth is shorter for a uniform inlet distributor than for a point source.

There are many models which describe the liquid distribution in the packed bed. Tour and Lerman [5] proposed a random walk mechanism for

such a flow and found that it described the experimental results quite well. Based on their results and those of Chandrasekhar [6], Cihla and Schmidt [7] introduced the diffusion model which is described by the following equation.

$$D \left[\frac{\partial^2 f}{\partial r^2} + \frac{1}{r} \frac{\partial f}{\partial r} \right] = \frac{\partial f}{\partial z} \quad [1.1]$$

where D represents the spreading coefficient. They proposed that since the spread of the liquid is of a probabilistic nature it might be expected that the process of distribution may be described by a differential equation of the diffusion type as in equation (1.1). To account for the preferential flow at the wall many investigators [7-12] have solved equation (1.1) with different boundary conditions arising out of different assumptions. These boundary conditions are given in Table 1.1. They encompass a wide range of physical phenomena that can take place at the wall, like the wall acting as a sink or as a perfect reflector for the liquid arriving at the wall. All the investigators mentioned above measured experimentally, the liquid distribution at the bottom of the packed column by using a collector consisting of several concentric walls. The spreading coefficient, D , was then evaluated from these experimental observations.

Although the diffusion model is based on the random walk concept, it is strictly valid only when the number of steps involved is large. This condition is not always satisfied in practical situations. In fact, the determination of the spreading coefficient, D , is carried out usually in

very short columns (Onda et al. [12]) which is equivalent only to a small number of steps. However, it has been shown (Patwardhan [13]) that the diffusion model predicts essentially the same cumulative liquid distribution as the random walk model even for very short columns and that the step length of a random walk model can be related to the spreading coefficient D .

The random walk mechanism postulates that each liquid element takes a random step radially as it flows down. Thus the flow paths would be random in character and would keep changing with time. However, it has been shown that the actual paths followed by the liquid rivulets are quite stable with respect to time (Lespinasse and Le Goff [14], Groenhoff [15]). In other words, liquid flows down the packing along preferred paths, because the rivulets prefer those paths which have been wetted by previous liquid elements. In spite of this, equation (1.1) has been found to describe the observed liquid distribution quite well. A probable explanation is that when leading liquid elements trace out the flow paths initially they do so at random. Thus the net aggregate of the flow paths, which are quite stable in time, are characterised by randomness in space. A similar explanation has been proposed by Groenhoff [15].

Equation (1.1) is based on the implicit assumption that the spreading coefficient " D " is constant throughout the bed. Stanek and Kolev [16] investigated the relationship between the local value of D and the local hydrodynamic conditions, which vary from point to point in the region of liquid distribution. They found that D depends upon the

local hydrodynamic conditions in certain regimes of operation. However, they concluded that in spite of this dependence, liquid distribution in packed bed can still be described by equation (1.1) with a constant D , provided a suitable effective value is assigned to D . In this study D is assumed to be constant.

Radial liquid distribution of liquid in a packed bed has been considered from a different view point by Gunn [1]. He considered the problem to be similar to that of a Darcy flow through a porous medium. The packed bed was divided into two regions, the central region of constant permeability and a thin wall region of higher permeability. The preferential flow near the wall was attributed to the higher permeability near the wall. He developed differential equations describing the stream function and solved them analytically for the case where the liquid was uniformly distributed at the packed bed inlet over the central region and where a separate uniform flow was provided over the wall region. Experimental verification of the equation was also presented by Farid and Gunn [17].

Crine et al. [18] developed a model based on a percolation theory, which considers preferential flow paths in the bed. These models could predict liquid distribution quite accurately at high liquid rates while for low liquid rates, they differ from each other. More recently, Stanek et al. [2] proposed a liquid distribution model that accounted for liquid maldistribution. It is also based on equation (1.1). They revealed two major points by extensive computation: the liquid maldistribution caused by poor initial distribution and wall flow.

Herskowitz and Smith [19] proposed a different deterministic model (shown in Fig. 1.1 and henceforth referred to as the HS model) to describe liquid spreading in a packed bed. The packed bed is regarded as an assembly of discrete spherical particles through which the liquid flows in rivulets. The radius of column and the bed depth are assumed to be divisible into an integral number of particles diameters. Each horizontal layer of particles of thickness d_p is divided into J (with $J = R/d_p$) concentric, annular rings and each ring is identified by its radial position i and bed depth n , where i and n represent integral numbers of particles. Radial transfer is visualised to occur by movement of liquid from one annular ring to the next ring by flow to, and mixing at, the contact points between consecutive rings, i.e. at the points where particles in adjacent rings are in contact with each other. Part of the liquid flowing in annular ring (i,n) moves radially to ring $(i+1, n+1)$ or $(i-1, n+1)$ via contact points, and the rest of it flows downwards to ring $(i, n+1)$ bypassing the contact points.

Similarly, the liquid flow at the wall at stage n, w_n , partly goes to the annular ring $(J, n+1)$ through contact points, and the rest of it remains at the wall itself. A typical flow diagram depicting this situation is shown in Fig. 1.2. They applied this model to a variety of regular and irregular packings and reported the values of the model parameters determined from experimental observations. It was shown later by Gianetto et al. [20] that this model represents a discrete version of the diffusion model and the parameters of the two models can be related to each other.

In short, to describe the liquid flow in a packed column completely the spreading of the liquid over the packing and its interaction with the wall have to be considered simultaneously. All the boundary conditions listed in Table 1.1 involve the process of interchange of liquid between the central flow i.e. flow over the packings and the wall flow, which ultimately results in the establishment of an equilibrium between the two. The model proposed by Herskowitz and Smith [19] results in a linear dependance between the equilibrium values f^* and w^* , i.e. the axial flux and wall flow at equilibrium respectively. A similar dependance has been used earlier by Dutkai and Ruckenstein [11]. Onda et al. [12] reported a non-linear dependance between f^* and w^* . However, they found that the wall flow profile predicted by their equations was almost identical to that calculated from the equations of Dutkai and Ruckenstein [11]. Thus, for the purpose of predicting the liquid distribution in a packed bed, the assumption of a linear dependance between f^* and w^* seems adequate.

In the following analysis of this study, the model proposed by Herskowitz and Smith [19] is used. Firstly, their procedure is presented in a matrix form which makes it possible to handle long columns packed with small particles without undue increase in the computational effort. Then it is shown that the liquid distribution which depends upon quite a large number of parameters, may be conveniently represented in a generalised way by combining the parameters into certain groups.

1.3 DEVELOPMENT OF WALL FLOW

Herskowitz and Smith [19] assumed the radius of the packed column, R , to be an integral multiple of the particle diameter d_p such that $R = J d_p$. They divided the bed into J concentric annuli of width d_p . The bed was vertically divided into a number of stages, each of height d_p . Based on their physical model, they derived equation for central flow and wall flow whereby it is possible to predict the flow distribution in the various annuli at the $(n+1)^{\text{th}}$ stage, if the same is known at the n^{th} stage. The detailed description of their model is given in previous section. Their equations can be represented in a compact manner in the following way in terms of matrices:

$$G_{n+1} = G_n P \quad [1.2]$$

$$\text{where } G_n = [F_{1,n}, F_{2,n}, \dots, F_{J+1,n}] \quad [1.3]$$

$F_{i,n}$ = total flow in the i th annulus at the n th stage

$F_{J+1,n}$ = the total wall flow at the n th stage

and the matrix P of dimension $(J+1, J+1)$ is given by

$$P_{i,j} = \left. \begin{array}{l} = \frac{S(i-1)}{2(2i-1)} \quad \text{for } j = i-1 \\ = 1-S/2 \quad \text{for } j = i \\ = \frac{S_i}{2(2i-1)} \quad \text{for } j = i+1 \\ = 0 \quad \text{otherwise} \end{array} \right\} \quad \text{for } 2 \leq i \leq J-1 \quad [1.4]$$

$$\begin{aligned}
 P_{1,1} &= 1 - S/2 \\
 P_{1,2} &= S/2 \\
 P_{J,J-1} &= (S/4) (2J-2) / (2J-1) \\
 P_{J,J} &= Sq J / (2J-1) + S(J-1) / (2J-1) + 1-S \\
 P_{J,J+1} &= (1-q) SJ / (2J-1) \\
 P_{J+1,J} &= q^2 \\
 P_{J+1,J+1} &= 1-q^2
 \end{aligned}
 \tag{1.5}$$

and S and q are the spreading and wall flow parameters respectively.

G_0 is the liquid distribution at the inlet to the packed bed, and is known. Then a repeated application of equation (1.2) gives the liquid distribution at any point in the packed bed. From equation (1.2) it follows that

$$G_{n+m} = G_n P^m \tag{1.6}$$

Thus, if it is desired to calculate the liquid distribution in a packed bed at successive axial positions separated by, say, a distance of 50

stages, then p^{50} can be calculated once for all, and then equation (1.6) may be used with $m = 50$, which involves only one matrix multiplication for 50 stages. Equation (1.5) can be modified for taking into account any non-linear dependence between f^* and w^* if required.

In order to calculate the wall flow at any axial position in the column under consideration, it is necessary to know the numerical values of S, q, R, J and n . However, in spite of the large number of parameters involved, it is possible to represent wall flow in a generalised manner, as shown in Fig. 1.3. It is seen from this figure, which is based on the assumption of an initially uniform distribution, that for a given equilibrium wall flow, the fractional wall flow at any particular axial position depends almost exclusively on the dimensionless axial distance ns/J^2 . It varies to some extent with column diameter (i.e. J), and S , but this variation is small enough to be neglected over the parameters ranges investigated which are wide enough to cover most of the practical situations. The different curves in Fig. 1.3 can be represented by

$$\frac{w}{w^*} = 1 - \exp(-\alpha_1 ns/J^2) \quad [1.7]$$

where α_1 is a curve fitting parameter and depends only upon w^* as shown in Fig. 1.4. The wall flow predicted by equation (1.7) is shown in Fig. 1.3 by solid lines. This figure covers the range of $S = 0.2$ to 1.0. The upper limit of $S=1$ is imposed inherently by the HS model itself.

The lowest value of S reported by Herskowitz and Smith [19] is about 0.4. For absorption packings, S turns out to be about 0.25. Therefore the range of S considered in Fig. 1.3 is wide enough to encompass all practical values. $J=5$ corresponds to small laboratory columns. $J=20$ was the largest value reported in Fig. 1.3, because it was found that $J>20$ leads to predictions which are identical to those for $J=20$. In small laboratory columns, as much as half the liquid may flow along the wall at equilibrium. In large industrial columns, the wall flow may be a much smaller fraction of the total flow. These situations are covered by the range of $W^*=0$ to 0.6 used in Fig. 1.3 (no points are shown for $W^*=0$ because this case is represented by the horizontal line at the top). The numerical value of f to be used in the HS model were calculated by using the equation for equilibrium wall flow [18].

$$W^* = \left[1 + \frac{f^2 J}{S(1-f)} \right]^{-1} \quad [1.8]$$

It is seen from Fig. 1.3 that equation (1.7) can predict the wall flow at any axial position quite satisfactorily.

The initial distribution used for generating Fig. 1.3 was uniform. The other kind of liquid source used commonly, especially in small diameter column is a central point source whereby liquid is introduced in the column by a single outlet at the centre of the column. Development of the wall flow for a point source distributor is quite different from that for a uniform source distributor. A small portion

TH-418

of the column at the top has no wall flow of liquid at all. This is so because the liquid introduced at the center of the column travels downwards to some extent before it reaches the wall by radial spreading. This fact is illustrated in Fig. 1.5. This downward distance travelled always appears to correspond to $ns/J^2 = 0.2$. Consequently the curves in Fig. 1.5 can be represented by

$$\begin{aligned} \frac{W}{W^*} &= 0 \quad \text{for } ns/J^2 < 0.2 \\ &= 1 - \exp[-\alpha_2(ns/J^2 - 0.2)] \end{aligned} \quad [1.9]$$

where α_2 is a curve fitting parameter for point source distribution and depends upon the equilibrium wall flow W^* . The dependence of α_2 on W^* is shown in Fig. 1.6. The solid lines in Fig. 1.5 correspond to equation (1.9) and the points to the predictions of the HS model. The two are seen to be in good agreement. Figures 1.3 and 1.5 cover the same ranges of parameters like W^* , S , J and f . It is also seen from these figures that for $ns/J^2 = 2.0$, the wall flow may be assumed to have reached an equilibrium with the central flow.

1.4 MASS TRANSFER IN PACKED COLUMNS

It is well known that the liquid flow rate in a packed column has a strong effect on its overall mass transfer characteristics. If the liquid distribution in a packed column is uniform everywhere, then the local mass transfer characteristics would also be uniform which in addition would be equal to the overall mass transfer characteristics.

66.023; 66.021.3(043)
SHR

However, the local hydrodynamic conditions change as a result of developing wall flow (which reduces the total flow rate in the central part of the column), as shown in the earlier section. Here we consider the effect of the developing wall flow on the overall mass transfer characteristics. The HS model discussed earlier is used for calculating the overall mass transfer characteristics in presence of a developing wall flow over a wide range of relevant variables. A simplified procedure is then proposed and shown to give predictions which are very close to calculations based on the HS model.

Let us consider a liquid phase controlled absorption process like the absorption of a pure gas or a relatively insoluble gas into a liquid in a packed column. The volumetric mass transfer coefficient of interest is then the $k_L a$ value. The numerous correlations available in literature lead to the following dependence of $k_L a$ on the liquid flow rate.

$$k_L a = \alpha_3 f^r \quad [1.10]$$

where f is the axial liquid flux; and α_3 is a constant depending upon the system properties, packing size and type etc. We make the reasonable assumption that even in changing hydrodynamic conditions, equation (1.10) represents the local $k_L a$ value. The overall $k_L a$ value is then given by

$$(k_L a)_{av} = \frac{1}{V} \int_V (k_L a) dV \quad [1.11]$$

If the initial liquid distribution is axi-symmetric, the symmetry is maintained everywhere in the column and we can write equation (1.11) as

$$(k_L a)_{av} = \frac{1}{\pi R^2 Z} \int_0^Z \int_0^R \alpha_3 f^r 2\pi r dr dz \quad [1.12]$$

Under the hypothetical condition of uniform distribution of liquid everywhere in the column, we get

$$(k_L a)_{ideal} = \alpha_3 \left(\frac{Q}{\pi R^2} \right)^r \quad [1.13]$$

Equations (1.12) and (1.13) lead to

$$E = \frac{2}{\bar{\beta}} \int_0^{\bar{\beta}} \int_0^1 \left[\frac{f}{Q/(\pi R^2)} \right]^r \alpha d\alpha d\beta \quad [1.14]$$

where $E = (k_L a)_{av} / (k_L a)_{ideal}$

and

$$\beta = zS / (J^2 d_p)$$

$$\bar{\beta} = \beta \text{ at } z = Z, \text{ and } \alpha = r/R$$

f is the local axial flux which varies with axial and radial position due to the existence of a developing wall flow. E represents the ratio of the

overall mass transfer coefficient under the conditions of a developing wall flow and the overall mass transfer coefficient that would be realised under the (hypothetical) condition of uniform flow with zero wall flow. Application of the HS model described earlier gives the axial flux as a function of α and β which may be used in equation (1.14) to calculate E.

The calculations involved in this procedure are quite considerable. In the following section, a simplified procedure is suggested as an alternative, and the predictions based on both the procedures are compared to each other.

1.5 SIMPLIFIED PROCEDURE

1.5-1 Uniform distributor

It is seen from Fig. 1.3 that in this case wall flow starts developing right from the top of the packed column, and equilibrium between the wall flow and the central flow is approached very closely at a packed height corresponding to $\beta = 2.0$. The total wall flow at any axial position is given by equation (1.7). If it is assumed that the central flow which is equal to $Q(1-W)$ is uniformly distributed over the cross section of column, then equation (1.14) simplifies to

$$E(\bar{\beta}) = \frac{1}{\bar{\beta}} \int_0^{\bar{\beta}} (1-W)^r d\beta \quad [1.15]$$

using equation (1.7) we get

$$E(\bar{\beta}) = \frac{1}{\bar{\beta}} \int_0^{\bar{\beta}} \left[1 - W^* (1 - \exp(-\alpha_1 \beta)) \right]^r d\beta \quad [1.16]$$

For $\beta > 2$, $\exp(-\alpha_1 \beta) \ll 1$, and equation (1.16) can be further simplified as

$$E(\bar{\beta}) = \frac{2E(2.0) + (\bar{\beta} - 2) (1 - W^*)^r}{\bar{\beta}} \quad \text{for } \bar{\beta} > 2 \quad [1.17]$$

1.5-2 Point source distributor

In this case, some portion of the packed column at the top has zero wall flow, because by the time the liquid reaches the wall it has already trickled down to some extent. The height of this portion corresponds to $\beta = 0.2$. By the time the liquid has travelled downward to a height corresponding to $\beta = 2$, the wall flow approaches equilibrium quite closely. Thus, the wall flow is zero for $0 \leq \beta \leq 0.2$, then changes significantly for $0.2 \leq \beta \leq 2.0$ and may be taken to have attained its equilibrium for $\beta > 2.0$. In the top region i.e. $0 \leq \beta \leq 0.2$, the flow is strongly non-uniform. The flow distribution here can be represented quite accurately [Patwardhan, 13] by following analytical solution given by Onda [12].

$$f(r, z) = \frac{Q}{4\pi D z} \exp\left(-\frac{r^2}{4 D z}\right) \quad [1.18]$$

Substituting this into equation (1.14) and using the relationship $D = d_p S/4$ [Gianetto et al. [20], Patwardhan, [13]] we get

$$E(\bar{\beta}) = \frac{1}{\tau \bar{\beta}} \int_0^{\bar{\beta}} \beta^{(1-\tau)} (1 - \exp(-\tau/\beta)) d\beta \quad \text{for } \beta \leq 0.2 \quad [1.19]$$

Figure 1.7 shows the dependence of E on τ and $\bar{\beta}$ for $\bar{\beta} \leq 0.2$ which covers the practical range of τ . In the lower region of packed column (i.e. $\beta > 0.2$) the wall flow (which is non-zero) is obtained by using equation (1.9). Also, the central flow (which is equal to $Q(1-W)$) is assumed to be uniform. Equation (1.14) can now be written as

$$E(\bar{\beta}) = \frac{1}{\bar{\beta}} \left\{ 0.2 E(0.2) + \int_{0.2}^{\bar{\beta}} [1 - W^* (1 - \exp(-\alpha_2(\beta - 0.2)))]^\tau d\beta \right\} \quad \text{for } \bar{\beta} > 0.2 \quad [1.20]$$

Neglecting the exponential term for $\beta > 2$, we get

$$E(\bar{\beta}) = \frac{2E(2.0) + (\bar{\beta} - 2)(1 - W^*)^\tau}{\bar{\beta}} \quad \text{for } \bar{\beta} > 2 \quad [1.21]$$

The integral in equations (1.16), (1.19) and (1.20) can be evaluated by standard numerical techniques.

The results calculated using the simplified procedure are shown

in Fig. 1.8 and 1.9 for a uniform source and a point source respectively, for several values of various parameters.

It is seen that they compare very well with the exact calculation based on the HS Model. Thus it appears that the reduction in $(k_L a)_{av}$ value arises primarily because of the existence of wall flow which is taken into account by the approximate procedure. The approximate procedure involves only one dimensional integrations which can be easily performed using standard numerical techniques.

Figs. 1.8 and 1.9 are based on $\tau = 1.44$. The values of τ reported in literature cover a range of about 0.44-1.44. Figure 1.10 shows a comparison of the HS model and the approximate procedure for $\tau = 1.0$, and Fig. 1.11 shows the same for $\tau = 0.44$, for specific values of other parameters. It is again seen that the approximate procedure gives predictions which match well with those based on the HS model.

1.6 COMPARISON WITH EXPERIMENTAL DATA

The effect of packed height on the average $(k_L a)$ values in a packed column for the absorption of CO_2 was investigated experimentally by Mangers and Ponter [3] who found that $(k_L a)_{av}$ decreases as packed height increases. They also determined the wall flow of liquid under the same conditions as a function of packed height. They used a five point distributor in a 10 cm diameter column using 1 cm glass raschig rings. In order to apply the theory developed here to their experimental

data, it is necessary to estimate the values of several parameters for the experimental conditions used by these authors.

1.6-1 Estimation of parameter values

(1) Spreading factor, S - Mangers and Ponter [3] did not report the S values. However, Herskowitz and Smith [19] have given a graph for wettable cylindrical particles (their Fig. 10) which can be used to get $S = 0.62$ for 1 cm particles.

(2) Equilibrium wall flow, W^* - Mangers and Ponter [3] reported the wall flow as a function of liquid flow rate for three different column heights, i.e. 25, 50, and 75 cm. Since they used a 5 cm radius column and 1 cm packings, $J = 5$. Also, n corresponding to the largest height is calculated as 75. Therefore, for their 75 cm tall column, $nS/J^2 = 1.86$. It has been shown in the earlier sections that wall flow may be assumed to be very close to equilibrium at $nS/J^2 = 2.0$. The wall flow corresponding to $nS/J^2 = 1.86$ may therefore be taken as the approximate value of W^* . Referring to Fig. 7 of Mangers and Ponter [3], we may take $W^* = 0.5$.

(3) The exponent, Υ - The same authors have investigated the relationship between $(k_L a)$ and liquid flow rate in another study using the same experimental set-up [22]. From this study, we get $\Upsilon = 1.44$.

(4) Distributor type - These authors used a five-point distributor with all five points located around a circle of 7 cm diameter. This type of distributor lies obviously in between the two limiting

cases of a point source and a uniform distributor.

The ratios of $k_L a$ values corresponding to column heights of 25, 50 and 75 cm were calculated using their Fig. 6 [3] and are shown in Fig.1.12 as circles. From Fig.1.9(a) for a point source we get $(k_L a)_{\text{uniform}} / (k_L a)_{75 \text{ cm}} = 1.22$ for $nS/J^2 = 1.86$, $W^* = 0.5$, $\gamma = 1.44$ and $R = 5$. Similarly, from the same figure, we get $(k_L a)_{25 \text{ cm}} / (k_L a)_{\text{uniform}} = 0.65$ for $nS/J^2 = 0.62$. Using these two values,

$$\frac{(k_L a)_{25 \text{ cm}}}{(k_L a)_{75 \text{ cm}}} = \frac{1.22}{0.65} = 1.88 \text{ for a point source}$$

This is shown as the solid line in Fig. 1.12. A similar calculation made with Fig.1.8 gives

$$\frac{(k_L a)_{25 \text{ cm}}}{(k_L a)_{75 \text{ cm}}} = 1.36 \text{ for a uniform source}$$

Figure 1.12 also shows comparisons of $(k_L a)$ for 25 and 50 cm packed heights. The five-point distributor used by Manqers and Ponter [21] lies somewhere in between a point source and a uniform source, as mentioned earlier. Figure 1.12 shows that the $(k_L a)$ ratios obtained from their experimental data indeed lie in between the lines for the point source and a uniform source. This figure also shows that the

liquid flow rate does not significantly affect the $k_L a$ ratios, both experimental and predicted.

1.7 CONCLUSIONS

A simple approximate procedure was developed for predicting the effect of wall flow in packed columns on the mass transfer characteristics. The HS model (which is mathematically equivalent to the diffusion equation) was used as the basis. Simple equations were developed (equations (1.7) and (1.9)) for correlating the wall flow as a function of axial position for the two common sources used, i.e. a uniform source and a point source. They were shown to match quite well with the calculations based on the HS model over wide ranges of several parameters. The simple procedure proposed consists of using these wall flow equations and assuming that the remaining flow is uniformly distributed throughout the cross section. The prediction of the average $k_L a$ based on this procedure is shown to agree well with the predictions of the HS model and also with the experimental data of Mangers and Ponter [3].

NOTATION

D	spreading coefficient (cm)
d_p	particle size (cm)
E	ratio of $(k_L a)_{av}$ under developing wall flow and $(k_L a)$ under the hypothetical conditions of uniform flow with zero wall flow
f	local axial liquid flux ($\text{cm}^3/\text{cm}^2 \text{ s}$)
f^*	equilibrium value of f ($\text{cm}^3/\text{cm}^2 \text{ s}$)
F	total liquid flow in an annulus (cm^3/s)
$F_{i,n}$	liquid flow rate in the i th annulus after n stages (cm^3/s)
G_n	the flow vector for the n th stage (defined by equation (1.3))
i, j	radial and axial indices
J	R/d_p (total number of rings H.S. model)
$(k_L a)$	volumetric mass transfer coefficient (s^{-1})
$(k_L a)_{ideal}$	defined by equation (1.13) s^{-1}
$(k_L a)_{av}$	average value of $k_L a$
m	r/d_p (HS model)
n	z/d_p (HS model)
$P_{i,j}$	fractional flow from i th annulus to the j th annulus during one stage, or the elements of the matrix
P	the matrix defined by equations (1.2) - (1.5)
q	fraction of wall flow going to contact points during one stage (a parameter referring to the HS model)
Q	total liquid flow to the packed column (cm^3/s)
r	radial distance (cm)

R	column radius (cm)
S	liquid spreading parameter of HS model
V	column volume (cm ³)
w	wall flow p.u. periphery (cm ³ /cm.s)
w [*]	equilibrium wall flow p.u. periphery (cm ³ /cm s)
W	total wall flow / Q
W ⁺	equilibrium value of W
z	axial distance from top of the column (cm)
Z	column height (cm)

Greek letters

α	r/R
α_1, α_2	defined in equations (1.7) and (1.9)
α_3	a coefficient defined by equation (1.10)
β	ns/J ²
$\bar{\beta}$	value of β for z = Z
τ	value of power on equation (1.10)
θ_{1-4} θ'_2, θ'_3 }	constants appearing in table 1.1
\emptyset	function appearing in table 1.1

REFERENCES

1. Gunn D.J., Chem. Eng. Sci. 33, 1211 (1978)
2. Stanek V., Hanika J., Hlavacek V. and Tranka O., Chem. Eng.Sci. 36, 1045 (1981)
3. Mangers R.J. and Ponter A.B., Chem. Eng. J¹. 19, 139 (1980)
4. Morris G.A. and Jackson J., 'Absorption Towers' 1953 (London: Butterworths Scientific Publications)
5. Tour R.S. and Lerman F., Trans. Am. Inst. Chem. Engr. 35, 719 (1939)
6. Chandrasekhar S., Rev. Mod. Phys. 15, 2 (1943)
7. Cihla Z. and Schmidt C., Cole. Czech. Chem. Comm. 22, 896 (1957)
8. Porter K.E. and Jones M.C., Trans. Inst. Chem. Engr. 41, 240 (1963)
9. Porter K.E., Trans. Inst. Chem. Engr., 46, T 69 (1968)
10. Kolar V. and Stanek V., Colln. Czech. Chem. Comm. 30, 1054 (1965)
11. Dutkai E. and Ruckenstein E., Chem. Eng. Sci., 23, 1365 (1968)
12. Onda K., Takeuchi H., Maeda Y. and Takeuchi N., Chem. Eng. Sci. 28, 1677 (1973)
13. Patwardhan V.S., Paper presented at Ind. Inst. Chem. Engr. Annual Symp., Madras (1980)
14. Lespinasse B. and Le Goff P., Rev. Inst. Pr. Pet. 17, 1 (1962)

.....

15. Groenhoff H.C., Chem.Eng. J1, 14, 181 (1978)
16. Stanek V. and Kolev N., Chem. Eng. Sci. 33, 1049 (1978)
17. Farid M.M. and Gunn D.J., Chem. Eng. Sci., 33, 1221 (1978)
18. Grine M., Marchot P. and L'Homme G.A., AIChE 72nd Annual Meeting, San Francisco (1979)
19. Herskowitz M. and Smith J.M., AIChE J1. 24, 439 (1978)
20. Gianetto A., Baldi G., Specchia V. and Sicardi S., AIChE J1. 24, 1087 (1978)
21. Jameson J.B., Trans. Inst. Chem. Engr. 44, T 198 (1966)
22. Mangers R.J. and Ponter A.B., I and EC Proc. Des. and Dev. 19, 530 (1980)

TABLE 1.1: BOUNDARY CONDITIONS USED BY VARIOUS WORKERS

Investigator	Ref.	Boundary condition
1. Chila Z. and Schmidt O.	[7]	$\left(\frac{\partial f}{\partial r}\right)_{r=R} = 0$
2. Porter K.E. and Jones M.C.	[8]	$f(R, z) = \theta_1 w(z)$
3. Porter K.E.	[9]	$f(R, z) = \theta [w(z)]$
4. Volar V. and Stanek V.	[10]	$-\left(\frac{\partial f}{\partial r}\right)_{r=R} = \frac{\theta_2}{D} \left\{ f(R, z) - \theta_2' w(z) \right\}$
5. Dutkai E. and Ruckenstein E.	[11]	$-2\pi RD \left(\frac{\partial f}{\partial r}\right)_{r=R} = \theta_3 f(R, z) - \theta_3' w(z)$ $= \frac{dW(z)}{dz}$
6. Onda et al.	[12]	$-2\pi RD \left(\frac{\partial f}{\partial r}\right)_{r=R} = \theta_4 \left\{ w^*(z) - w(z) \right\}$ $= \frac{dW(z)}{dz}$

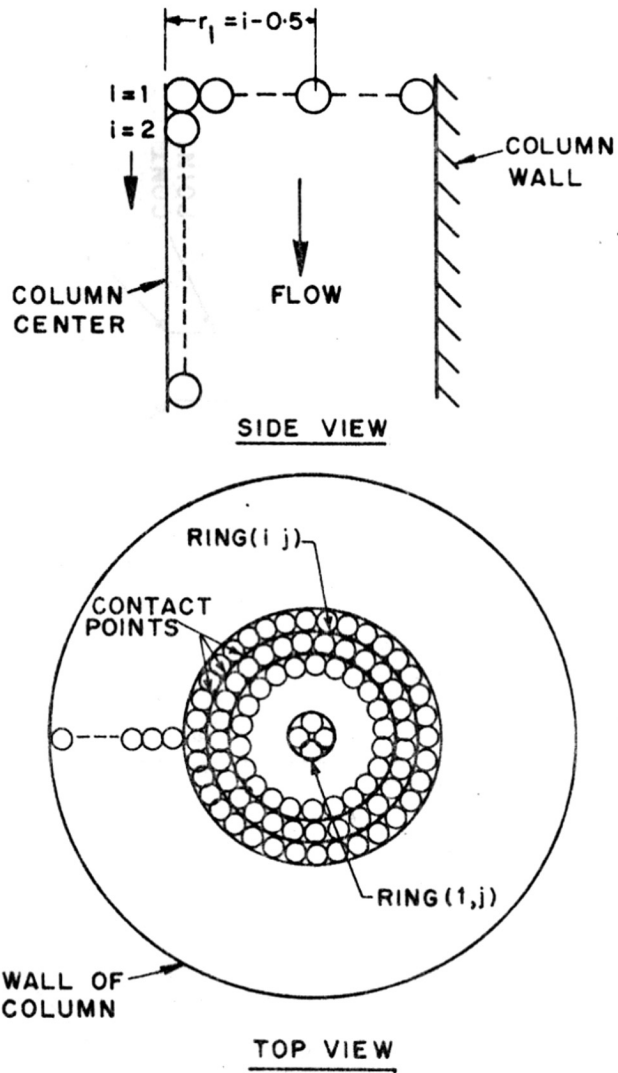


FIG. 1.1 : NOTATION FOR FLOW MODEL (H.S.)

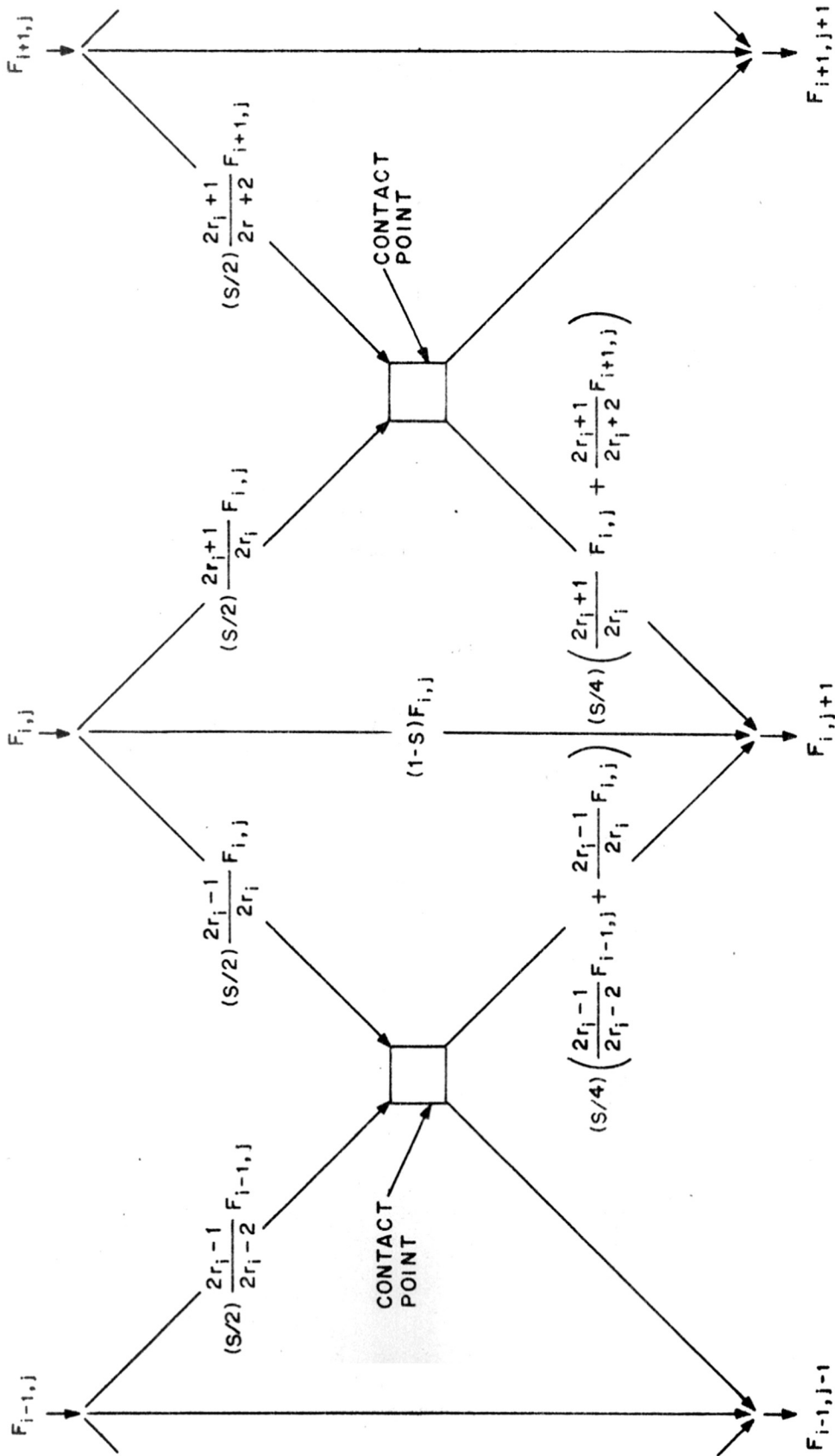


FIG. 1-2 (a) : FLOW NETWORK IN BED.

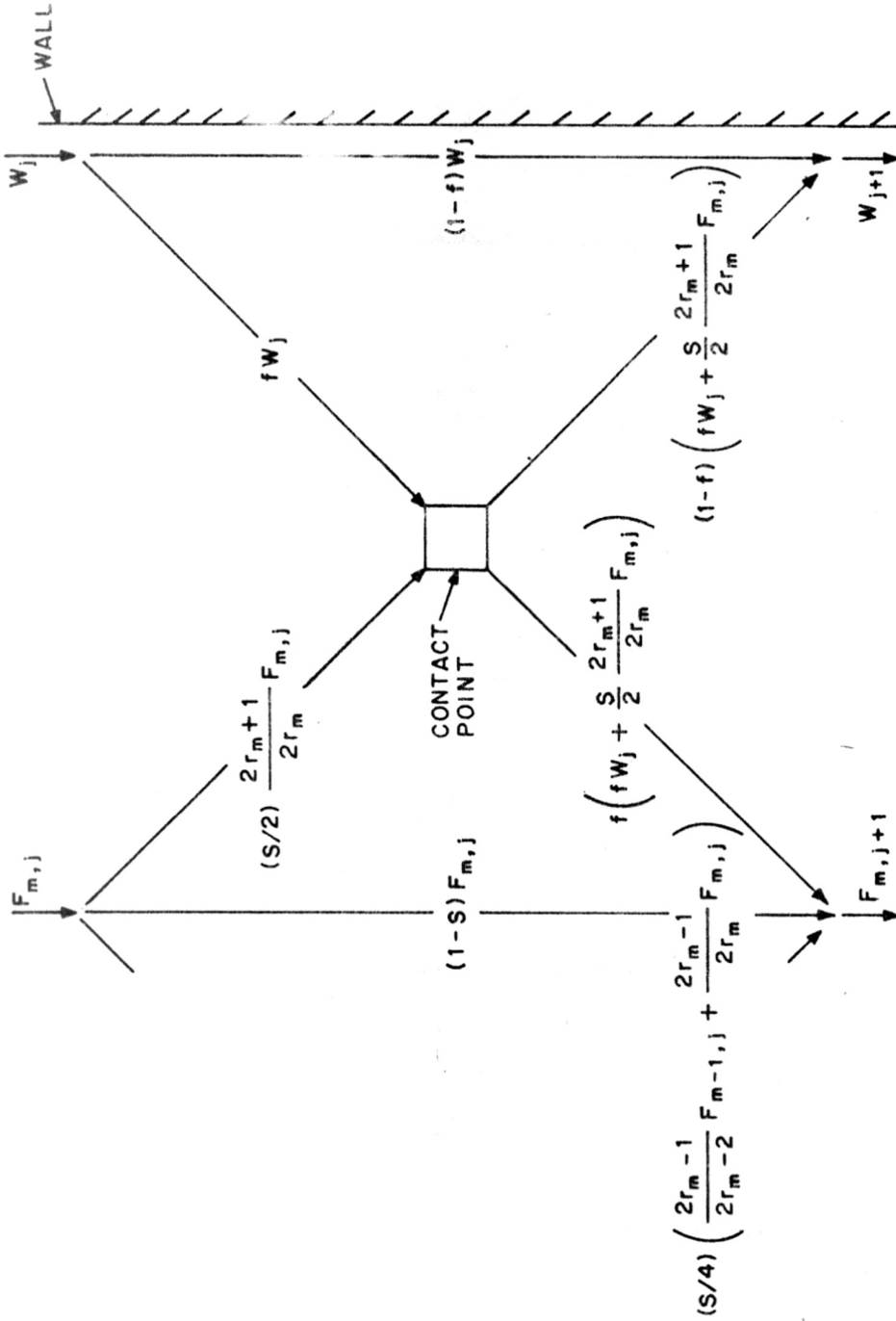


FIG. 1-2 (b) : FLOW NETWORK NEAR COLUMN WALL.

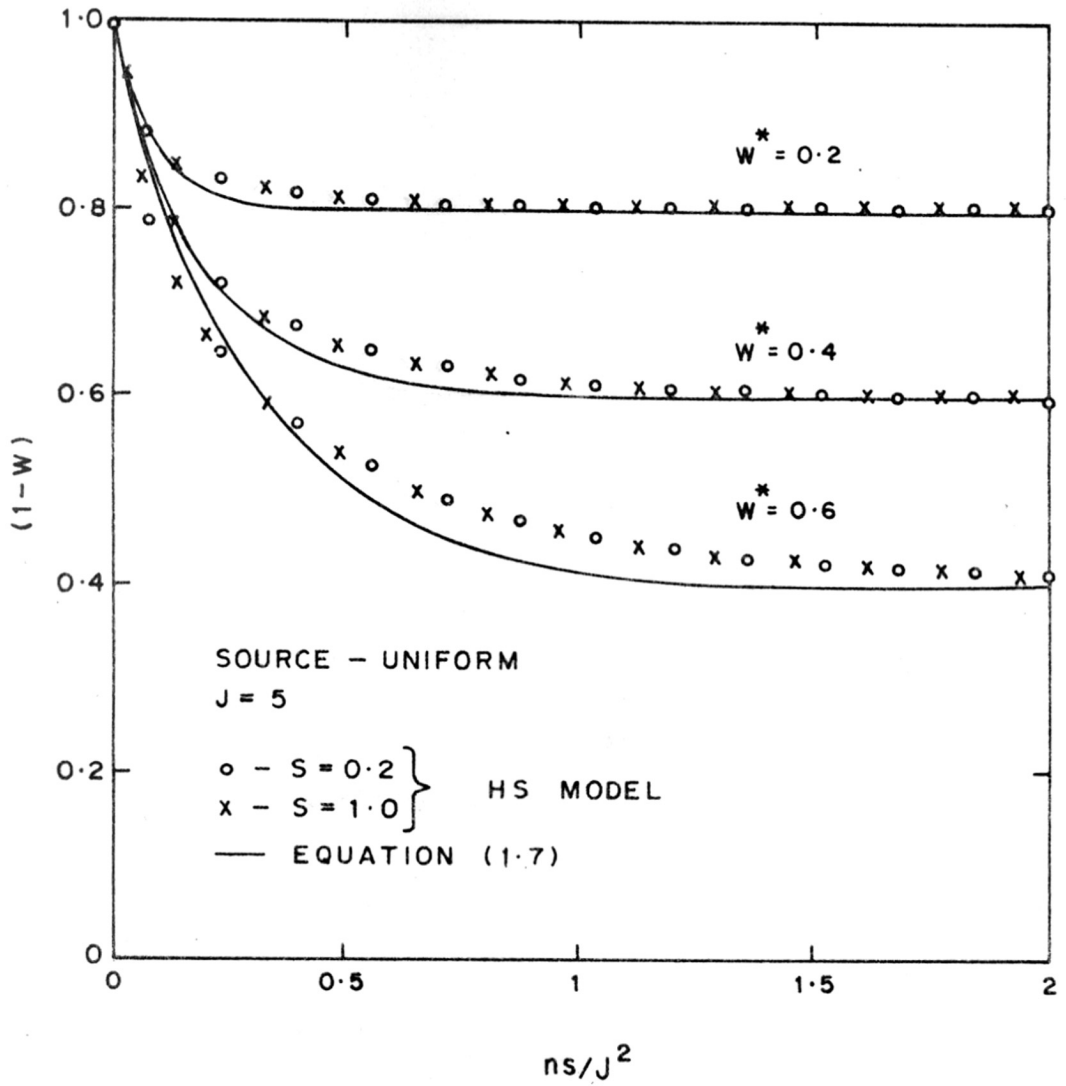


FIGURE - 1.3(a) : DEVELOPMENT OF WALL FLOW

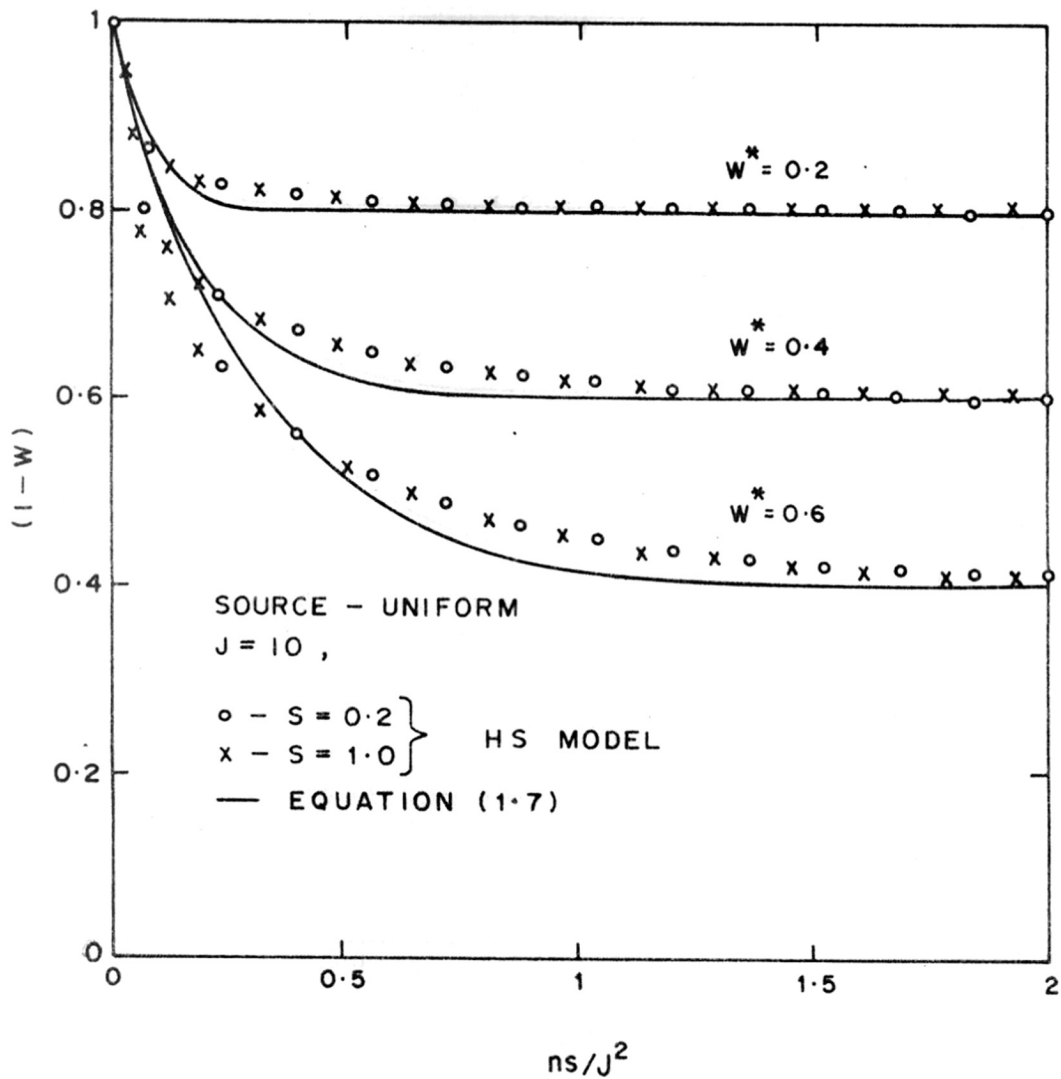


FIGURE -1.3 (b) DEVELOPMENT OF WALL FLOW.

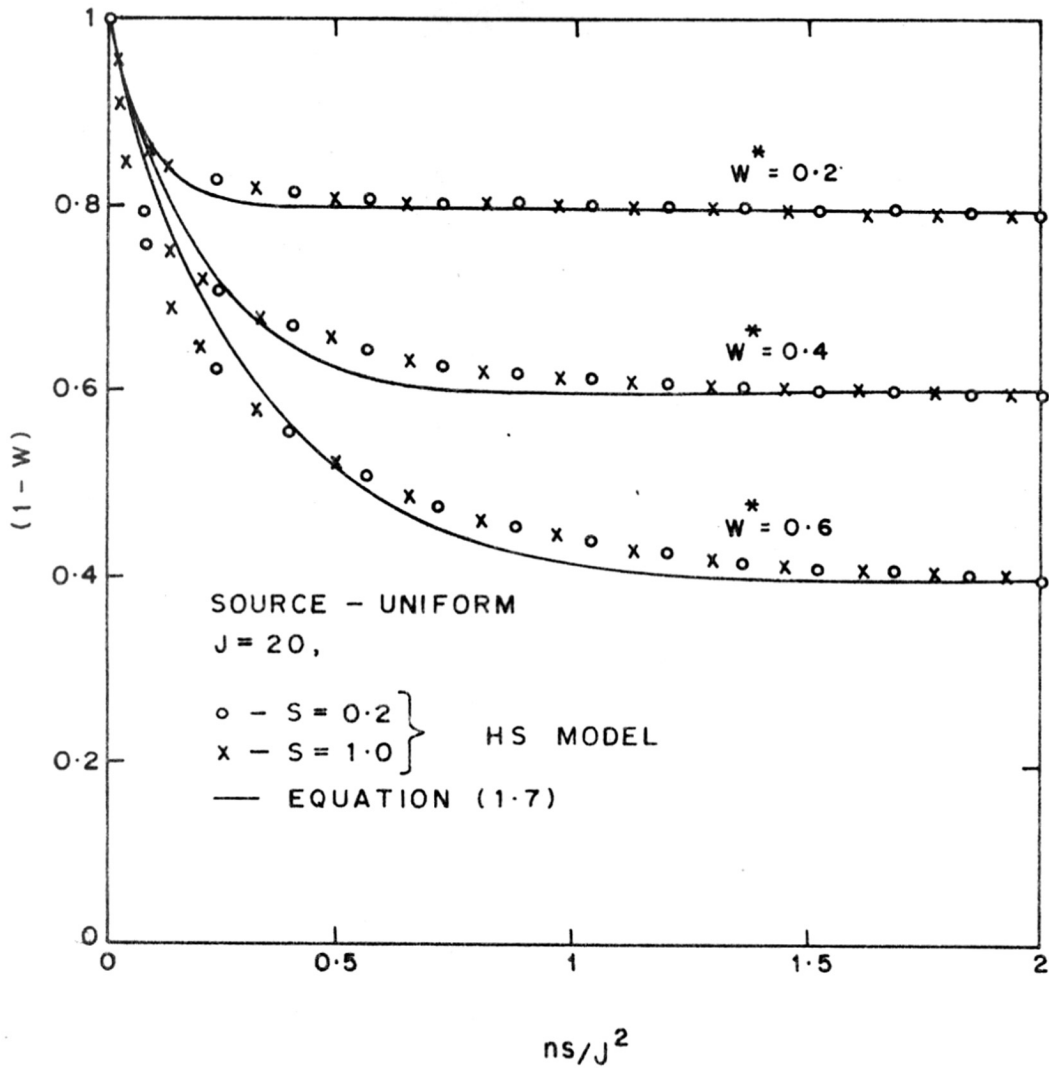


FIGURE -1.3 (c) : DEVELOPMENT OF WALL FLOW.

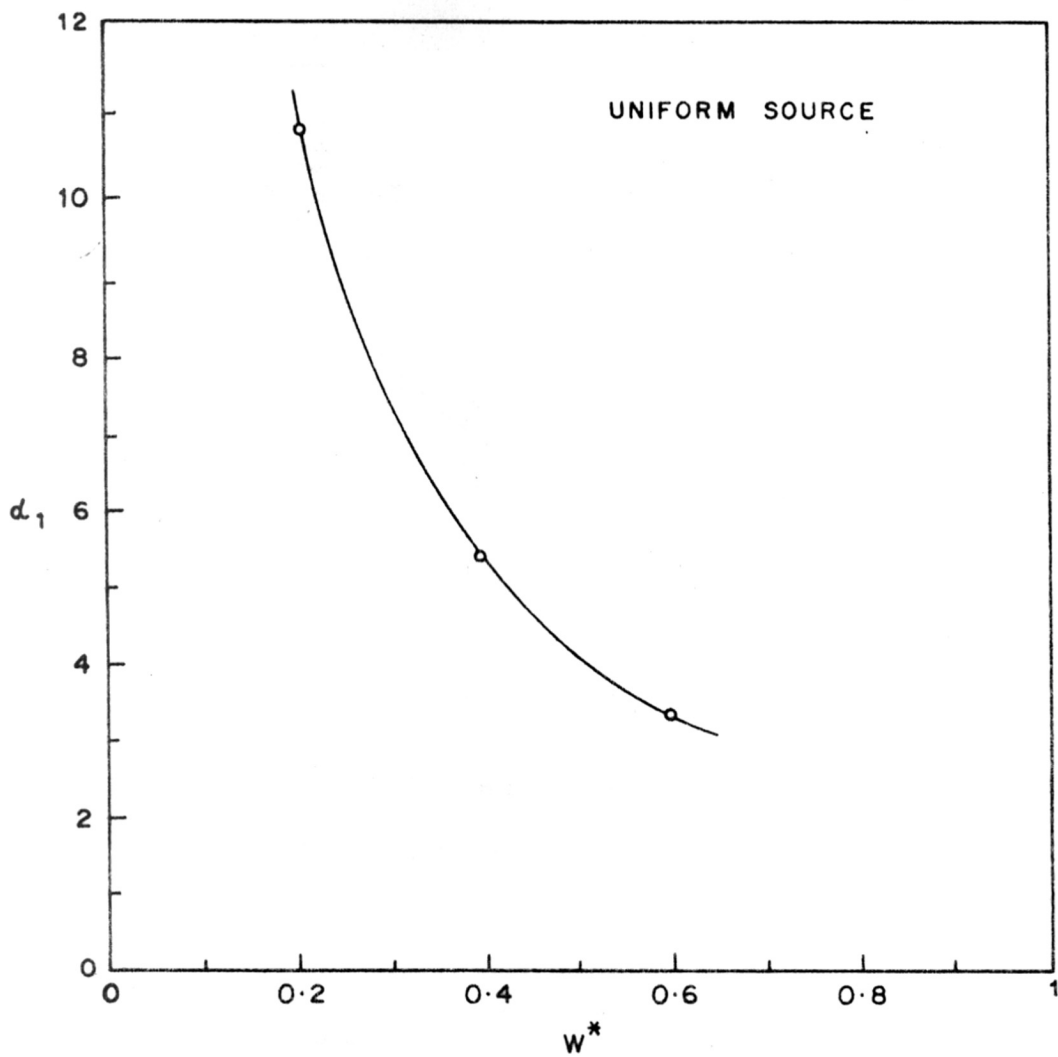


FIGURE-1.4 : α_1 AS A FUNCTION OF W^*

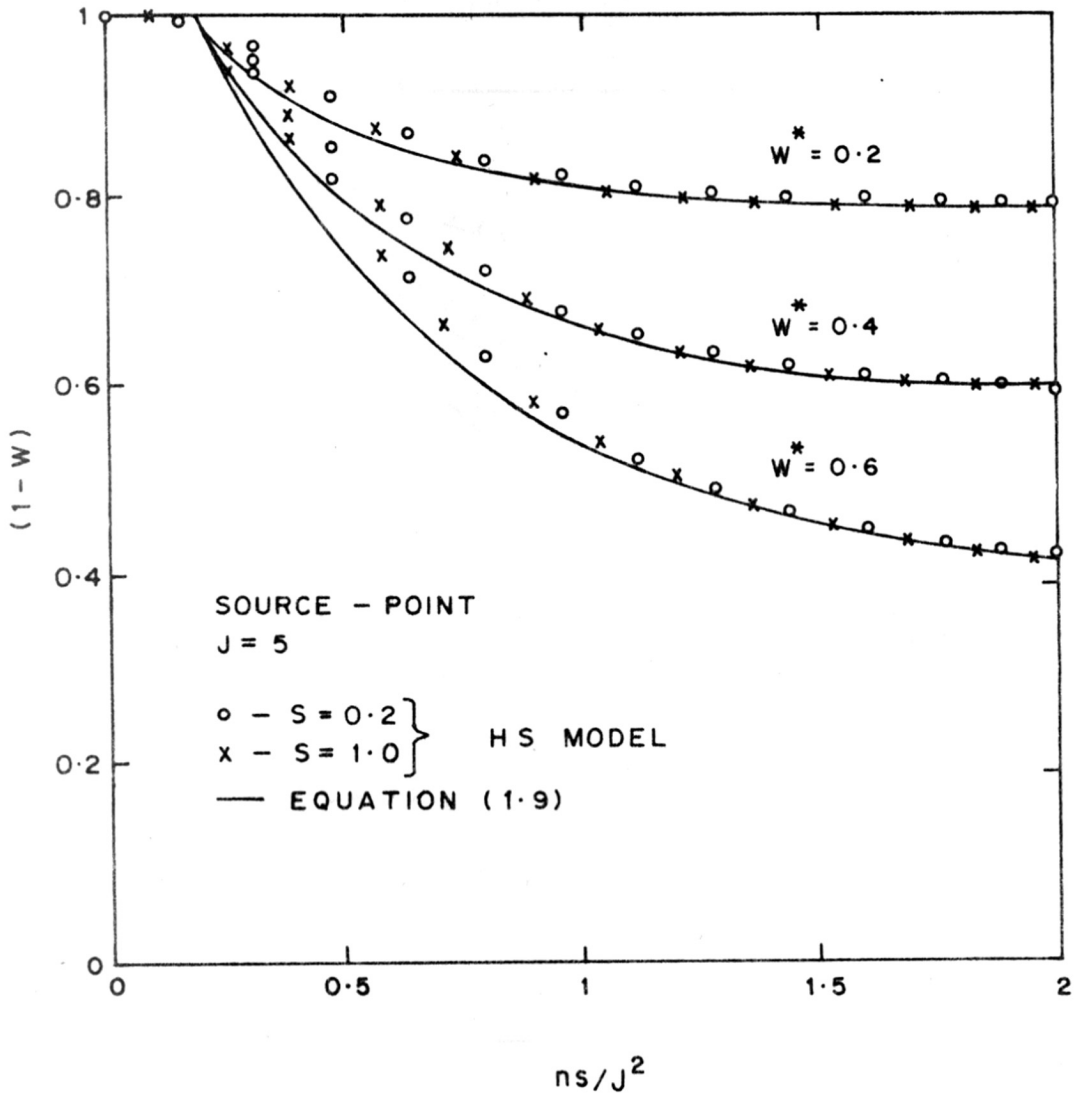


FIGURE -1.5(a) : DEVELOPMENT OF WALL FLOW

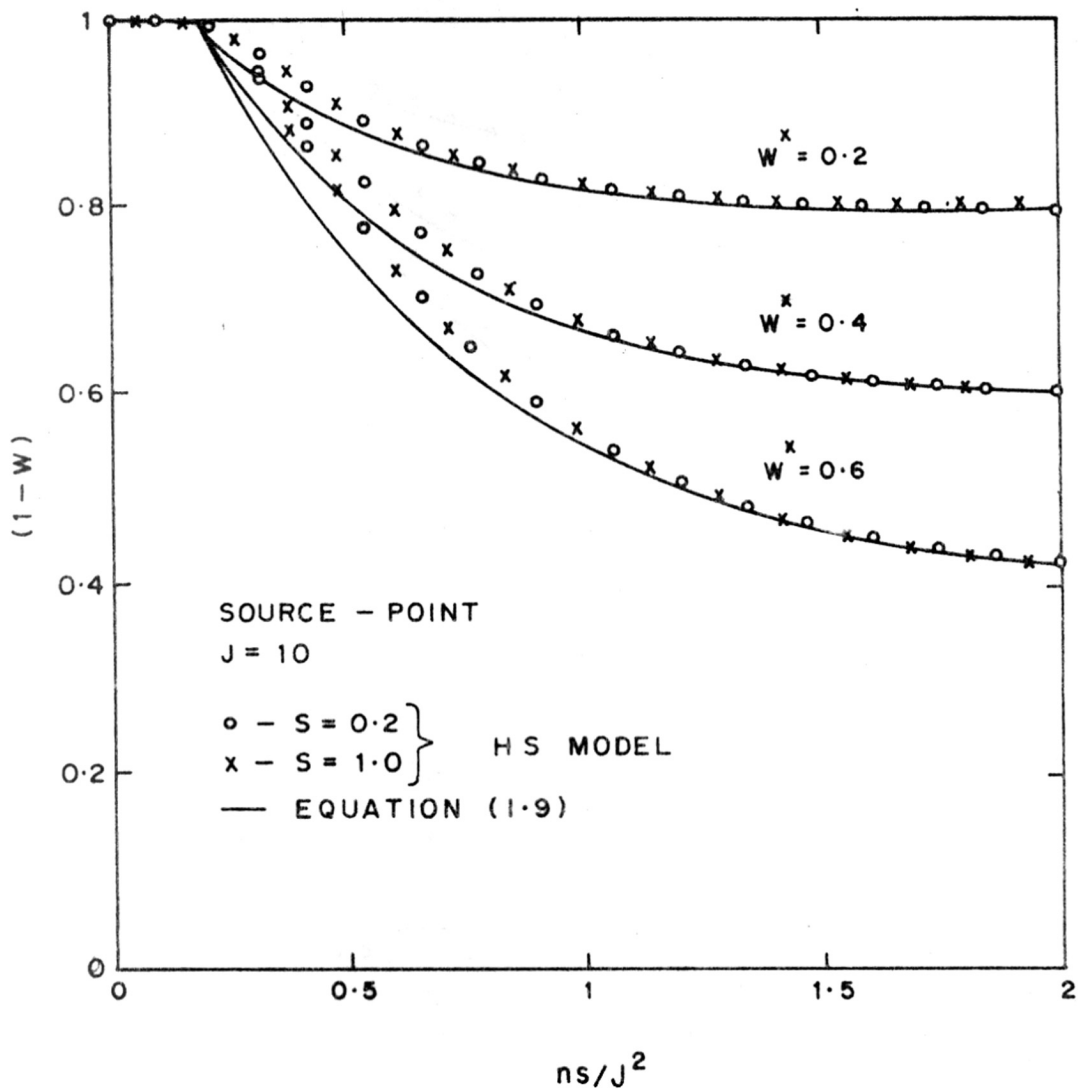


FIGURE -1.5 (b) : DEVELOPMENT OF WALL FLOW

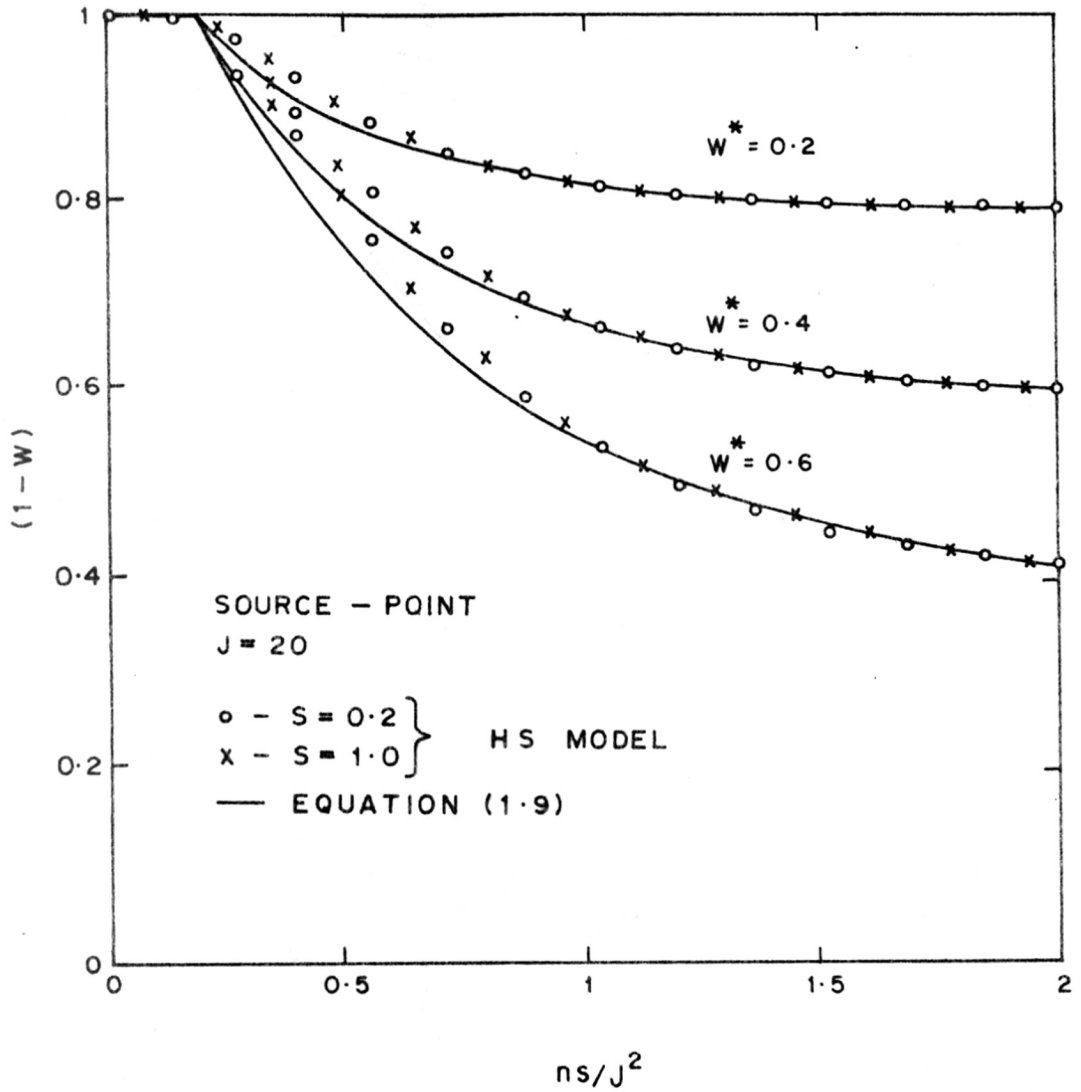


FIGURE-1.5(c) : DEVELOPMENT OF WALL FLOW

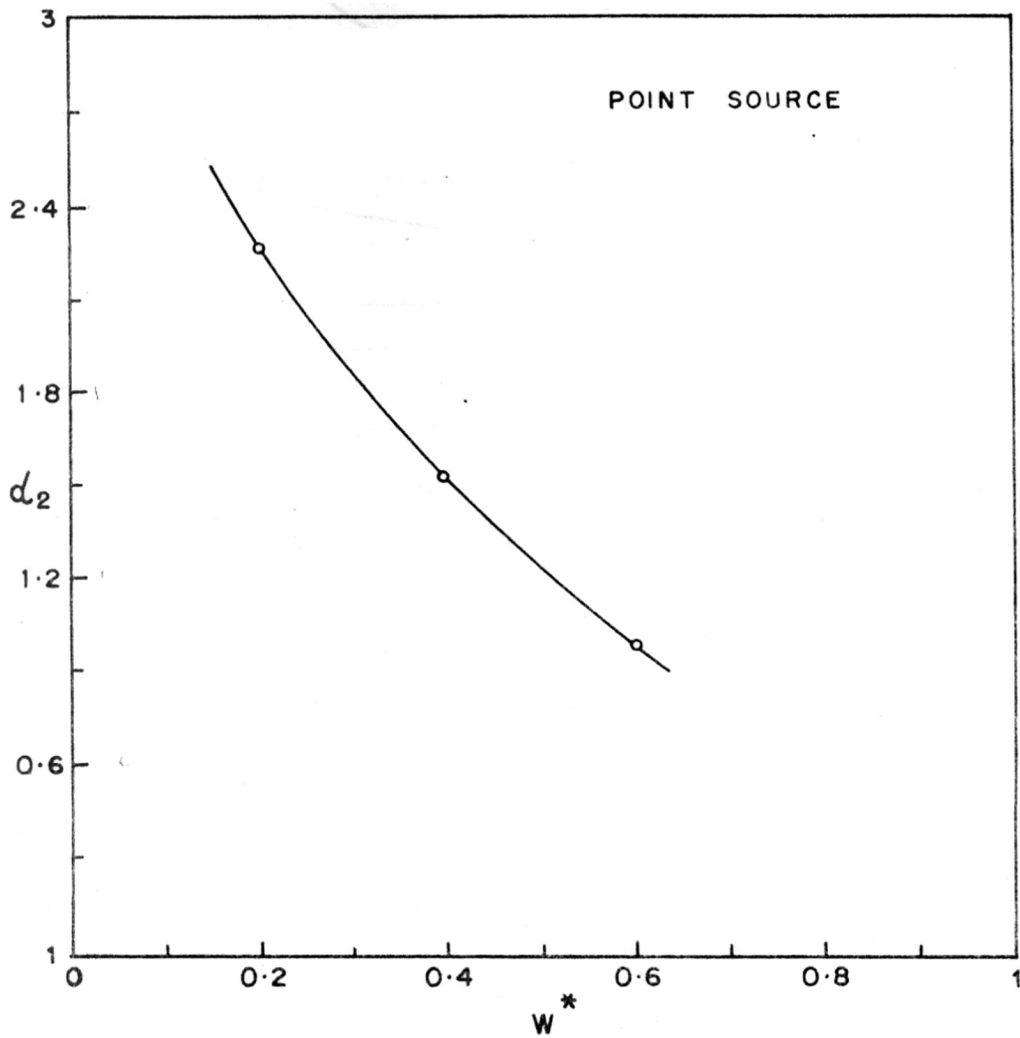


FIGURE -1.6 : α_2 AS A FUNCTION OF W^*

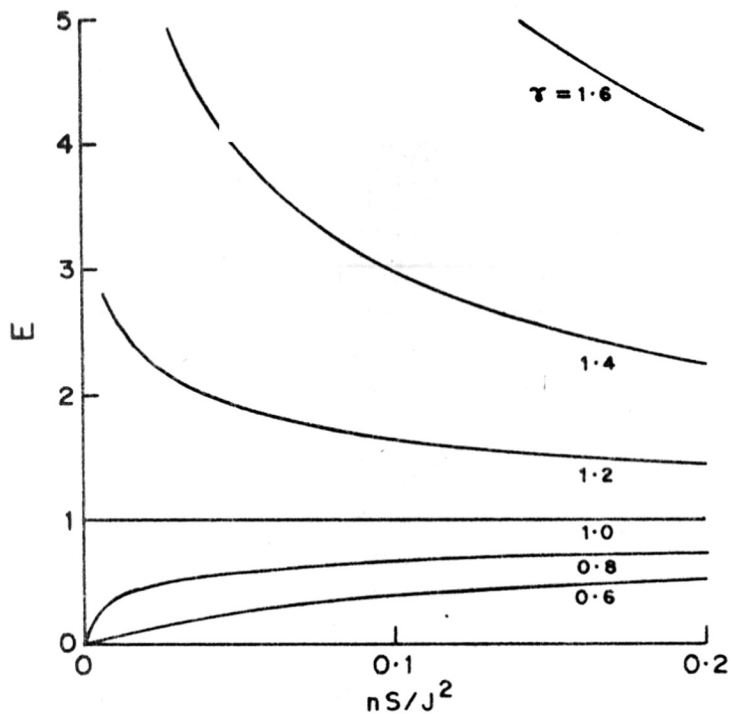


FIGURE-1.7(a): E AS A FUNCTION OF nS/J^2 AND γ FOR A POINT SOURCE.

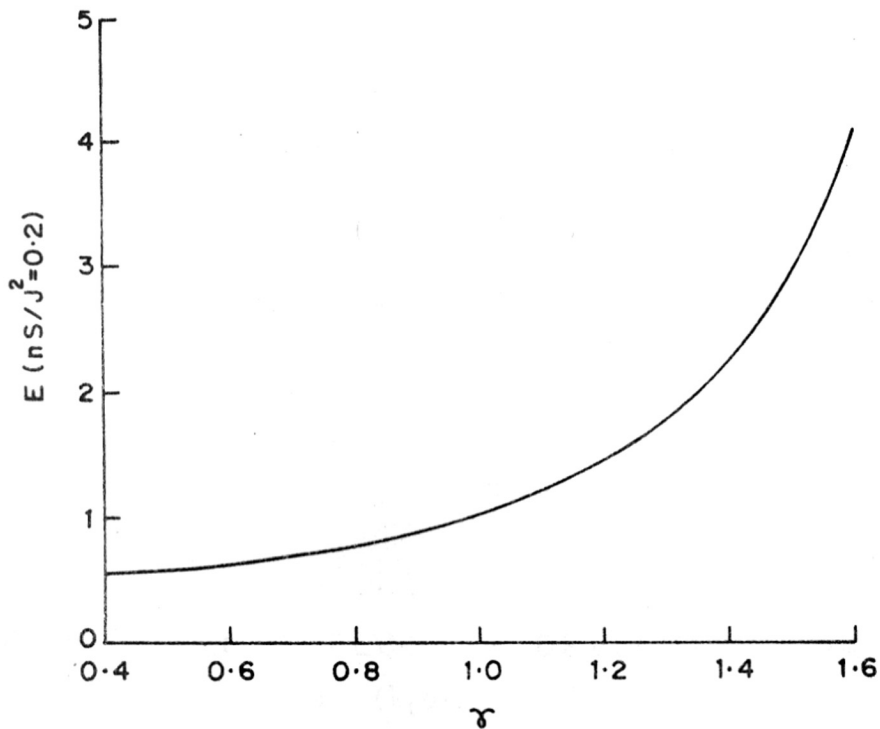


FIGURE-1.7(b): E AS A FUNCTION OF γ FOR $nS/J^2 = 0.2$ FOR A POINT SOURCE.

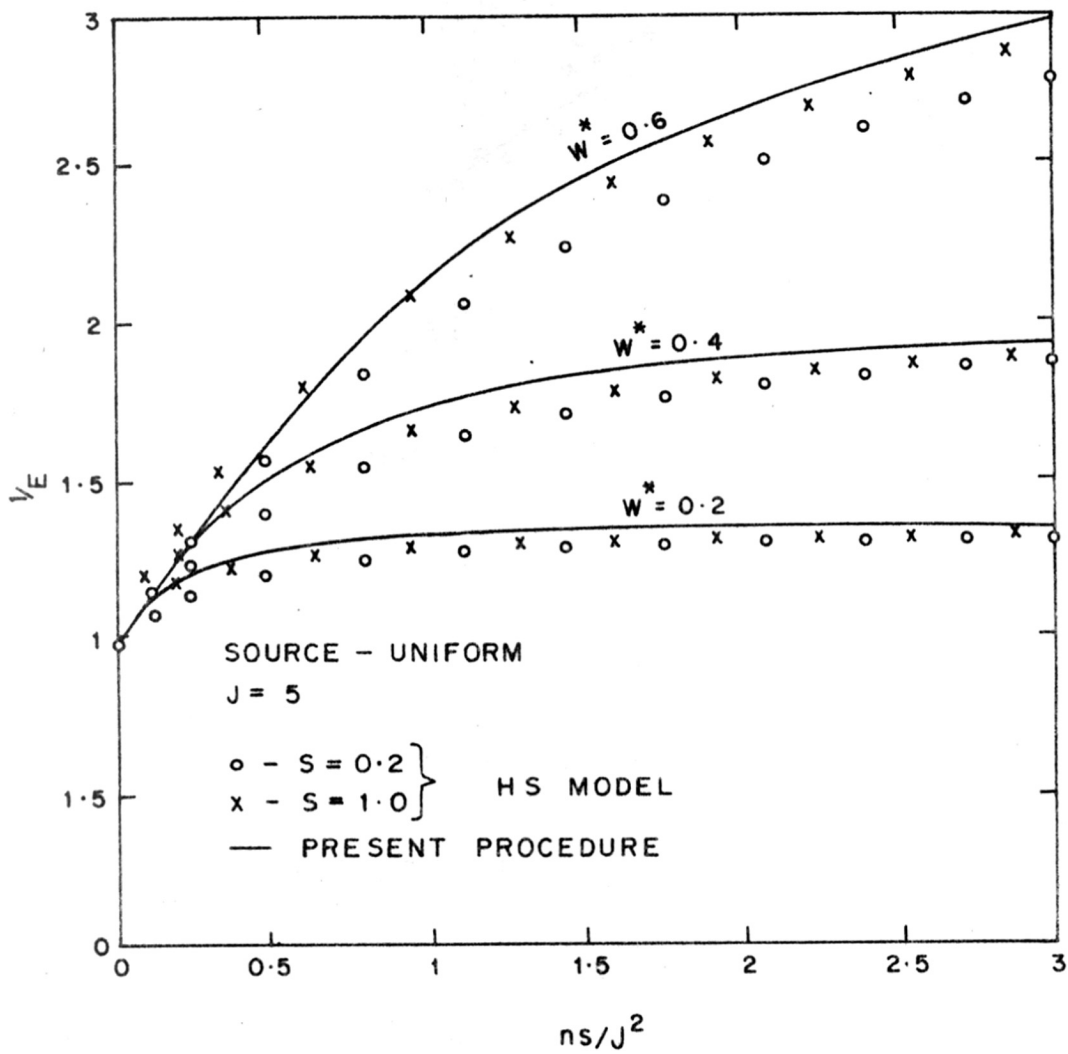


FIGURE - 1.8 (a) : EFFECT OF DEVELOPING WALL FLOW ON $(k_L a)_{av}$.

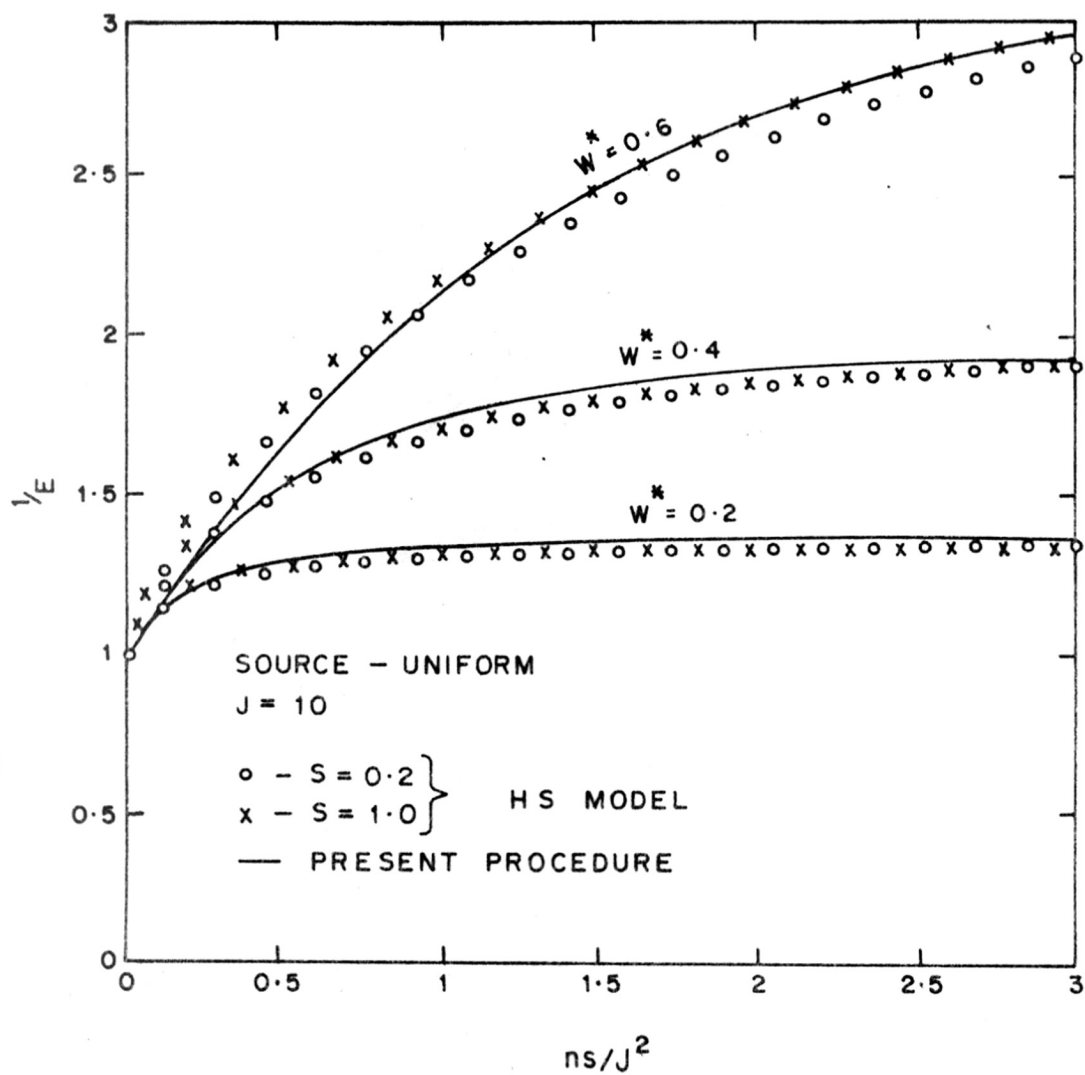


FIGURE-1.8(b) : EFFECT OF DEVELOPING WALL FLOW ON $(kLa)_{av}$

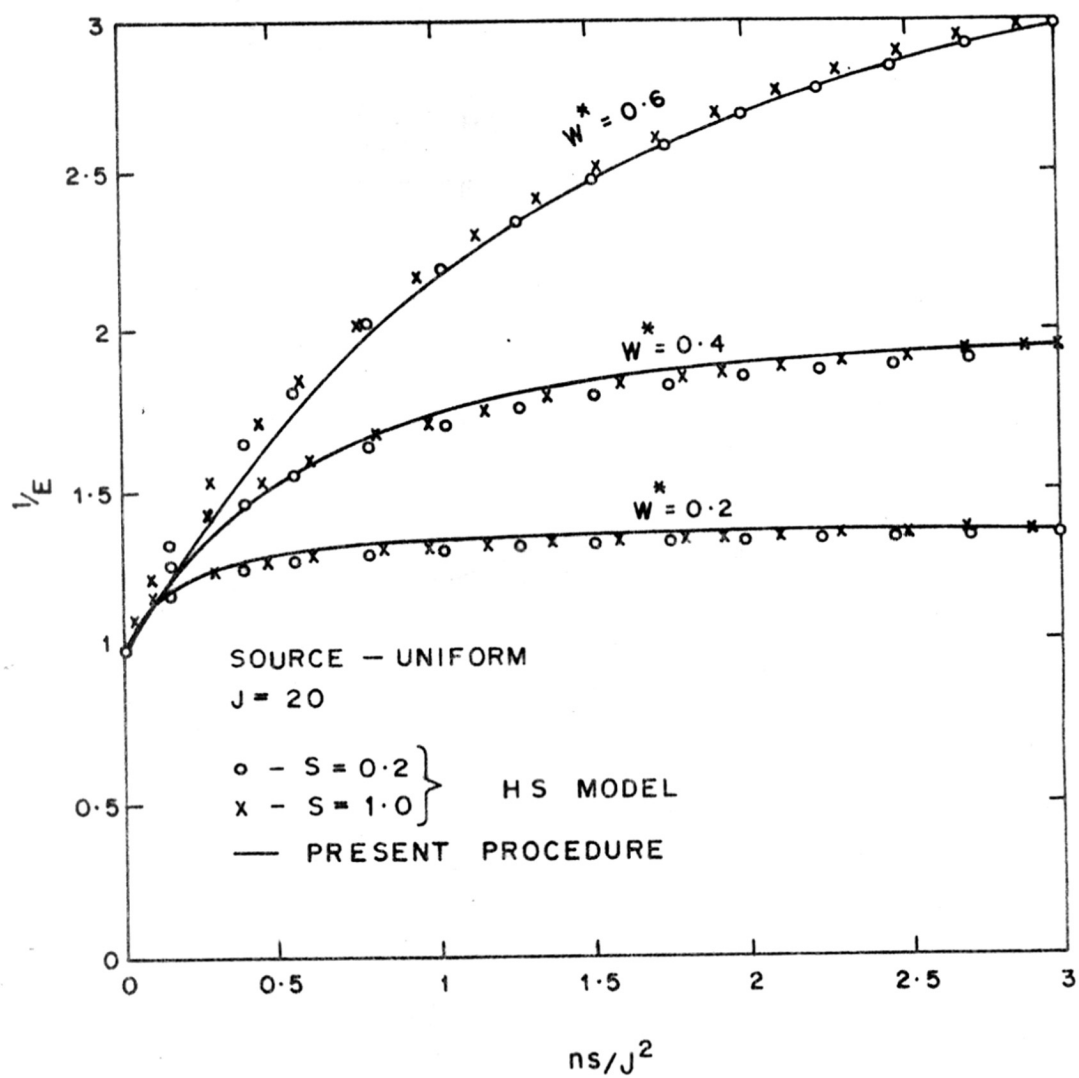


FIGURE-1.8(c) : EFFECT OF DEVELOPING WALL FLOW ON $(kLa)_{av}$.

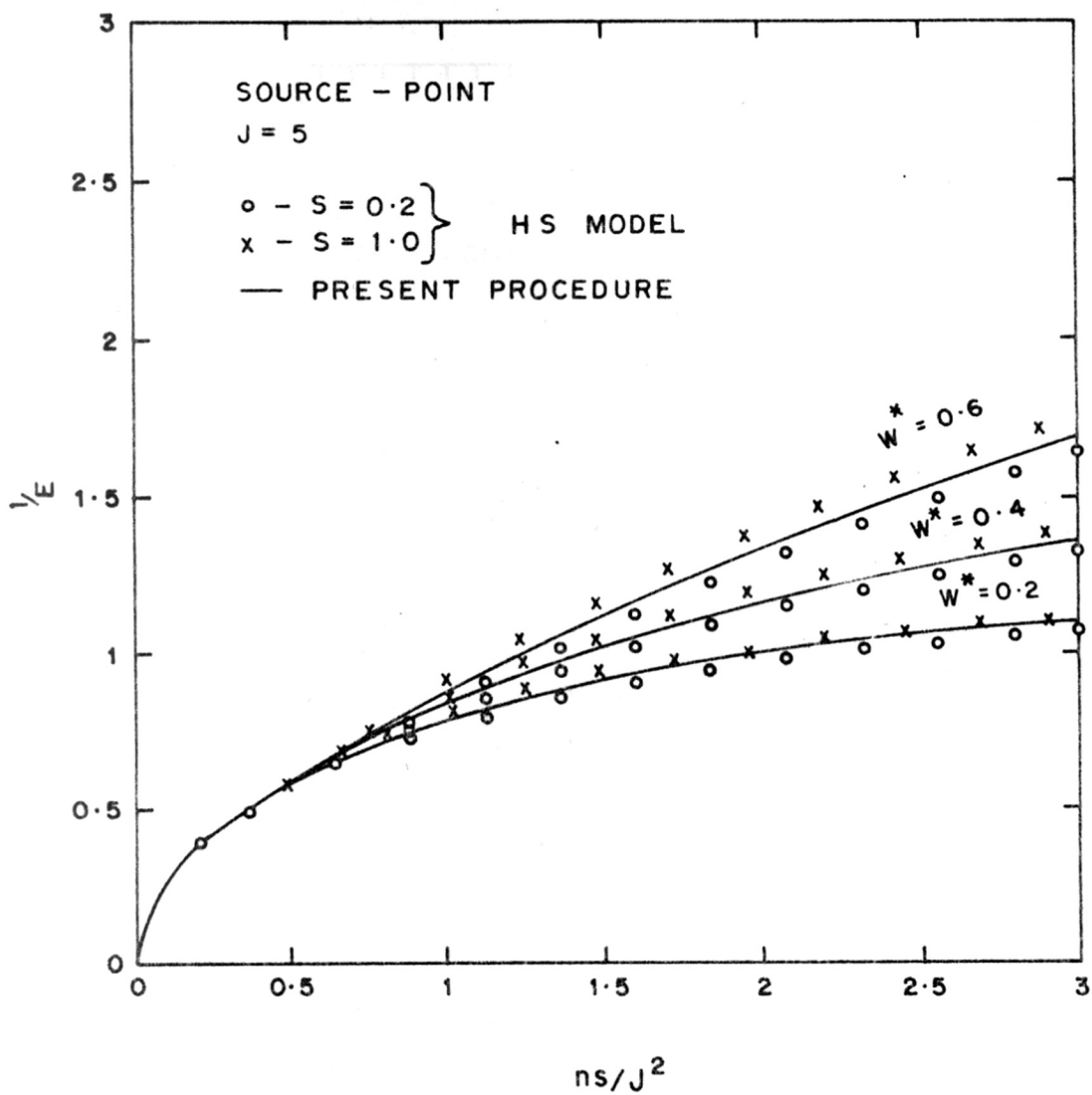


FIGURE - 1.9(a) : EFFECT OF DEVELOPING WALL FLOW
 ON $(kLa)_{av}$.

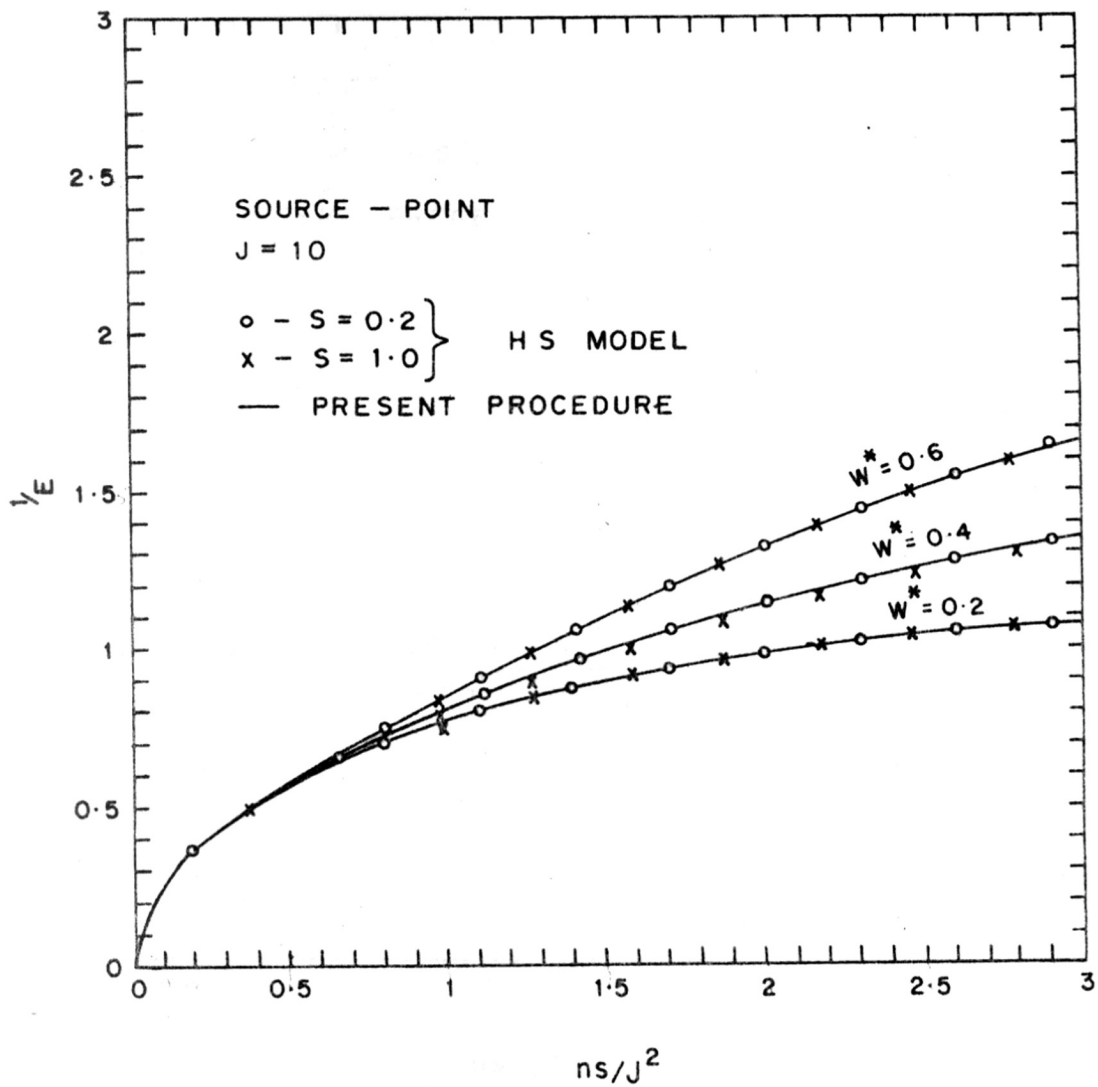


FIGURE -1.9 (b) : EFFECT OF DEVELOPING WALL FLOW ON $(k_L a)_{av}$.

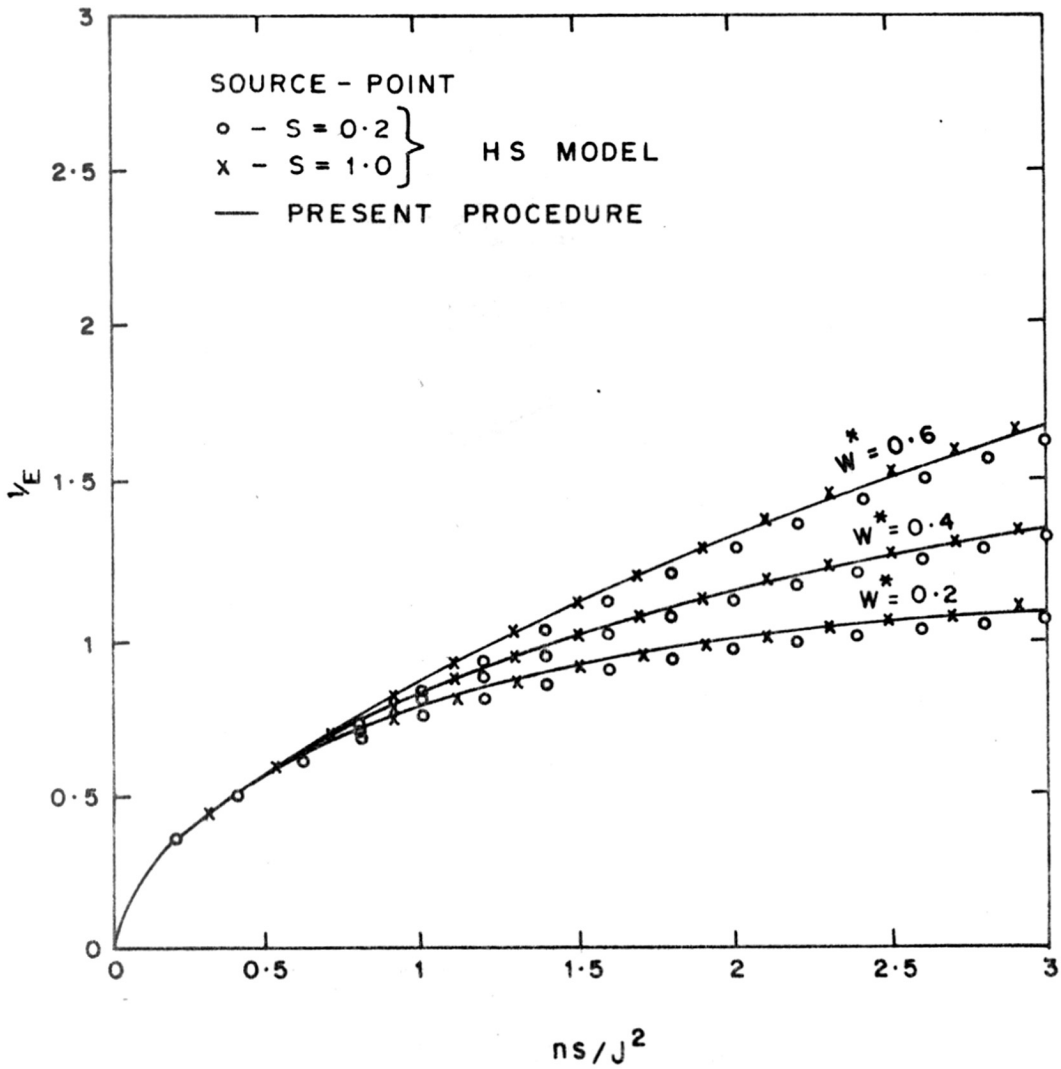


FIGURE - 1.9(c) : EFFECT OF DEVELOPING WALL FLOW ON $(k_L a)_{av}$.

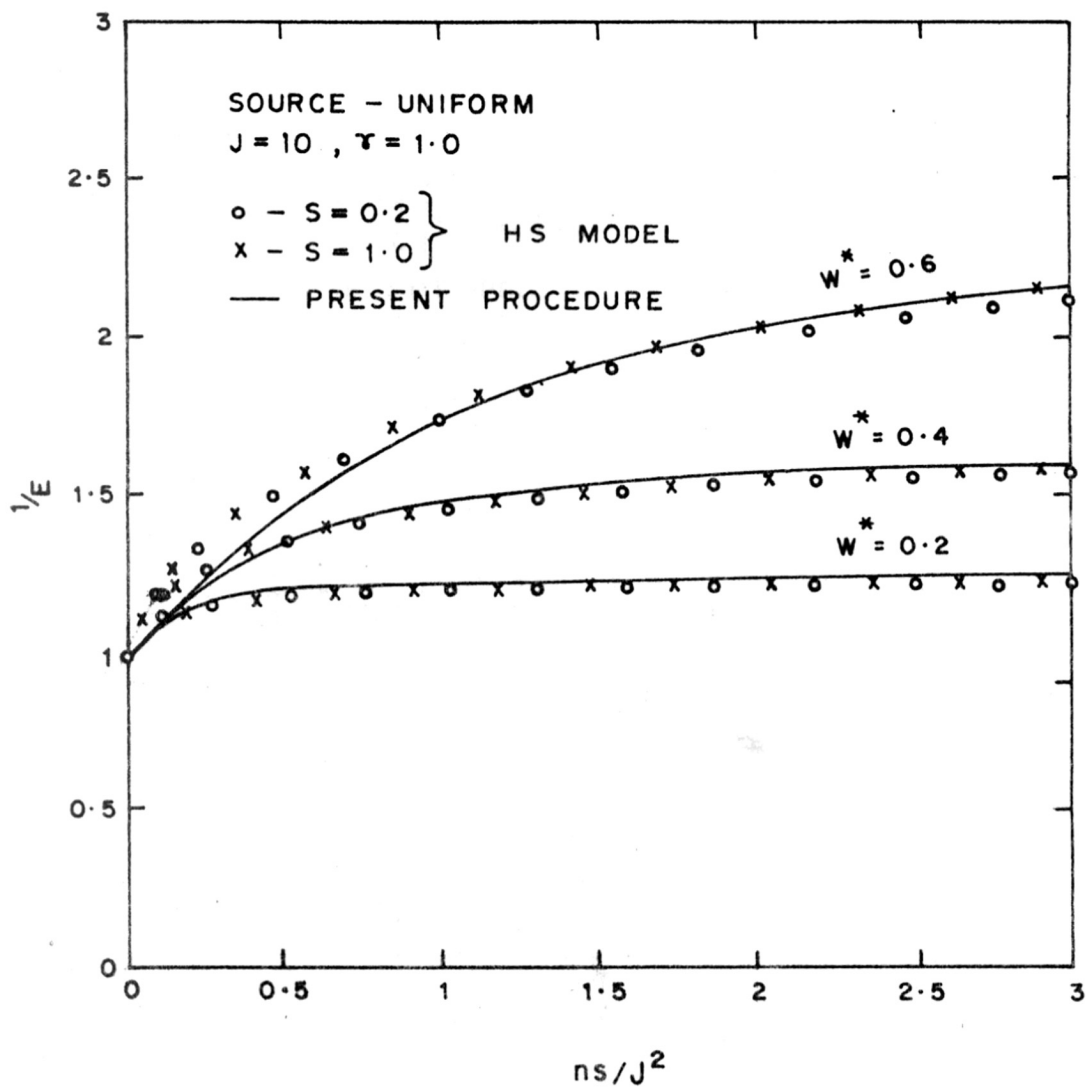


FIGURE-1.10: EFFECT OF DEVELOPING WALL FLOW ON
 $(k_L a)_{av}$ FOR $\gamma = 1.0$

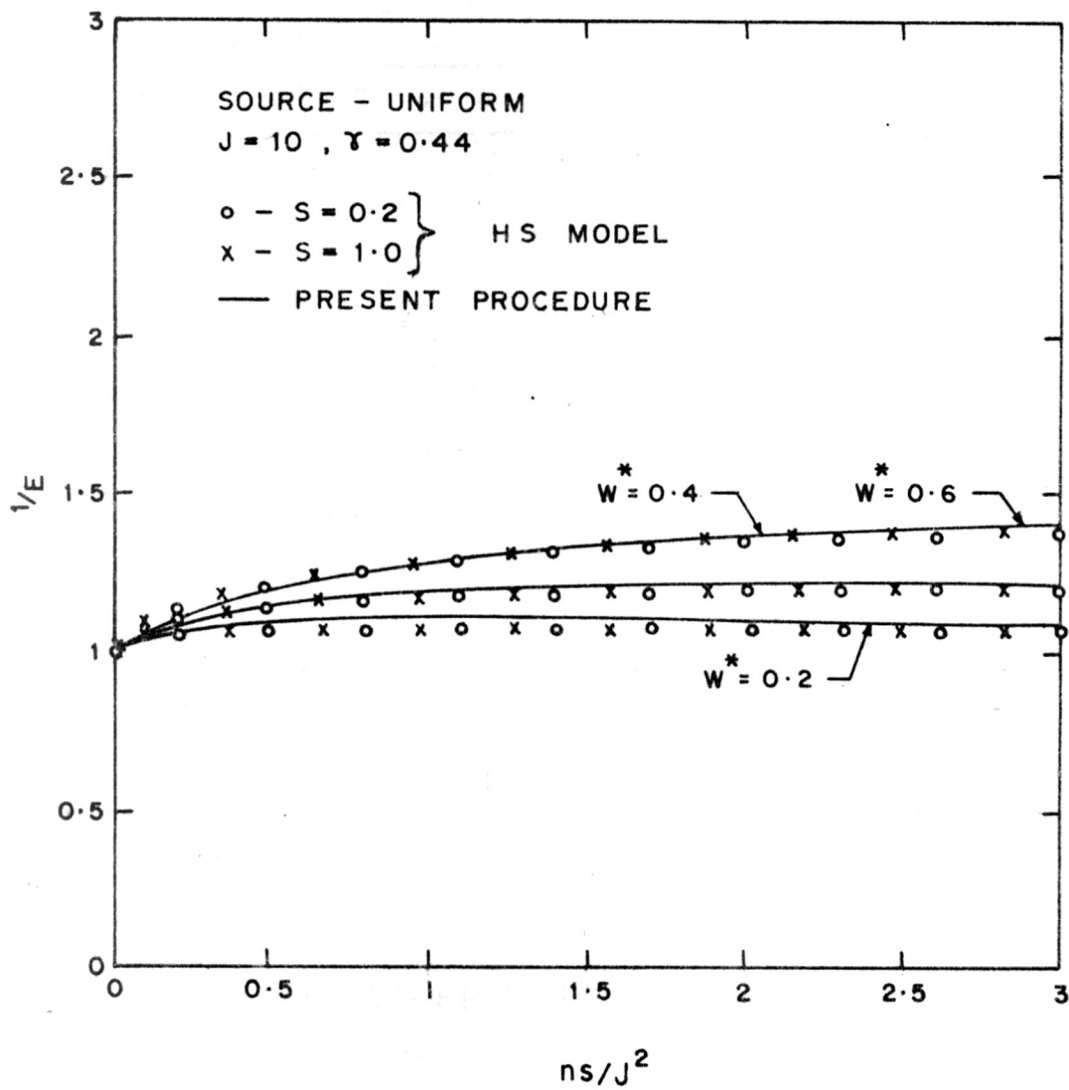


FIGURE-1-11 : EFFECT OF DEVELOPING WALL FLOW ON
 $(k_L a)_{av}$ FOR $\gamma = 0.44$

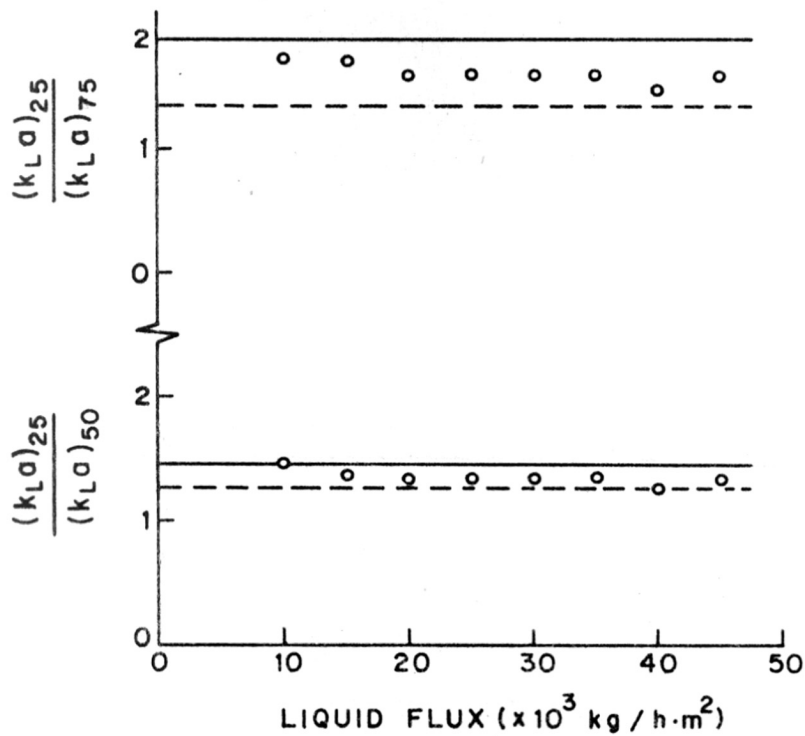


FIGURE-1.12 : EFFECT OF COLUMN HEIGHT ON $(k_{La})_{av}$

○ EXPERIMENTAL [Ref.3]

— PRESENT PROCEDURE (POINT SOURCE)

---- PRESENT PROCEDURE (UNIFORM SOURCE)



CHAPTER.2
DYNAMIC HOLD-UP FOR WETTABLE AND
NON-WETTABLE PACKINGS.

2.1 INTRODUCTION

Packed columns operated under trickle flow conditions and packed trickle bed reactors are widely used for conducting mass transfer operations with or without chemical reactions. This category of contactors renders several advantages like ease of construction and low cost of operation. The liquid in such columns is distributed over the top of the column and gradually descends through the packings. The performance of the packed column depends directly upon the hydrodynamic and mass transfer characteristics of the column. One of the important hydrodynamic parameters is the liquid hold-up in the column. The total hold-up of the liquid can be considered to be made up of two parts, i.e. the dynamic hold-up and the static hold-up. The liquid hold-up is related directly to the average residence time of the liquid in the column. It is also indirectly related to mass transfer parameters like the interfacial area. The subject of liquid hold-up in a packed column has been covered in several reviews (1-5).

2.2 PREVIOUS WORK

Liquid hold-up in packed columns has been studied by a number of workers (6,8-16). Discrepancies between vaporisation and gas absorption data have been correlated with total and dynamic hold-ups by several workers (9,17). Warner (18) investigated the absorption of zinc vapours in molten lead and proposed the quantity called effective hold-up ratio. Onda et al. (7) have taken hold-up into account for correlating the liquid film mass transfer coefficients. In catalytic packed trickle bed reactor the liquid hold-up is one of the measures of contacting

effectiveness between the liquid and the catalyst. Dynamic hold-up is also directly related to the mass transfer coefficient, the interfacial area and heat transfer coefficients [Matsura et al. (19) and Muroyama et al. (20)]. Out of the many correlations available for the dynamic hold-up, the important ones are listed in Table 2.1. In these correlations various parameters have been employed, like the flow parameter proposed by Lockhart and Martinelli (21,22), and dimensionless numbers like Reynolds number, Fanning number and Weber number. Some empirical correlations are also available in literature which are of the type $h = \alpha L^\beta$ [Charpentier and Favier (23), Bakos and Charpentier (24)]. Davidson (25) has presented a correlation which is purely based on theoretical considerations. Generally most of the workers have employed equations similar to that of Otake and Okada (26) with different constants. Most of the investigators have used porous or non-porous wettable packings like ceramic, glass or metal packings of different shapes and sizes. Some have used non-uniform particles of alumina or silica. Considering the factors like cost, durability, weight, corrosion resistance etc. non-wettable packings made of materials like polypropylene are potentially good substitutes for conventional packings. Some initial studies on mass transfer and distillation with such packings have been conducted by Gaston et al. (27). They observed that the results obtained with polypropylene packings are comparable with the traditional ceramic packings. For measuring dynamic hold-up they used the correlation given by Jesser and Elgin (13). Andrieu (28), who worked on the silicone coated packings of two sizes and shapes using the air-water system, presented an equation which is similar to that of Otake and Okada (26). It is shown that the wettability of the packing

can influence characteristics like interfacial area and equilibrium wall flow quite strongly (29,30). The influence of wettability on dynamic hold-up, however, has not been investigated thoroughly. The only information in this respect which is available in literature (28) was collected with air-water system. The purpose of the present study was to investigate the effect of liquid properties like viscosity and surface tension on the dynamic hold-up for both wettable and non-wettable packings, and to determine whether the same form of correlation is adequate for both types of packings. A simplified form of correlation was also tested with all the packings. Seven different packings were used in this study. Liquid properties were varied over wide ranges by using appropriate additives.

2.3 EXPERIMENTAL

The schematic representation of our experimental set up is shown in Figure 2.1. A pyrex glass column of 7.8 cm internal diameter and 100 cm length was used. The packings employed were of two types: (1) three different non-wettable packings of polypropylene i.e. 1.27 and 0.635 cm Raschig rings and 1.27 cm Pall rings, (2) four different wettable ceramic packings i.e. 1.27, 0.938 and 0.635 cm Raschig rings and 1.27 cm partition rings. The irrigating liquids employed were distilled water and aqueous solutions of two additives i.e. CEPOL and ALK-5, covering a wide range of viscosities and surface tensions. It was found that the addition of CEPOL, a polymeric additive, to water changed both its viscosity and surface tension simultaneously. However, the addition of ALK-5, a surface active agent, to water affected only

its surface tension. The irrigating liquid from the inlet was distributed over the top of the bed through a 20 point globe type of distributor. The distributor was found to work satisfactorily even at the minimum liquid flow rate. The outlet liquid was made to pass through a conductivity cell connected to a conductivity meter and an automatic recorder. This recorder and the conductivity bridge were pre-calibrated and frequently checked.

Measurement of liquid hold-up may be carried out by various methods which can be grouped into 3 types (1) local measurement of hold-up by placing optical probe in packing [Hewitt (31)]. (2) Semi-integral method dealing with some section of the packing which is geometrically well defined like a diametral line or a column cross section and employing x-ray or γ -ray techniques [Jones and Zuber (32)]. (3) Integral measurement methods which apply to the total volume of packing in the reactor. Prominent among them are (a) weighing of packing method [Shulman et al. (10)]. (b) liquid collection method in which the flow of irrigating liquid is stopped simultaneously at inlet and outlet [Larkins et al. (22)]. (c) residence time distribution method involving the determination of the mean residence time of a tracer [Rothfield and Ralph (33)].

In packed columns with trickling liquid, the liquid maldistribution at the microscopic level is always significant due to the rivulet-like flow of the liquid, so local probe or semi-integral methods may incorporate experimental errors. Liquid collection method is a time-consuming one. Continuous reactor weighing method needs a specially designed set up. The tracer method is comparatively easy and fast.

Therefore it has been widely used by many workers (22,33-36). In this method, the hold-up is evaluated from the mean residence time of the liquid phase obtained from the first moment of the exit age distribution using a pulse input of a tracer. The results obtained by this method were also compared with the liquid collection method and were found to be in excellent agreement.

Prior to each run, a high flow rate of the irrigating liquid was maintained through the column for at least 10 minutes to ensure a steady state. The desired flow rate was then adjusted through the pre-calibrated rotameter and again continued for the next five minutes to reach a steady state. NaCl solution of 1 N served as the tracer and was introduced at the centre of the distributor and as close as possible to the packings. The corresponding event was marked on the recorder. The tracer quantity was kept very small (<2 ml) for the following practical reasons. (1) Tracer quantity should not influence the total liquid flow rate at inlet and outlet. (2) The physical properties of the irrigated liquid e.g. viscosity, surface tension and density should not be altered after the addition of tracer.

The connection between the packed column and the conductivity cell was kept short so as to minimise the time lag. To minimise back-mixing and air bubbles in the connecting tube, the size of the connecting tube was kept as small as possible. It was observed experimentally that it did not lead to any build up of liquid level in the column even at the highest flow rates. The R.T.D. curve was found to be reproducible. Operation of the conductivity meter at high sensitivity allowed an accurate determination of very low tracer concentration (<0.001 N) at

the outlet of the column. The run was continued until the outlet concentration of liquid approached zero very closely. All the packings gave R.T.D. curves without much tailing for all liquid flow rates except for very low rates where tailing was significant.

The relation between mean residence time and the hold-up in the equipment is shown by following equation:

$$\bar{t} = \frac{h_t V_c}{Q} = \int_0^{\infty} t E(t) dt \quad [2.1]$$

and

$$E(t) = \frac{Q C_T(\text{exit})(t)}{M_T} \quad [2.2]$$

Schiesser and Lapidus (38) questioned the validity of the tracer measurements because of somewhat different results for hold-up obtained for various forms of tracer inputs. However, the determination of the volume of the system given by Eq.(2.1) is based on the central volume principle which is proved theoretically by Stephenson (39). Further, the validity of the tracer measurements and the equivalence of results for different tracer inputs has been demonstrated and confirmed by Rothfield and Ralph (33), Patwardhan and Shrotri (40) and Ross (41). Generally, the residence time distribution is measured outside the column in tracer communication method. Van Swaaij (35) used a special type of arrangement which enabled them to evaluate conductivity of the liquid flowing internally and thus calculate the residence time distribution. In the present work, the residence time distribution is measured outside the column. A volume correction is applied to the results to account for the liquid volume in the tube connecting the column bottom to the conductivity cell.

Collected experimental data for wettable and non-wettable packings is shown in Tables 2.7 and 2.8 respectively.

2.4 RESULTS AND DISCUSSION

The properties of the liquid phase used in this study were varied over wide ranges as shown in Table 2.2. The static hold-up was determined with the usual weighing method. It is observed that for non-wettable packings the static hold-up is about 20% higher than the wettable packings. Andrieu (28) reported the static hold-up to be 20% less than that for wettable packings. Our results of static hold-up are in agreement with the results obtained by Gaston et al. (27). These results are compared in Table 2.3. It is quite likely that the static liquid on the non-wettable surface forms droplets due to its large contact angle. This may cause the higher static hold-up in case of non-wettable packings. Pall rings show higher static hold-up than Raschig rings of the same size. This may be due to the additional surfaces present in Pall rings.

It was found in this study that the dynamic hold-up for non-wettable packings was less than that for similar wettable packings (42). One of the objectives of this study was to investigate the effect of liquid properties like viscosity and surface tension on the dynamic hold-up. In order to correlate the results in terms of dimensionless groups, the following equation was used first:

$$h_d = k_1 \text{Re}^{\alpha_1} \text{Ga}^{\beta_1} \quad [2.3]$$

This is similar to the equations used by earlier workers as listed in Table 2.1. The Reynolds number and the Gallilio number incorporate liquid viscosity but not the surface tension. This equation can be transformed into a linear equation by taking logarithms of both sides, and the constants k_L , α_1 and β_1 can be determined by linear regression analysis of the experimental data. The results of such analysis are shown in Table 2.4 for all the packings used in this study. It is seen that the multiple correlation coefficient is quite high. The calculated F ratio are very high, indicating that the regression is highly significant. The mean squares of the residuals for the four ceramic packings are comparable. The mean squares of residuals for the polypropylene packings are comparatively higher and also show more variation, from packing to packing. It appears that the variability of experimental results is higher for non-wettable packings. This is expected, because liquid does not wet the solid surface for polypropylene packings. The nature of liquid flow in a column consisting of random packings is stochastic. The wetting of packing surface by liquid in case of ceramic packings probably tends to stabilise the liquid flow paths to some extent, thus reducing the experimental variations. In spite of the higher experimental variation for polypropylene packings, the calculated F ratios are quite high. The hold-up values predicted by Eq.(2.3) with appropriate values of the constants taken from Table 2.4 and those obtained experimentally are plotted in Figure 2.2. The predictions of Eq. (2.3) are seen to be satisfactory. A similar plot is presented in Figure 2.3 for polypropylene packings.

Ceramic packings are wetted by aqueous solutions, while polypropylene packings are not. The effect of surface tension on the dynamic hold-up of wettable packings has been investigated and is known to be insignificant. Since the entire surface is wetted, the cross-sectional geometry of the fast flowing zones of liquid is probably not affected very much by any change in surface tension. However, in case of polypropylene packings, the cross-section of a liquid rivulet might be determined mainly by surface tension forces, and thus might get affected considerably by changes in surface tension. To test this possibility, the experimental data were reanalysed using the following equation:

$$h_d = k_2 \text{Re}^{\alpha_2} \text{Ga}^{\beta_2} \text{We}^{\gamma_2} \quad [2.4]$$

where We, the Weber number, incorporates the liquid surface tension. The results of this analysis for the seven different packings used are shown in Table 2.5. The multiple correlation coefficients are seen to be slightly higher, on an average, as compared to those in Table 2.4. This is expected, since Eq. (2.4) has an additional independent variable. The SS_{reg} values are slightly higher in Table 2.5 than in Table 2.4. This increase can be directly attributed to the inclusion of Weber number in Eq. (2.4). The marginal sum of squares listed in Table 2.5 is the difference in the SS_{reg} values in Tables 2.4 and 2.5. It is also equal to the mean square attributable to the Weber number. This is used for calculating the marginal F values listed in Table 2.5. It is seen that in five cases the calculated F is insignificant. Only in two cases it is statistically significant.

However, even in these two cases, the calculated marginal F for Weber number is much smaller than the F_{reg} values in Table 2.4. Therefore, we can safely conclude that the Weber number does not have a significant effect on the dynamic hold-up. The experimental and predicted values of h_d for both types of packings are shown in Figures 2.4 and 2.5.

It is seen from Table 2.1 that in most correlations previously determined, the power on Re is approximately twice the power on Ga , but is opposite in sign. The same also holds good for the results of regression analysis shown in Table 2.4. Since Re^2 / Ga is equal to another dimensionless number, i.e. the Froude number, it is interesting to see whether the dynamic hold-up can be correlated with Froude number alone. The following equation was considered:

$$h_d = k_3 Fr^{\alpha_3} \quad [2.5]$$

The results of the statistical analysis of experimental data employing Eq. (2.5) for all the packings used are shown in Table 2.6. It is seen that the multiple correlation coefficients are quite comparable to those in Table 2.4. The SS_{reg} values in Tables 2.4 and 2.5 are also comparable to each other. In other words, using just one dimensionless number, i.e. Fr , gives a correlation which is almost as good as that based on two dimensionless numbers, i.e. Re and Ga , with two independent exponents. The calculation of Re and Ga needs the knowledge of liquid viscosity and surface tension, while Fr can be calculated knowing only the packing size and superficial liquid velocity. Thus, for estimating the

dynamic hold-up for a new liquid, Eq. (2.5) is more convenient. The experimental hold-up values and those predicted by Eq. (2.5) are shown in Figure 2.6 and 2.7 for all the packings used.

The several correlations for the dynamic hold-up, listed in Table 2.1 are quite similar in form, though they differ in terms of the numerical values of the various constants. In order to compare these correlations with each other, and also with correlations developed in this work, all these were applied to a hypothetical system, i.e. that of air and water, for 1.27 cm ceramic Raschig rings. The results are shown in Figure 2.8. It is seen that our correlation compares quite well with earlier ones. Also, the predictions based on Eqs. (2.3) and (2.5) are almost identical. A similar comparison is shown in Figure 2.9 for 1.27 cm polypropylene Raschig rings. There is only one earlier correlation, i.e. that by Andrieu (28), which is applicable for non-wettable packings.

2.5 CONCLUSIONS

It was found that liquid viscosity and surface tension do not affect the dynamic hold-up in trickle flow packed columns significantly. The same form of correlation is applicable both to wettable and non-wettable packings. Predictive correlations based on the Froude number, Eq. (2.5), are almost as accurate as those based on two dimensionless numbers, i.e. Re and Ga . The dynamic hold-up for polypropylene packings is less than that for ceramic packings of comparable size.

NOTATION

a	packing geometrical area per unit column volume (cm^{-1})
C_T	concentration of tracer in liquid phase (gm/lit)
d_p	nominal packing diameter (cm)
d_t	hydraulic diameter of the packing
E	exit age distribution
Fi	film number ($=Fr/Re$)
Fr	Froude number ($V^2/d_p g$)
g	acceleration due to gravity (cm/s^2)
Ga	Gallileo number ($d_p^3 g \rho^2 / \mu^2$)
h_t	total fractional hold-up
h_s	fractional static hold-up
h_d	fractional dynamic hold-up
k_1, k_2, k_3	constants in Eqs. (2.3)-(2.5)
M_T	mass of tracer injected (gm)
N	number of packings/unit column volume
Q	liquid flow rate, cm^3/sec
Re	Reynolds number ($V \rho d_p / \mu$)
t	time (s)
\bar{t}	mean residence time of liquid phase (s)
We	Weber number ($V^2 d_p \rho / \sigma$)
V	superficial liquid velocity (cm/s)
V_c	volume of the column

Greek letters

- $\alpha_1, \alpha_2, \alpha_3$ constants used in Eqs. (2.3)-(2.5)
- $\beta_1, \beta_2, \beta_3$ constants used in Eqs. (2.3)-(2.5)

.....

- τ_2 constant used in Eq. (2.4)
- μ liquid viscosity (poise)
- ρ liquid density (gm/cm^3)
- σ liquid surface tension (dynes/cm)
- ϵ porosity of dry packing

REFERENCES

1. Charpentier J.C., Chem. Eng. Jl. 11, 161 (1976)
2. Hofmann H.P., Catal. Rev. Sci. Eng. 17, 21 (1978)
3. Satterfield C.N., AIChE J. 21, 209 (1975)
4. Gianetoo A., Baldi G., Specchia V. and Sicardi S., AIChE, 24, 1087 (1978)
5. Herskowitz M. and Smith J.M., AIChE J. p. 29, 1 (1983)
6. Hochman J.M. and Effron E., I & EC Fundamentals, 8, 63 (1969)
7. Onda K., Sada E. and Murase Y., AIChE J. 5, 235 (1959)
8. Payne J.M. and Dodge B.F., Ind. Eng. Chem. 24, 630 (1932)
9. Shulman H.L., Savini C.G. and Edvin R.V., AIChE J. 9, 479 (1963)
10. Shulman H.L., Ullrich C.F. and Wells N., AIChE J., 1, 247 (1955)
11. Kan K.M. and Greenfield P.F., I & EC Proc. Des. Dev. 18, 740, (1979)
12. Mayo F., Hunter T.G. and Nash A.W., JSCI, 54, 375 (1935)
13. Jesser B.W. and Elgin J.C., Trans. Amer. Inst. Chem. Engrs. 39, 277 (1943)
14. Varier C.B.S. and Rao K.R., Trans. Ind. Inst. Chem. Engr. 13, 29 (1961)
15. White R.E. and Othmer D.F., Trans. Amer. Inst. Chem. Engr. 38, 1067 (1942)
16. Shulman H.L., Ullrich C.F., Wells N. and Proulx A.X., AIChE J. 1, 259 (1955)
17. Yoshida F. and Koyanagi T., AIChE J., 8, 309 (1962)
18. Warner N.A., Chem. Eng. Sci., 11, 161 (1959)
19. Matsuura A., Akehata T. and Shirai T., Kagaku Kogaku Ronbunshu, 5, 167 (1979)
20. Muroyama K., Hishimoto K. and Tomita T. Kaya, Kogaku Kagaku Ronbunshu, 3, 612 (1977)
21. Lockhart R.W. and Martinelli R.C., Chem. Eng. Progr. 45, 39 (1949)

22. Larkins R.P., White R.R. and Jeffrey D.W., *AIChE J.* 7, 231 (1961)
23. Charpentier J.C. and Favier M., *AIChE J.* 21, 1213 (1975)
24. Bakos M. and Charpentier J.C., *Chem. Eng. Sci.* 25, 1822 (1970)
25. Davidson J.F., *Trans. Inst. Chem. Engrs.* 37, 131 (1959)
26. Otake T. and Okada K., *Kagaku Kogaku (Chem. Eng. Jap.)*, 17, 176 (1953)
27. Gaston-Bonhomme J., Chevalier J.L. and Cunin G., *Chem. Eng. Sci.*, 35, 1163 (1980)
28. Andrieu J., *Chem. Eng. Sci.* 30, 217 (1975)
29. Linek V., Stoy V., Machon V. and Krivsky Z., *Chem. Eng. Sci.* 29, 1955 (1974)
30. Patwardhan V.S. and Pataskar S.G., *Chem. Eng. JI.* 23, 145 (1982)
31. Hewitt G.F., Academic Press N.Y. 1978, 116-128
32. Jones O.C. and Zuber N., *Inter. J. Multiphase Flow*, 2, 273 (1975)
33. Rothfield L.B. and Ralph J.L., *AIChE J.*, 9, 852 (1963)
34. Colombo A., Baldi G. and Sicardi S., *Chem. Eng. Sci.*, 31, 1101 (1976)
35. Van Swaaij W.P.M., Charpentier J.C. and Villèrmaux J., *Chem. Eng. Sci.*, 24, 1083 (1969)
36. Schwartz J.G., Weger E. and Duducovic M.P., *AIChE J.* 22, 894, (1976)
37. Gilbe H., *Chem. Eng. Sci.*, 23, 1401 (1968)
38. Schiesser W.E. and Lapidus, *AIChE J.* 7, 163 (1961)
39. Stephenson J.L., *Bull. Math. Biophysics*, 22, 1 (1960)
40. Patwardhan V.S. and Shrotri V.R., Paper presented at the 34th Annual Session of the IChE, held in Madras, India (1981)
41. Ross L.D., *Chem. Eng. Progr.* 61, 77 (1965)
42. Mohunta D.M. and Laddha G.S., *Chem. Eng. Sci.*, 20, 1069 (1965)
43. Specchia V. and Baldi G., *Chem. Eng. Sci.*, 32, 515 (1977)
44. Buchanan J.E., *Ind. Eng. Chem. Fund.* 6, 400 (1967)

Table 2.1: Some previous studies on dynamic hold-up in packed columns

Investigators	Packing type	Reynolds No. range	Liquid phase	Correlation
1. Otake & Okada (26)	0.65 to 2.2 cm spheres, 1.27, 2.54 cm Raschig rings and Berl saddles	10-2000	Water	$h_D = 1.29(Re)^{0.675} (Ga)^{-0.44} (ad_p)$
2. Gilbe (37)	Raschig rings, Lessing rings	10 ⁻³ - 100	Water, glycerol and alcohols	$h_D = 1.59(dt/dp)^{-5/9} (We/Fr)^{-1/7} (Ga) Re^n$
3. Buchannan (44)	Raschig rings	10-1000 0.5-1	Water, petro- wet solutions	$Re < 1, n = 1/3$ $Re > 1, n = 5/11$ $h_D = 2.2 Fi^{1/3} + 1.8 Fr^{1/2}$
4. Specchia and Baldi (43)	Raschig rings, Berl and Intalox saddles, glass cylinders, non-uniform particles, carbon heads and cylinder	0.3-300	Water, sucrose solutions, glycerol solutions, alcohols	$h_D = 3.86(Re)^{0.545} (Ga)^{-0.42} \left(\frac{ad_p}{\epsilon}\right)^{0.65}$
5. Mohunta & Laddha (42)	Raschig and Lessing rings, spheres	10-100	Water, aqueous solution of CMC	$h_D = 16.13 \left(\frac{\mu V^3 N}{g^2}\right)^{1/4} (N d_p^3)^{-1/2}$
6. Andrieu (28)	Silicon coated non-wettable rings	10-100	Water	$h_D = 0.765 (Re)^{2/3} (Ga)^{-1/3}$

Table 2.2: Range of parameters investigated

Parameter		Range
Liquid viscosity	μ	1-14 cP
Surface tension	σ	20-72 dynes/cm
Liquid flow rate	Q	40-1400 cc/min

Table 2.3: Comparison of static hold-up for non-wettable packings

	This work			Andrieu (28)	Gaston et al. (27)
	0.635 cm RR	1.27 cm RR	1.27 cm Pall rings	1.27 cm RR	1.27 cm RR
h_s	6.1	5.68	5.92	2.3	5.81
%					

Table 2.4 : Statistical analysis of experimental data using Eq. (2.3)

Packing material	Wettable			Non-wettable		
	P.R.	R.R.	partition rings	P.R.	R.R.	Pall rings
Packing size & type	0.635 cm	0.938 cm	1.27 cm	0.635 cm	1.27 cm	1.27 cm
k_1	3.031	7.57	9.81	1.87	3.06	2.05
α_1	0.655	0.65	0.84	0.726	0.623	0.649
β_1	-0.360	-0.486	-0.49	-0.359	-0.376	-0.36
Multiple correlation coefficient						
	0.878	0.912	0.894	0.906	0.757	0.612
Sum of squares	Total corr.					
	9.531	17.12	16.2	13.29	10.25	17.3
Degree of freedom	Req.					
	8.37	15.6	14.4	12.05	8.15	14.33
Mean square	Res.					
	1.16	1.49	1.72	1.25	2.09	2.79
F0.99(2,df res)	Req.					
	2.00	2.00	2.00	2.00	2.00	2.00
F0.99(2,df res)	Res.					
	57	51	51	53	46	50
Mean square	Req.					
	4.18	7.81	7.24	6.02	4.08	6.14
F0.99(2,df res)	Res.					
	0.02	0.029	0.033	0.024	0.045	0.156
Freq	205.04	267.67	214.67	256.34	89.65	39.36
F0.99(2,df res)	5.00	5.05	5.05	5.03	5.12	5.06

Table 2.5 : Statistical analysis of experimental data using Eq. (2.4)

Packing material	Wettable			Non-wettable			
	0.635 cm R.R.	0.938 cm R.R.	1.27 cm R.R.	0.635 cm R.R.	1.27 cm R.R.	1.27 cm R.R.	
Packing size & type			partition rings			Pall rings	
K_2	2.75	3.01	108.8	1.94	0.053	0.455	1.18
α_2	0.606	0.54	1.58	0.739	-1.12	0.174	0.757
β_2	-0.332	-0.258	-0.929	-0.366	0.661	-0.081	-0.357
γ_2	0.0247	0.213	-0.364	-0.0065	0.876	0.240	-0.046
Multiple correlation coefficient	0.878	0.928	0.903	0.906	0.854	0.614	0.828
Sum of squares	9.53	17.12	16.2	13.29	10.25	20.08	17.3
Req.	8.36	15.88	14.6	12.05	8.753	12.33	14.33
Res.	1.16	1.24	15.5	1.25	1.501	7.743	2.97
Deg. of freedom	3.0	3.0	3.0	3.0	3.0	3.0	3.0
Req.	56	50	50	52	45	49	40
Res.	2.79	5.29	4.88	4.02	2.918	4.11	4.77
Mean square	0.021	0.024	0.0312	0.024	0.033	0.158	0.074
Marginal s.s. due to Me	0.013	0.22	0.14	0.00	0.59	0.05	0.00
Marginal F value due to Me	0.63	8.87	4.49	-	17.73	0.316	-
$F_{0.99}(1,df_{res})$	7.11	7.17	7.17	-	7.24	7.18	-

Table 2.6 : Statistical analysis of experimental data using Eq. (2.5)

Packing material	Wettable			Non-wettable			
	0.635 cm R.R.	1.27 cm R.P.	1.27 cm Partition rings	0.635 cm R.R.	1.27 cm R.R.	1.27 cm Pall rings	
K_3	1.95	6.12	2.55	2.00	1.07	1.01	1.43
α_3	0.327	0.479	0.398	0.364	0.294	0.315	0.336
Multiple correlation coefficient							
Sum of square	9.53	17.12	16.2	13.29	10.25	20.08	17.3
Req.	8.19	15.6	13.98	12.05	7.649	12.08	14.19
Res.	1.34	1.515	2.21	1.249	2.605	8.018	8.11
Degree of freedom							
Req.	1	1	1	1	1	1	1
Res.	58	52	52	54	47	51	42
Mean square							
Req.	8.195	15.6	13.98	12.05	7.649	12.06	14.19
Res.	0.023	0.029	0.0427	0.0231	0.055	0.157	0.074
Freq	356.3	536.08	327.4	523.9	523.9	76.71	191.76
F _{0.99(1,df_{res})}							
	7.10	7.15	7.15	7.13	7.21	7.16	7.28

TABLE 2.7

EXPERIMENTAL DATA FOR
WETTABLE PACKINGS

No.	Liquid flow rate (c.c./min)	Viscosity (centi poise)	Surface tension (-dynes/cm)	Liquid hold-up c.c.
1	2	3	4	5

PACKING TYPE - 0.635 C.M. WETTABLE RASCHIG RINGS

1.	1110	1	72	404
2.	750	1	72	320
3.	690	1	72	263.6
4.	850	1	72	334
5.	915	1	72	362.6
6.	710	1	72	300
7.	600	1	72	272
8.	385	1	72	206.4
9.	360	1	72	190.4
10.	210	1	72	161.6
11.	375	1	72	230
12.	145	1	72	122.4
13.	435	1	72	221
14.	890	3.25	39	387.2
15.	700	3.25	39	324
16.	350	3.25	39	114
17.	480	3.25	39	248
18.	650	3.25	39	298
19.	215	3.25	39	183.6
20.	300	3.25	39	188.6
21.	170	3.25	39	68.8
22.	900	4.8	35	392
23.	675	4.8	35	311
24.	600	4.8	35	296
25.	375	4.8	35	215
26.	500	4.8	35	240
27.	280	4.8	35	184
28.	225	4.8	35	185
29.	850	4.8	35	368

.....

1	2	3	4	5
30.	1075	9	26	562
31.	700	9	26	380
32.	560	9	26	318.4
33.	375	9	26	260
34.	175	9	26	198
35.	405	9	26	251.6
36.	940	9	26	448
37.	1000	1	30	400
38.	935	1	30	371
39.	740	1	30	315
40.	640	1	30	280
41.	490	1	30	234
42.	275	1	30	169
43.	300	1	30	188
44.	420	1	30	212
45.	150	1	30	116
46.	950	1	45	378
47.	800	1	45	344
48.	610	1	45	265
49.	450	1	45	230
50.	180	1	45	132
51.	300	1	45	182
52.	440	1	45	224
53.	1150	1	55	466
54.	750	1	55	320
55.	940	1	55	411
56.	575	1	55	282
57.	400	1	55	216
58.	180	1	55	133
59.	300	1	55	188
60.	800	1	55	376

.....

1	2	3	4	5
---	---	---	---	---

PACKING TYPE - 0.938 C.M. WETTABLE RASCHIG RINGS

61.	1480	1	72	611
62.	1920	1	72	805
63.	800	1	72	216
64.	1025	1	72	288
65.	680	1	72	178
66.	440	1	72	118
67.	620	1	72	134
68.	220	1	72	66
69.	350	1	72	100
70.	1400	3.5	37	484
71.	1240	3.5	37	356
72.	950	3.5	37	264
73.	760	3.5	37	218
74.	510	3.5	37	133
75.	400	3.5	37	120
76.	280	3.5	37	83
77.	705	3.5	37	180
78.	1300	6	33	428
79.	1250	6	33	410
80.	950	6	33	302
81.	850	6	33	232
82.	720	6	33	204
83.	560	6	33	139
84.	400	6	33	104
85.	300	6	33	92
86.	1240	13.5	25	555
87.	980	13.5	25	352
88.	700	13.5	25	240
89.	800	13.5	25	312
90.	530	13.5	25	193
91.	450	13.5	25	176

.....

1	2	3	4	5
92.	900	1	62	248
93.	675	1	62	176
94.	850	1	62	232
95.	575	1	62	155
96.	355	1	62	109
97.	450	1	62	140
98.	160	1	62	68
99.	925	1	40	256
100.	740	1	40	197
101.	800	1	40	222
102.	580	1	40	192
103.	510	1	40	164
104.	260	1	40	106
105.	360	1	40	118
106.	170	1	40	69
107.	1000	1	25	360
108.	775	1	25	270
109.	740	1	25	256
110.	475	1	25	168
111.	400	1	25	158
112.	240	1	25	99
113.	250	1	25	100
114.	800	1	25	248

PACKING TYPE - 1.27 C.M. WETTABLE RASCHIG RINGS

115.	375	1	72	95
116.	165	1	72	72
117.	310	1	72	65
118.	625	1	72	140
119.	315	1	72	86
120.	475	1	72	116
121.	580	1	72	134
122.	650	1	72	168
123.	655	1	72	170

.....

1	2	3	4	5
	1320			
124.	75000	1	72	200
125.	122000	1	72	277
126.	84050	1	72	229
127.	81020	1	72	219
128.	108070	1	72	240
129.	108000	2.7	38	240
130.	71500	2.7	38	189
131.	74500	2.7	38	198
132.	83000	2.7	38	192
133.	68050	2.7	38	178
134.	60500	2.7	38	154
135.	33000	2.7	38	92
136.	52500	2.7	38	139
137.	22000	2.7	38	66
138.	11500	2.7	38	52
139.	69000	4	35.5	181
140.	86500	4	35.5	220
141.	43500	4	35.5	125
142.	25000	4	35.5	80
143.	12000	4	35.5	44
144.	130000	4	35.5	324
145.	87500	7.5	29	223
146.	55500	7.5	29	138
147.	43500	7.5	29	104
148.	29500	7.5	29	101
149.	10000	7.5	29	52
150.	125000	1	56	260
151.	95000	1	56	188
152.	80000	1	56	152
153.	65005	1	56	116
154.	45005	1	56	68
155.	27000	1	56	38

.....

1	2	3	4	5
156.	1320	1	50	277
157.	1000	1	50	200
158.	800	1	50	152
159.	650	1	50	116
160.	520	1	50	105
161.	270	1	50	46
162.	1400	1	46	296
163.	1100	1	46	268
164.	800	1	46	184
165.	660	1	46	145
166.	425	1	46	96
167.	225	1	46	50
168.	950	1	46	188

PACKING TYPE - 1.27 C.M. WETTABLE PARTITION RASCHIG RINGS

169.	1075	1	72	261
170.	1200	1	72	248
171.	690	1	72	153
172.	725	1	72	134
173.	835	1	72	227
174.	635	1	72	138
175.	225	1	72	77
176.	555	1	72	182
177.	210	1	72	94
178.	455	1	72	160
179.	160	1	72	75
180.	740	2.5	40	196
181.	740	2.5	40	324
182.	600	2.5	40	164
183.	500	2.5	40	140
184.	295	2.5	40	101
185.	175	2.5	40	79
186.	950	2.5	40	226

.....

1	2	3	4	5
187.	930	4.5	34	220
188.	660	4.5	34	171
189.	840	4.5	34	228
190.	450	4.5	34	122
191.	300	4.5	34	80
192.	220	4.5	34	66
193.	880	4.5	34	206
194.	1550	4.5	34	270
195.	900	7.2	29	248
196.	600	7.2	29	152
197.	660	7.2	29	171
198.	550	7.2	29	140
199.	400	7.2	29	136
200.	250	7.2	29	80
201.	150	7.2	29	56
202.	1100	7.2	29	268
203.	1800	1	60	464
204.	1100	1	60	312
205.	1300	1	60	324
206.	800	1	60	152
207.	890	1	60	174
208.	590	1	60	137
209.	750	1	60	170
210.	360	1	60	104
211.	1050	1	32	296
212.	1700	1	32	436
213.	800	1	32	200
214.	620	1	32	134
215.	420	1	32	111
216.	600	1	32	128
217.	200	1	32	80

.....

1	2	3	4	5
218.	1000	1	24	200
219.	1600	1	24	344
220.	800	1	24	168
221.	700	1	24	156
222.	530	1	24	172
223.	360	1	24	147
224.	175	1	24	65

TABLE 2.8

EXPERIMENTAL DATA FOR
NON-WETTABLE PACKINGS

No.	Liquid flow rate (c.c./min)	Viscosity (centi poise)	Surface tension (-dynes/ cm)	Liquid holdup (c.c.)
1	2	3	4	5

PACKING TYPE - 0.635 C.M. NON-WETTABLE RASCHIG RINGS

1.	150	1	72	61.0
2.	210	1	72	61.9
3.	370	1	72	120.6
4.	580	1	72	131.6
5.	960	1	72	195.6
6.	1000	1	72	200
7.	1200	1	72	230.1
8.	1320	1	72	290.6
9.	90	4.4	36	60.1
10.	160	4.4	36	69.6
11.	140	4.4	36	114.4
12.	300	4.4	36	153
13.	400	4.4	36	151
14.	600	4.4	36	202
15.	1280	4.4	36	336.4
16.	260	1	65	146.4
17.	350	1	65	165.5
18.	360	1	65	178
19.	380	1	65	170
20.	450	1	65	196
21.	570	1	65	253.6
22.	640	1	65	256.6
23.	740	1	65	261
24.	870	1	65	228.3
25.	990	1	65	281.7
26.	270	1	48	150.1
27.	300	1	48	154
28.	390	1	48	186.7
29.	585	1	48	225.7

.....

1	2	3	4	5
30.	705	1	48	266.1
31.	765	1	48	276
32.	870	1	48	295.6
33.	685	1	48	290.1
34.	115	2.86	38	73.9
35.	250	2.86	38	135
36.	280	2.86	38	137.4
37.	370	2.86	38	182
38.	460	2.86	38	177.4
39.	600	2.86	38	195
40.	1000	2.86	38	310
41.	1280	2.86	38	352
42.	140	7.48	29	120.6
43.	260	7.48	29	185.6
44.	300	7.48	29	251
45.	405	7.48	29	226.5
46.	540	7.48	29	255.8
47.	705	7.48	29	287.3
48.	800	7.48	29	313
49.	820	7.48	29	334

PACKING TYPE - 1.27 C.M. NON-WETTABLE RASCHIG RINGS

50.	150	9.12	26	107
51.	170	9.12	26	56.6
52.	220	9.12	26	114.4
53.	340	9.12	26	121.2
54.	390	9.12	26	115.4
55.	540	9.12	26	158.6
56.	560	9.12	26	148.6
57.	570	9.12	26	146
58.	120	5.06	34.5	71
59.	150	5.06	34.5	74
60.	190	5.06	34.5	87.1
61.	345	5.06	34.5	109.6

.....

1	2	3	4	5
62.	450	5.06	34.5	121.5
63.	540	5.06	34.5	142.
64.	600	5.06	34.5	157
65.	780	5.06	34.5	170
66.	160	1	72	40.6
67.	270	1	72	66.8
68.	510	1	72	102.5
69.	640	1	72	122.2
70.	690	1	72	119.9
71.	740	1	72	137.8
72.	880	1	72	151.0
73.	1080	1	72	180
74.	1215	1	72	217.6
75.	1315	1	72	230.3
76.	45.2	1.85	45	18.32
77.	134	1.85	45	24.95
78.	252	1.85	45	22.58
79.	300	1.85	45	25.8
80.	390	1.85	45	49.26
81.	492	1.85	45	49.78
82.	660	1.85	45	90.16
83.	672	1.85	45	91.12
84.	50	1	65	40
85.	180	1	65	91.6
86.	270	1	65	88
87.	450	1	65	124
88.	500	1	65	120
89.	600	1	65	148
90.	700	1	65	162
91.	760	1	65	208
92.	780	1	65	198.4
93.	960	1	65	190.2
94.	120	1	48	76
95.	210	1	48	93.4
96.	320	1	48	101.6
97.	390	1	48	112.6

.....

1	2	3	4	5
98.	620	1	48	153.6
99.	640	1	48	159.2
100.	700	1	48	218
101.	840	1	48	238.8
102.	1000	1	48	260

PACKING TYPE - 1.27 C.M. NON-WETTABLE PALL RINGS

103.	147.5	1	72	76.2
104.	250	1	72	90
105.	315	1	72	108.6
106.	410	1	72	158.6
107.	690	1	72	231
108.	892	1	72	258.3
109.	1340	1	72	389.6
110.	1710	1	72	415.6
111.	1730	1	72	422.9
112.	68	4	35.7	24.64
113.	147	4	35.7	66.14
114.	178	4	35.7	71.12
115.	244	4	35.7	82.36
116.	328	4	35.7	99.64
117.	546	4	35.7	155.18
118.	606	4	35.7	181.04
119.	702	4	35.7	171.56
120.	192	7.12	28.6	63.32
121.	368	7.12	28.6	80.6
122.	480	7.12	28.6	85.4
123.	704	7.12	28.6	158.04
124.	976	7.12	28.6	179.9

.....

1	2	3	4	5
125.	60	8.9	25.9	29.
126.	356	8.9	25.9	96.04
127.	440	8.9	25.9	133.4
128.	540	8.9	25.9	142.4
129.	560	8.9	25.9	165.4
130.	630	8.9	25.9	176.6
131.	752	8.9	25.9	155.48
132.	100	1	48	68
133.	240	1	48	114.4
134.	360	1	48	109.6
135.	600	1	48	148
136.	620	1	48	178.4
137.	700	1	48	197
138.	1020	1	48	189.4
139.	40	1	65	29.6
140.	180	1	65	109.6
141.	220	1	65	59.2
142.	320	1	65	69.6
143.	420	1	65	55.6
144.	580	1	65	107.6
145.	840	1	65	121.2
146.	1060	1	65	150.8

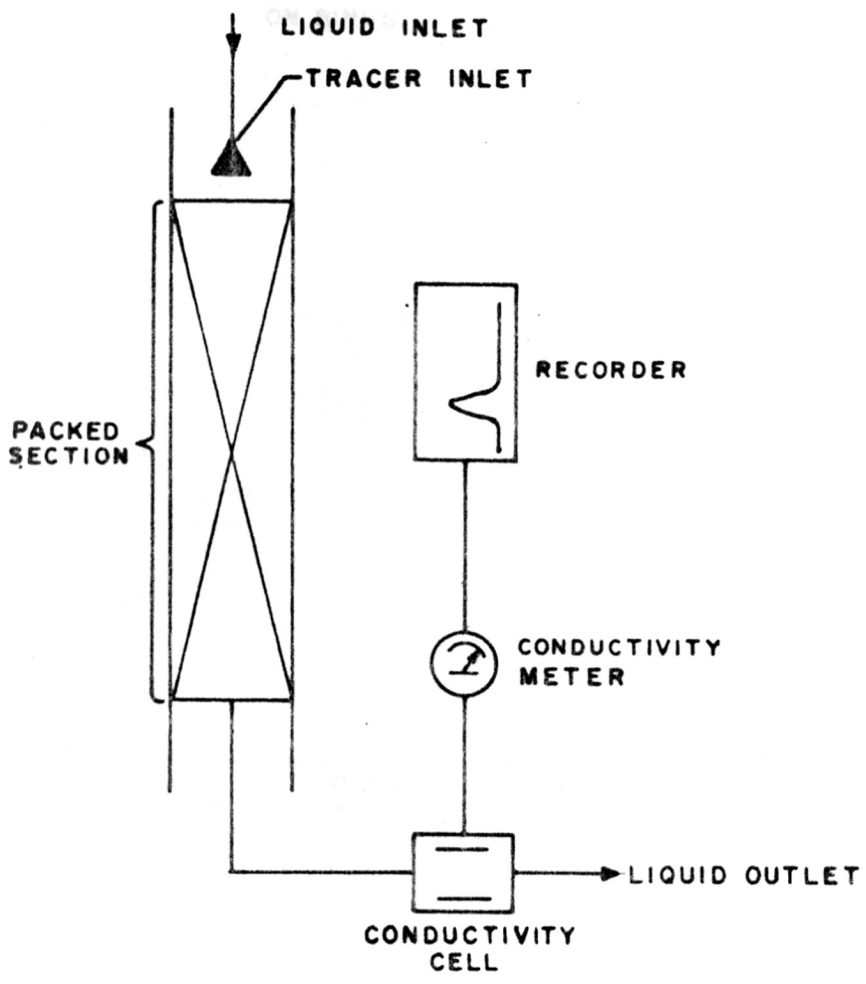


FIG.2-1:SCHEMATIC REPRESENTATION OF EXPERIMENTAL SET UP.

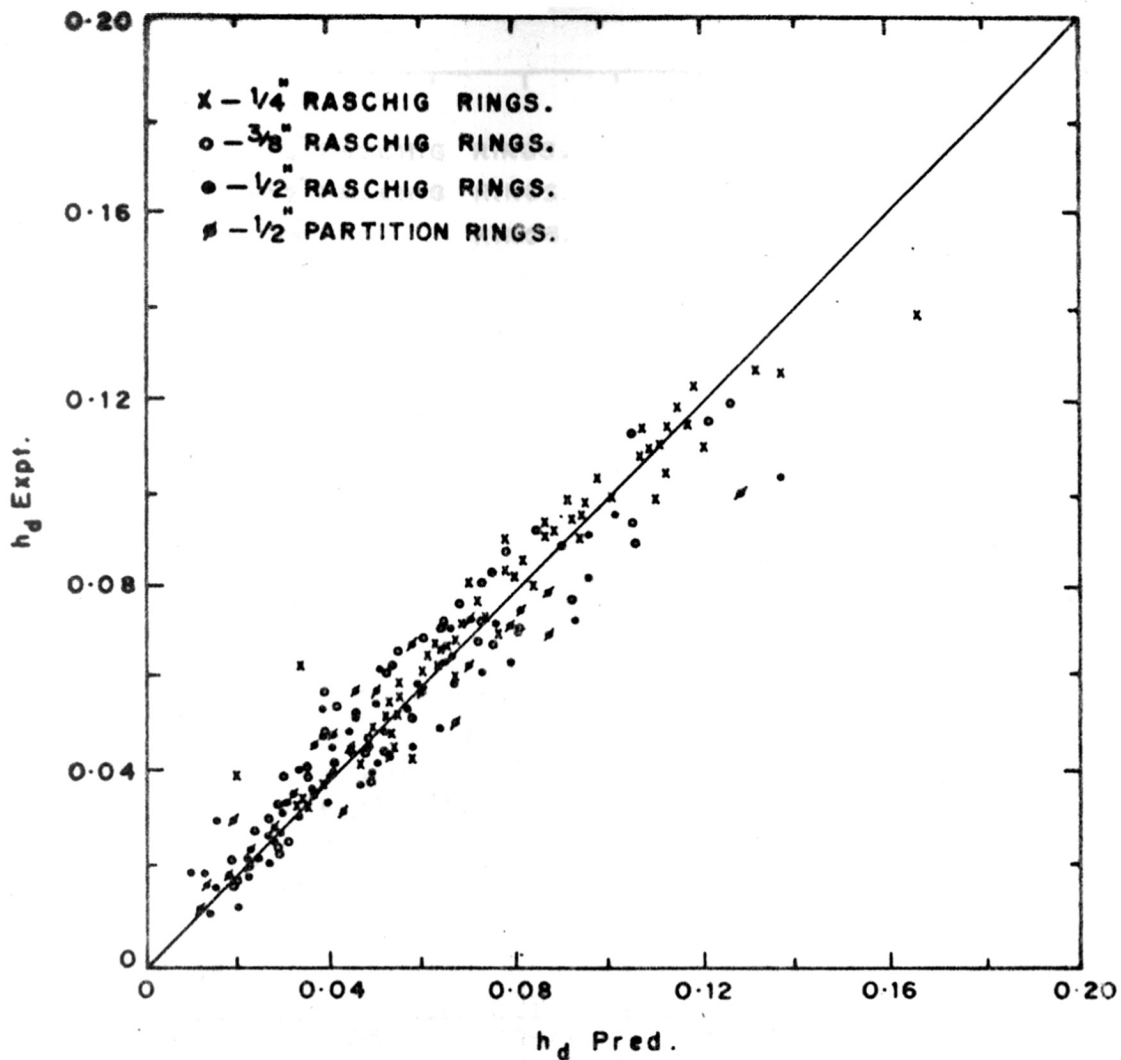


FIG.2-2: EXPERIMENTAL AND PREDICTED [Eqn.(2-3)] VALUES OF h_d FOR WETTABLE PACKINGS.

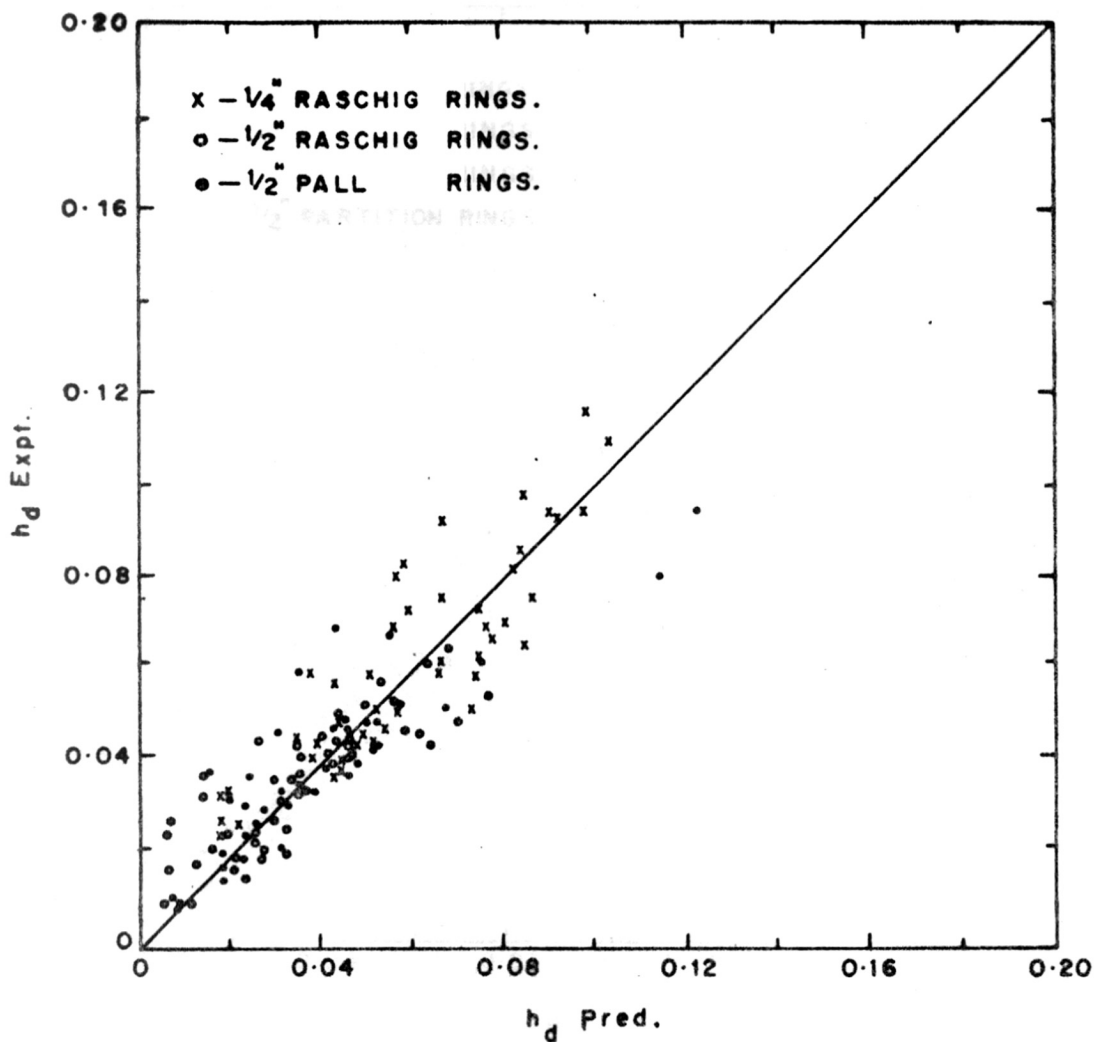


FIG.2.3: EXPERIMENTAL AND PREDICTED [Eqn.(2.3)] VALUES OF h_d FOR NON-WETTABLE PACKINGS.

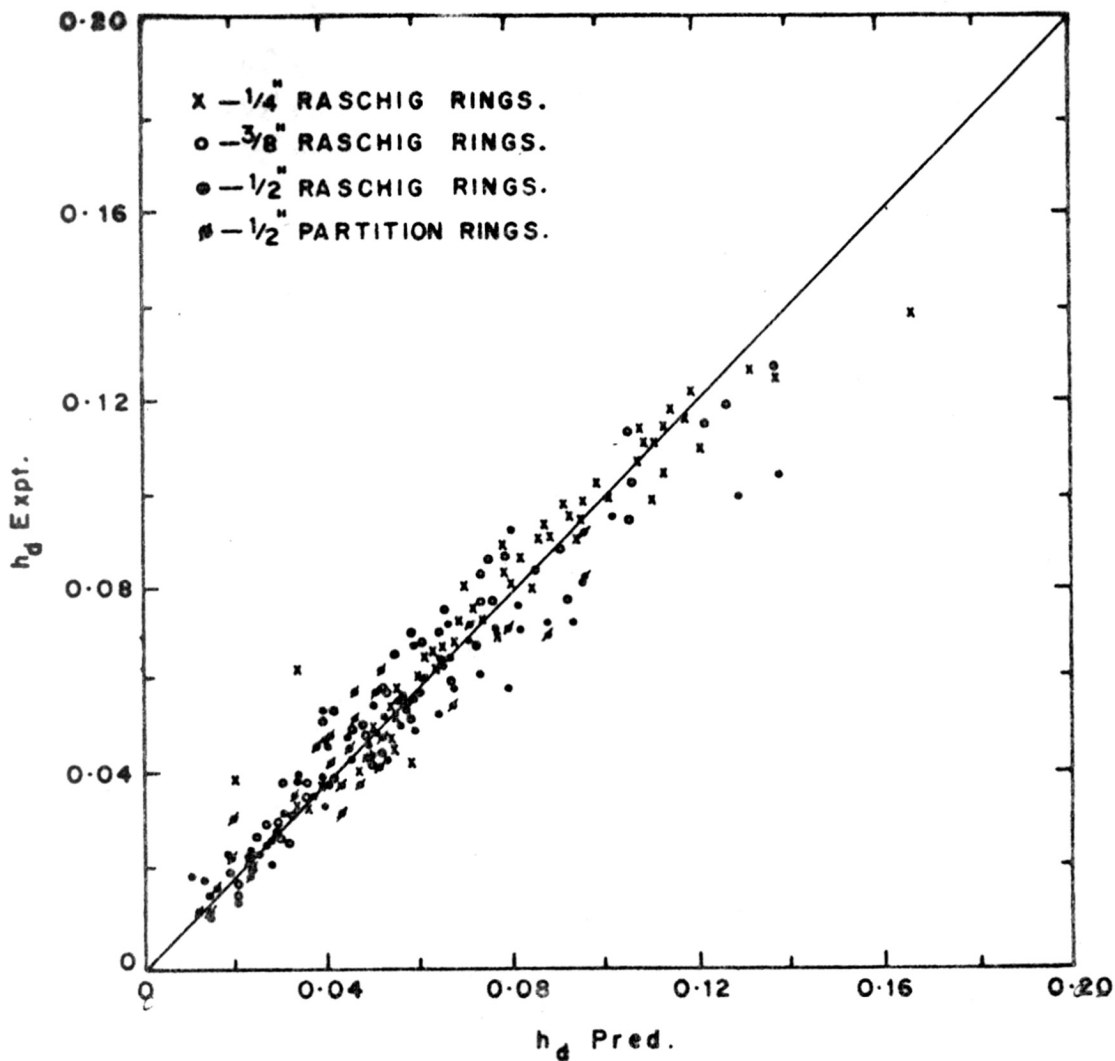


FIG.2-4: EXPERIMENTAL AND PREDICTED [Eqn.(2-4)] VALUES OF h_d FOR WETTABLE PACKINGS.

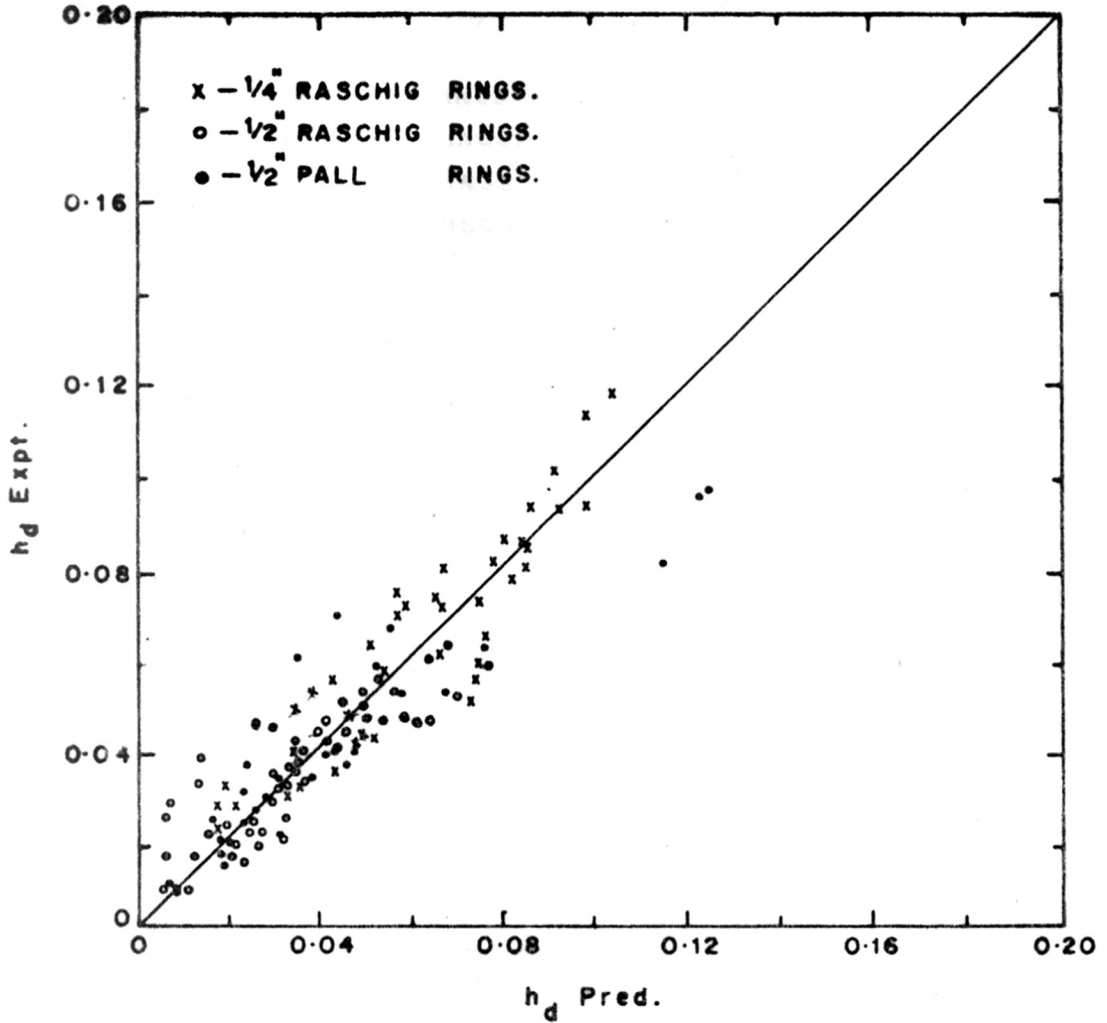


FIG.2-5: EXPERIMENTAL AND PREDICTED [Eqn.(2-4)] VALUES OF h_d FOR NON-WETTABLE PACKINGS.

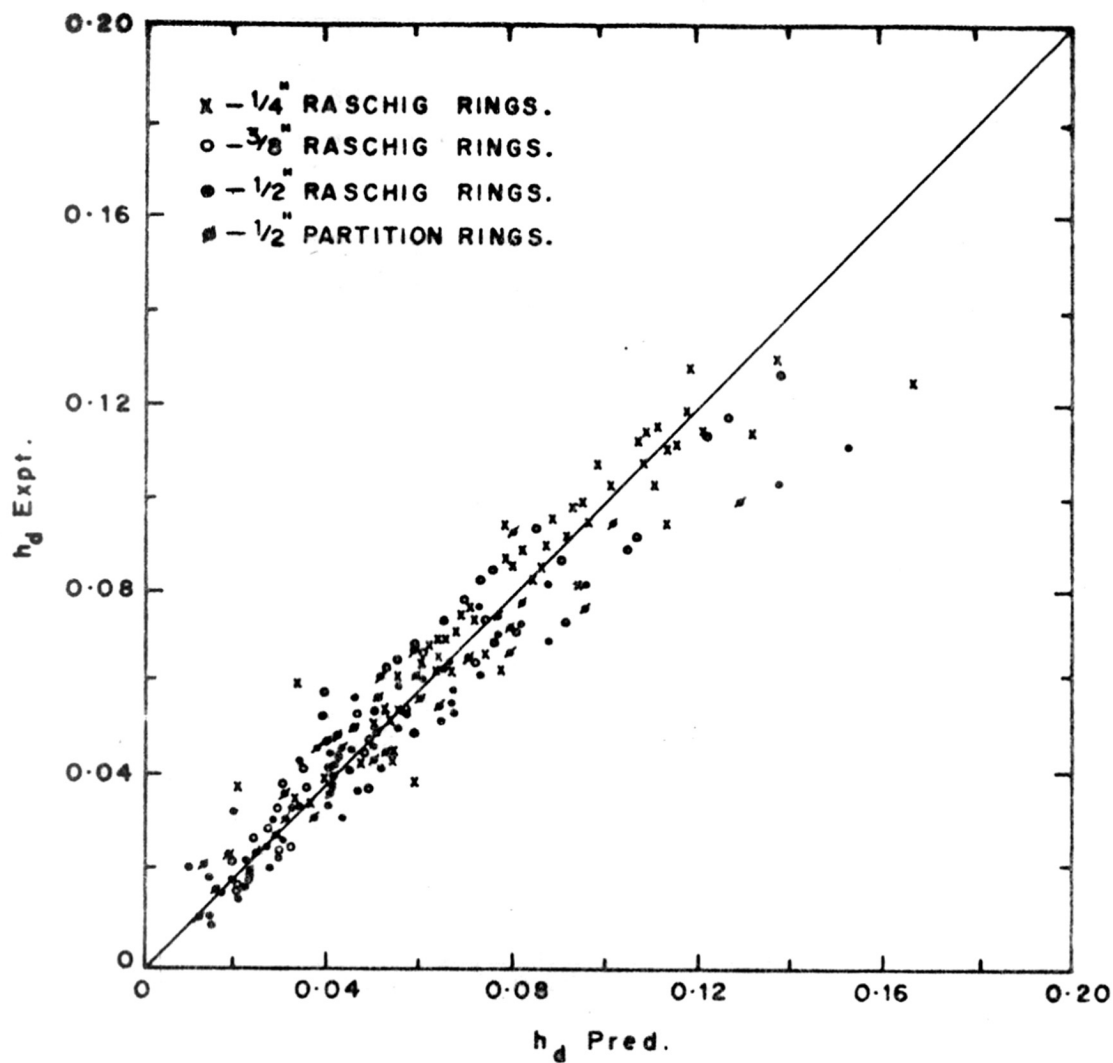
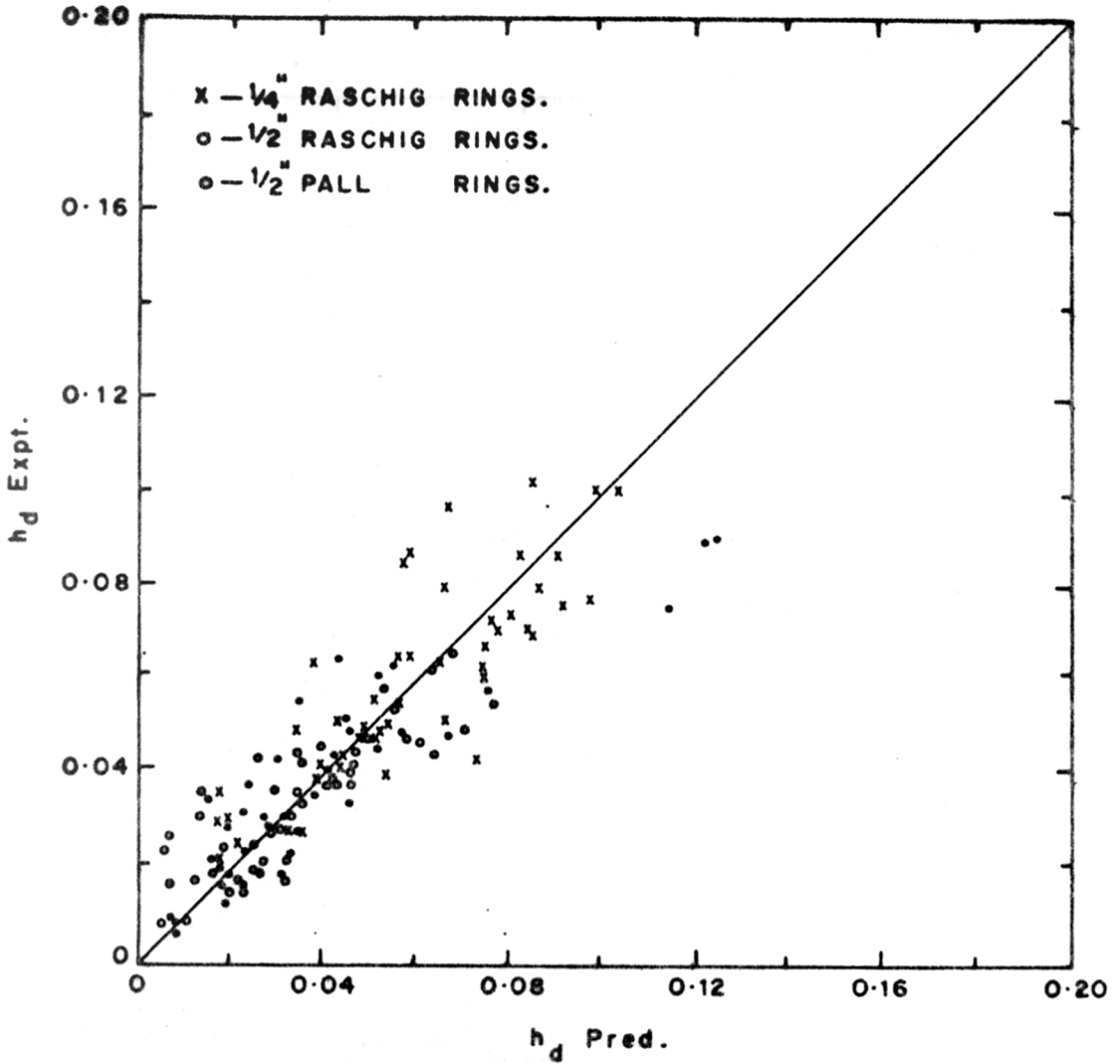


FIG.2.6: EXPERIMENTAL AND PREDICTED [Eqn.(2.5)] VALUES OF h_d FOR WETTABLE PACKINGS.



SUPERFICIAL

FIG.2-7: EXPERIMENTAL AND PREDICTED [Eqn.(2.5)] VALUES OF h_d FOR NON-WETTABLE PACKINGS.

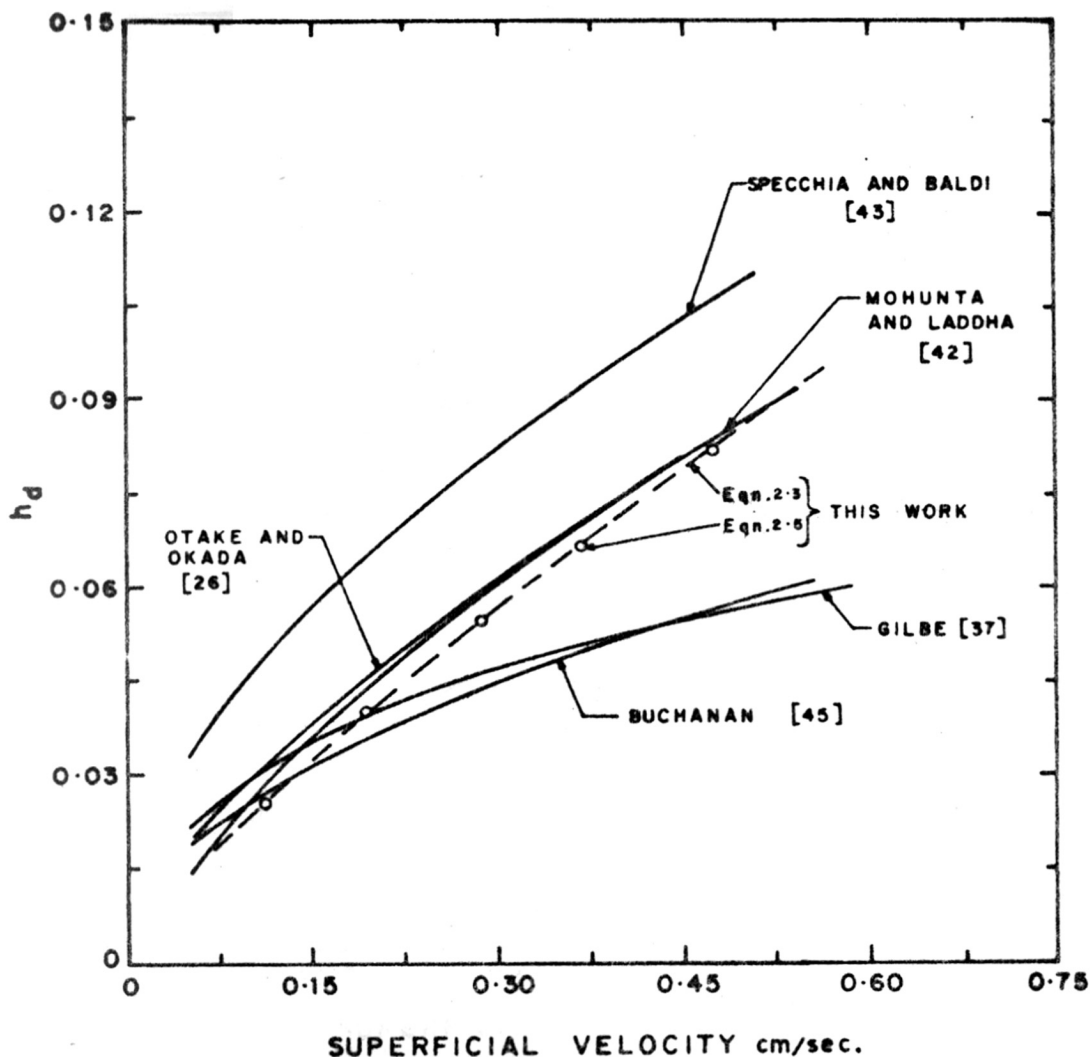


FIG.2-8:COMPARISON OF CORRELATIONS FOR DYNAMIC HOLD-UP IN WETTABLE PACKINGS.

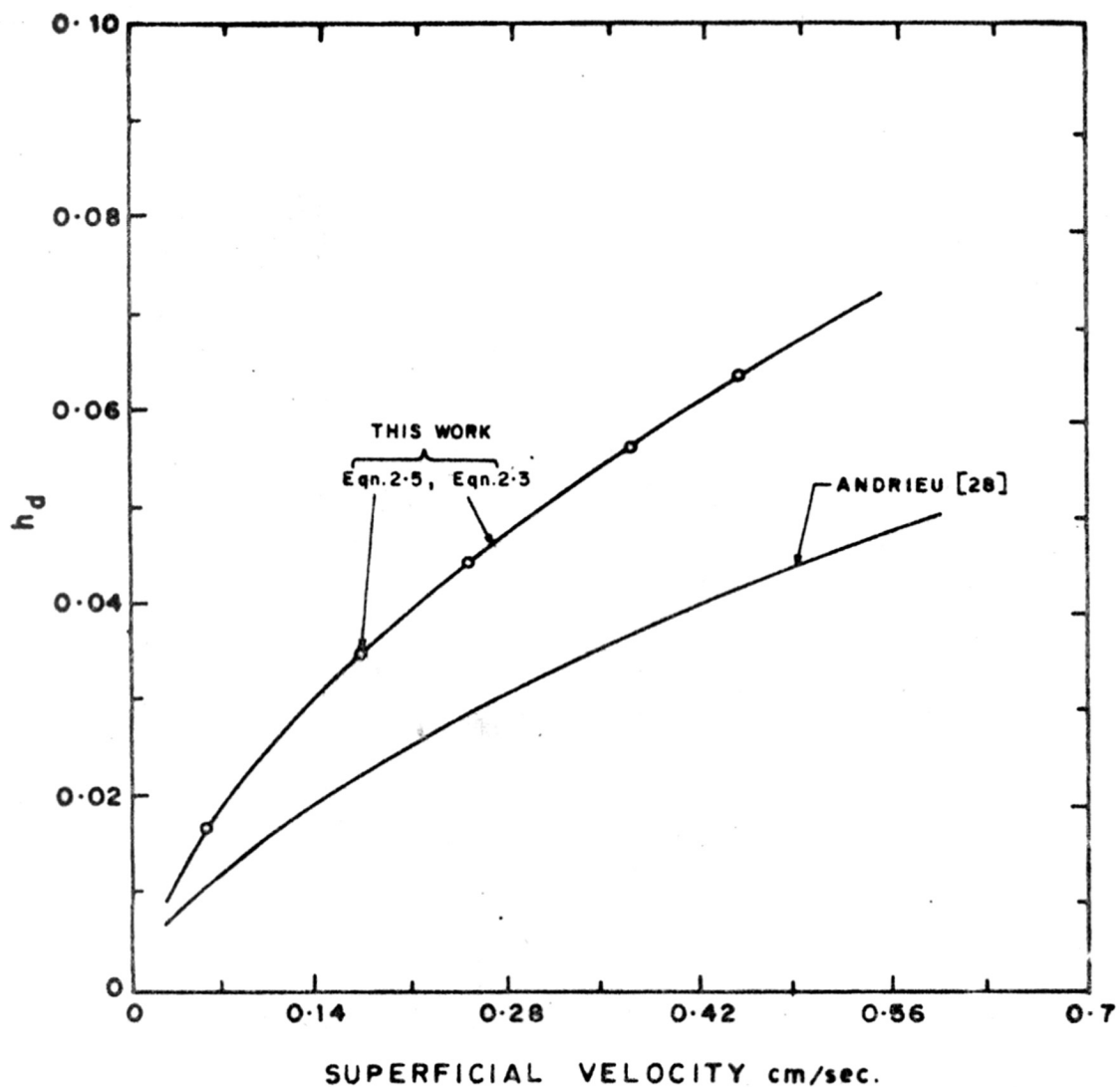
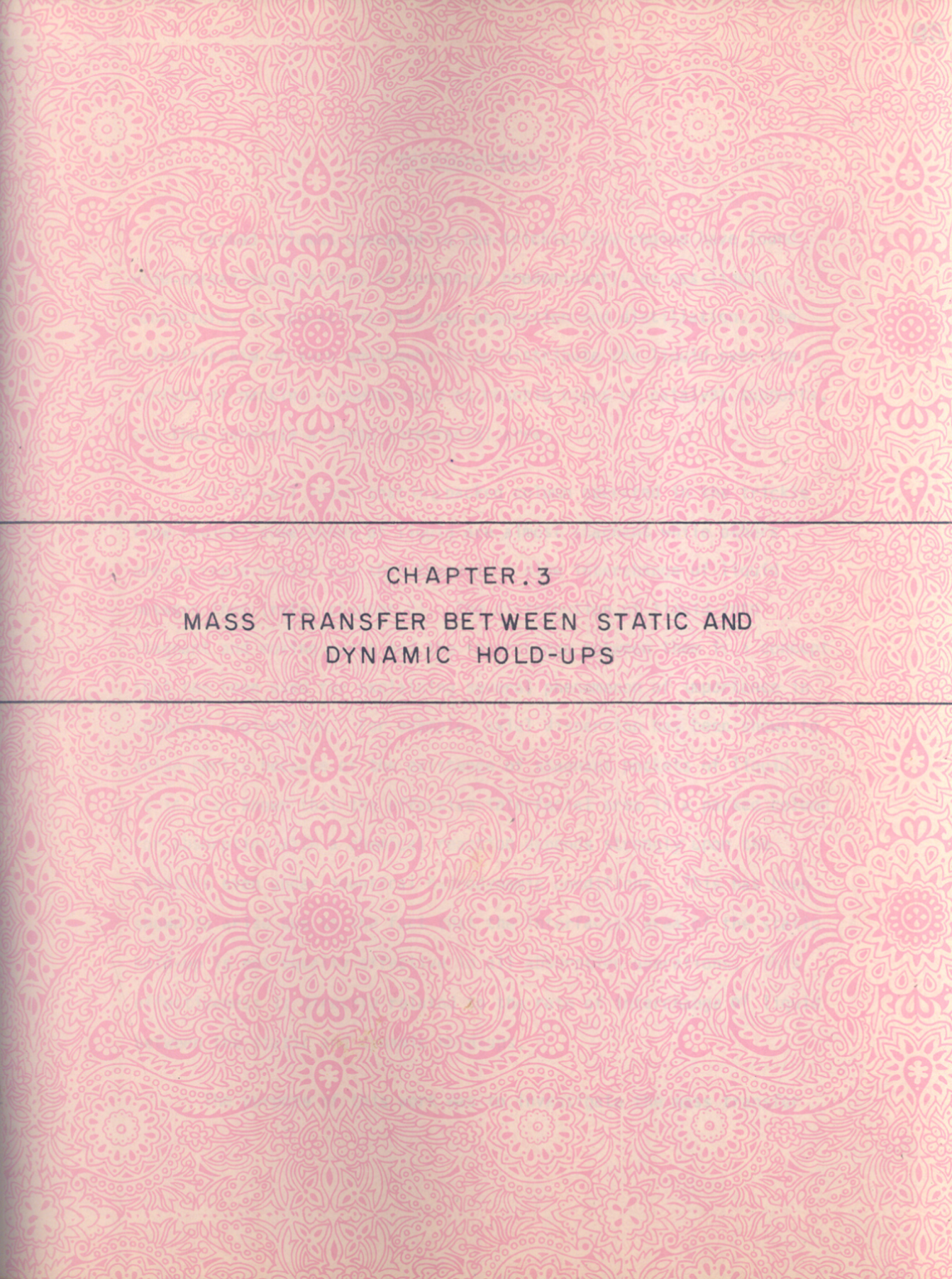


FIG.2-9: COMPARISON OF CORRELATIONS FOR DYNAMIC HOLD-UP IN NON-WETTABLE PACKINGS.



CHAPTER.3
MASS TRANSFER BETWEEN STATIC AND
DYNAMIC HOLD-UPS

3.1 INTRODUCTION

Packed columns operated in the trickle flow regime have found wide-spread applications in industry, predominantly as gas-liquid contactors, in operations like gas absorption and distillation. The principle aim of such equipment is to distribute the liquid over the surface of packing elements such as raschig rings or catalyst supports, and thus generate a large interfacial area.

It is well known that in a packed column operated in the trickle flow regime, some zones of liquid are almost stagnant while others are in rapid motion and that there is a slow interchange of liquid between them (refer chapter 2). The distribution of liquid into stagnant and moving parts and the interchange between them is a concept that has been used for explaining several phenomenon of importance in chemical engineering. For example, axial dispersion has been shown to arise partly because of the existence of stagnant pockets of liquid. It is also known that the effective interfacial area in a packed column for absorption with a chemical reaction depends strongly upon the kinetics even under identical hydrodynamic conditions. This has been shown to arise due to the fact that the interfacial area of the static hold-up is not equally effective in all absorption operations. This effectiveness is directly related to the rate of interchange of liquid between the static and dynamic hold-ups.

The purpose of this work was to investigate the mass transfer

coefficient between the static and dynamic hold-up in packed columns operated in the trickle flow regime, and to develop predictive correlations for the same. Several relevant factors like the liquid viscosity, surface tension, liquid flow rate, and the size and type of the packings were investigated. In addition, packings of two different materials i.e. ceramic and polypropylene, were used. Thus, the effect of wettability of the packing material on the liquid interchange rate was also studied. This study led to predictive correlations based on dimensionless groups.

3.2 PREVIOUS WORK

It is well known that the total liquid hold-up in a packed column can be split into two parts, i.e. the dynamic hold-up consisting of rapidly moving liquid and the static hold-up consisting of semistagnant zones of liquid. It is also known [1] that there is a slow interchange of liquid between the dynamic and the static hold-up. This interchange of liquid has been investigated by many workers who were mainly interested in the axial dispersion of liquid in the packed column. Earlier attempts to characterise axial dispersion in terms of an axial dispersion coefficient alone indicate that the tail of the tracer response curves (obtained with a pulse input) is not predicted well. The significant tailing of these response curves is due mainly to interchange between stagnant and dynamic zones. This was recognised by later workers like Hochman and Effron [2], Hoogendorn and Lipps [3], Schwartz and Roberts [4], who incorporated this exchange into their models and used the moment method

to evaluate model parameters. They, however, did not incorporate any axial dispersion coefficient. Villermaux and Van Swaij [5] proposed a model which incorporated both liquid interchange and an axial dispersion coefficient. They evaluated model parameters from the response curves obtained with a pulse input. This model was later used by others [6-8] for correlating their axial dispersion data. A comparison between the results of all these workers is available (Gianetto et al. [9]) and indicates a very poor agreement between the values of interchange coefficients reported by the earlier workers. They attributed this disagreement to the differences in the procedures adopted by different workers both for experiments and analysis. All these workers (with the exception of Bennett and Goodridge [6], whose work is discussed later) calculated their parameter values from response curves for a pulse tracer input by curve fitting techniques or by nonlinear regression. The tracer response curves used extended upto 1.5 to 3 times the liquid residence time in the column. The response curves in this period are governed mainly by axial dispersion, and only to a lesser extent, by interchange of liquid. Therefore, it would not be surprising if the calculated interchange coefficients had wide confidence limits. The confidence limits, however, have not been reported. More recent models involving a larger number of parameters suffer from the same shortcomings [10,11].

A different procedure was adopted by Bennett and Goodridge [6] who used a step decrease input of tracer rather than a pulse input. They found that the outlet concentration of tracer falls to a low value within

about two residence times and decreases further exponentially. The outlet tracer concentration, after 4-6 residence times, gives a straight line on a semilog plot, whose slope gives the interchange coefficient. It is shown later that this part of the tracer output curve is governed mainly by the liquid interchange and not by axial dispersion coefficient. The accuracy with which the interchange coefficient can be calculated, is thus expected to be higher. Accurate measurement of outlet tracer concentration at such high time is possible only with this procedure involving a step decrease input. A pulse input leads to outlet concentrations too low to be measured, at such high times. Bennett and Goodridge [6] were able to measure output concentration of tracer even after 14 residence times quite accurately.

Further evidence regarding the accuracy of the results of Bennett and Goodridge comes from another direction. It has been known for some time that the effective interfacial area in packed columns used for gas absorption with or without chemical reaction depends strongly upon the chemical kinetics even under comparable hydrodynamic conditions (Shulman et al. [12], Joosten and Danckwerts [13]). A semiquantitative explanation was provided later (Puranik-Vogelpohl [14]) which amounted to saying that the interfacial area of the static hold-up is not equally effective in all gas absorption operations. A more rigorous quantitative explanation was provided by the extended crossflow model proposed later [15]. The central idea behind this model is as follows. The effectiveness of the area of the static hold-up for gas absorption depends upon the concentrations of the gas and liquid components in the static hold-up.

The interchange of liquid and the absorption of gas through the interfacial area of the static hold-up affect these concentrations in opposite directions. It was shown [15] that by estimating the interchange coefficient from the correlation of Bennett and Goodridge [6], the discrepancies in the values of effective interfacial area for gas absorption can be satisfactorily explained by the extended crossflow model.

The correlation mentioned above was obtained using ceramic packings and the air-water system. This study was undertaken to develop a similar correlation which would be valid for wider ranges of parameter values like liquid properties and flow rate. A large number of packings were used which covered different sizes, shapes and also the packing materials. Some of the packings were made of ceramic which is wetted by aqueous solutions, while others were made of polypropylene, which is not wetted by aqueous solutions, but have other desirable properties like being lightweight and corrosion resistant.

3.3 THEORY

The total liquid hold-up in a packed column, h_t , is composed of two parts, i.e. dynamic or operating hold-up h_d , and static hold-up h_s . Interchange of liquid can take place between these two hold-ups. The stagnant liquid is found mostly at the points of contact. Assuming the radial dispersion to be negligible, the axial dispersion equation for a tracer is given by

$$D_L \frac{\partial^2 C}{\partial x^2} - \frac{L}{h_t} \frac{\partial C}{\partial x} - \frac{\partial C}{\partial t} = 0 \quad [3.1]$$

This, however, does not account for the presence of stagnant pockets. It can be modified by writing a mass balance over an incremental length of a packed column as

$$D_L \frac{\partial^2 C}{\partial x^2} - \frac{L}{h_d} \frac{\partial C}{\partial x} - \left[\frac{h_t - h_d}{h_d} \right] \frac{\partial q}{\partial t} - \frac{\partial C}{\partial t} = 0 \quad [3.2]$$

or in a dimensionless form as

$$\frac{1}{P_e} \frac{\partial^2 C}{\partial Z^2} - \frac{\partial C}{\partial Z} - \frac{h_s}{h_d} \frac{\partial q}{\partial \theta} - \frac{\partial C}{\partial \theta} = 0 \quad [3.3]$$

where P_e is axial Peclet number. Now, the mass transfer coefficient between the stagnant and dynamic regions is defined as

$$\frac{\partial q}{\partial t} = k [C - q] \quad [3.4]$$

When a step decrease of tracer is used, the outlet concentration decreases rapidly to a fairly low value and decreases further rather slowly in an exponential manner. A typical sample of these curves is shown in Fig. 3.1. The graph is seen to be divided into two parts. The first portion is due to dispersion taking place in the dynamic hold-up. In

this regime the effect of the static hold-up is very small. In the second region of exponential decrease, the dynamic portion is relatively free of the tracer, and the outlet response is caused by the tracer being transferred out of the static hold-up. In this region, C is very small compared with q , and equation (3.4) simplifies to:

$$\frac{\partial q}{\partial t} = -k q \quad [3.5]$$

In general, q may vary along the column height at any time. Let $q(x, t_0)$ represents the profile of q at any time t_0 . Then equation (3.5) is applicable to any point in the packed bed with the initial condition

$$q = q(x, t_0) \text{ at } t = t_0 \quad [3.6]$$

The total flow of the tracer from the static to dynamic hold-up is given as $A k h_s \int q dx$. The outlet concentration of the tracer thus becomes as

$$C_{out} = (h_s k / L) \int q dx \quad [3.7]$$

The solution of the equation (3.5) gives

$$q(x, t) = q(x, t_0) \exp(-k(t - t_0)) \quad [3.8]$$

If C_0 represents the outlet concentration of tracer at t_0 then equation (3.8) gives

$$C_{out} = [C_0 \exp (k t_0)] \exp (-k t) \quad [3.9]$$

Thus a plot of $\ln C_{out}$ vs. t at large t would give a straight line with a slope of $(-k)$ irrespective of the initial distribution of tracer in the static hold-up along the column height. Even if the initial tracer concentration in the static hold-up is not uniform, k can be evaluated from the slope of the semilog plot. A typical plot of $\log C_{out}$ vs t is given in Fig. 3.2 which shows it to be a reasonably good straight line.

3.4 EXPERIMENTAL

A schematic diagram of the experimental set up is shown in Fig. 3.3. The packed column used was of 7.8 cm I.D. and 67 cm long and was made up of pyrex glass. Two types of packings were employed to evaluate mass transfer coefficient between the static and dynamic hold-up. Four different types of wettable packings were used, i.e. 0.635 cm, 0.937 cm and 1.27 cm raschig rings and 1.27 cm partition rings. The three non-wettable packings used were 0.635 cm and 1.27 cm raschig rings and 1.27 pall rings. The liquid used was distilled water. The surface tension of the distilled water was varied by the addition of Nonyl phenol (< 0.005 wt.%). The viscosity of water was varied by adding the polymeric additive CEPOL (< 1.0 wt.%). Both the additives

were non-ionic and did not change the conductivity of distilled water. The ranges of parameters investigated in this study are shown in Table 3.1. An aqueous solution of NaCl (1N) was used as the tracer. The concentration of sodium chloride was measured by measuring the electrical conductivity, which varied linearly over the concentration range used. Initially, the conductivity meter and chart recorder were calibrated for different concentrations of the tracer solutions.

All the packings were first washed with chromic acid and then with distilled water to ensure that their surface was clean. After packing a column with the desired type of packing, it was flooded with the salt solution and kept for 15 minutes. Then the tracer solution was drained out completely over a period of 15 minutes. This resulted in a column with the entire static hold-up filled with the tracer solution. Flow of liquid with desired properties was then started through the 20-point distributor. This event was marked on the strip chart recorder kept running at the appropriate speed. The liquid level in the tank was maintained constant in order to keep a constant flow rate during the run. The electrical conductivity of the effluent liquid from the column was continuously measured by platinum cell, fixed in a specially made teflon jacket, and connected to the strip chart recorder. The length of the connections of the column to the cell was kept at a minimum. Each run was continued for a minimum of 10 minutes. This allowed sufficient time for the elutriation of most of the tracer from the static hold-up. The procedure was repeated to cover wide ranges of flow rates and liquid properties for the seven different packings mentioned earlier.

For each run, the slope of the straight line obtained on the semilog plot computed by linear regression. The entire experimental data collected for wettable and non-wettable packing is shown in Table 3.2 and Table 3.3 respectively.

3.5 RESULTS AND DISCUSSION

According to the procedure outlined in the earlier section, totally 224 and 154 runs were conducted, for wettable and non-wettable packings respectively, with widely different values of viscosity, surface tension and liquid flow rate. In the earlier study by Bennett and Goodridge [6], the mass transfer coefficient between static and dynamic hold-up was correlated as

$$k d_p = 1.95 \times 10^{-4} \text{Re}^{0.58} \quad [3.10]$$

which was obtained from data for the air-water system. This work was aimed at studying the effect of surface tension and viscosity which were varied over wide ranges. The following equation which incorporates surface tension in the form of Weber number was tried for all the packings to correlate the mass transfer coefficient k ,

$$\frac{k d_p \mu}{\sigma} = k_1 \text{Re}^{\alpha_1} \text{We}^{\beta_1} \quad [3.11]$$

Both the Reynold and Weber numbers are based on the interstitial

velocity, as used by Bennett and Goodridge [6]. It was found that if the Reynolds number is based on the superficial liquid velocity, it results in a poorer fit. The interstitial velocity is equal to the superficial velocity divided by the dynamic hold-up. The dynamic hold-up was calculated by applying our own correlations [Chapter 2]. Since these were developed using the same packings, they are expected to be more accurate for the purpose than similar correlations available in literature.

The analysis of variance for equation (3.11) is given in Table 3.4. The equation uses the dimensionless group $\left[\frac{k d_p \mu}{\sigma} \right]$ for the interchange coefficient. Bennett and Goodridge used a dimensional group as $(k d_p)$. Gianetto et al. [9] have presented the results of Bennett and Goodridge [6] in the form of the dimensionless group $(k d_p / \nu)$. However, it is seen from the work of Gianetto et al. [9] that such a representation leads to different lines for different packing sizes. The present correlation in terms of $(k d_p \mu / \sigma)$ gives a single line for various packings as is obvious from the results of Bennett and Goodridge [6], which cover two packing sizes. Equation (3.11) is transformed into a linear equation by taking logarithms of both sides and the constants, α_1 , β_1 and k_1 are obtained by linear regression analysis of our experimental data. As seen from Table 3.4, the multiple correlation coefficient is quite high, indicating that the regression is highly significant. The powers on Re and We do not vary much with packing type and size, though they seem to depend to some extent on the wettability. The power on Re obtained by Bennett and Goodridge [6] is much

lower than that obtained in this study. However, it must be mentioned here that the present study covers much wider ranges of independent parameters than those used by Bennett and Goodridge [6]. The power on Weber number suggests that surface tension is also important in determining the mass transfer coefficient between the static and dynamic hold-up, and must be incorporated in the correlation as done in equation (3.11). Figures 3.4 and 3.5 indicate the accuracy of predictions of $k_d \mu / \sigma$ from equation (3.11) using α_1 and β_1 from Table 3.4. The predictions are seen to match the experimental values very well over the range of parameters investigated.

It is seen from Table 3.4 that the multiple correlation coefficient for non-wettable packings is similar in magnitude as that for wettable packings. This implies that both types of packings have comparable experimental errors. Also it appears that the same type of correlation is applicable for both cases.

It was also thought worthwhile to try an equation of the following type (which was found to be satisfactory for correlating dynamic hold-ups) for both the kinds of packings separately.

$$\frac{k_d \mu}{\sigma} = k_2 \text{Re}^{\alpha_2} \text{Ga}^{\beta_2} \quad [3.12]$$

This equation has one more group, Ga, which accounts for the gravity factor. Equation (3.12) does not involve the surface tension. This equation, as explained in Chapter 2 was transformed into a linear equation

by taking logarithms of both sides and constants k_2 , α_2 and β_2 were determined by linear regression analysis of the experimental data. The results of analysis are shown in Table 3.5 for both wettable and non-wettable packings. It appears from this table that the multiple correlation coefficients are lower than those in Table 3.4, and the powers on Reynolds and Gallileo numbers are unusually large in magnitude. Therefore, equation (3.12) is not considered to be suitable for correlating the interchange coefficient.

3.6 CONCLUSION

A correlation was developed for the mass transfer coefficient between the stagnant and dynamic zones in a packed column operated in the trickle flow regime. The correlation is given by equation (3.11) with values of constants listed in Table 3.4, and involves only dimensionless group. This form of equation was found to be suitable for different types and sizes of packings, both wettable and non-wettable, over wide ranges of several parameters as shown in Table 3.1. It is seen that surface tension affects the interchange coefficient in a significant manner.

NOTATION

A	cross sectional area of packed column (cm^2)
C	tracer concentration in dynamic hold up (moles/cm^3)
C_{out}	tracer concentration at the column outlet (moles/cm^3)
C_0	C_{out} at t_0 (moles/cm^3)
d_p	packing size (cm)
D_L	axial liquid phase dispersion coefficient (cm^2/s)
h_t	total liquid hold-up dimensionless
h_d	dynamic liquid hold-up dimensionless
h_s	static liquid hold-up dimensionless
H	column height
k	mass transfer coefficient defined by equation (3.4) (s^{-1})
L	superficial liquid velocity (cm/s)
Pe	Peclet number based on length of bed, HV/D_L dimensionless
q	tracer concentration in static hold-up (moles/cm^3)
Re	$V d_p \rho / \mu$ dimensionless
t	time (s)
\bar{t}	residence time, H/V (s)
t_0	arbitrary starting value of t
V	interstitial velocity of liquid in the column (L/h_d) (cm/s)
We	$V^2 d_p \rho / \sigma$ dimensionless
x	axial distance (cm)
Z	x/H

.....

Greek letters

α β γ	constants obtained from equations (3.11) and (3.12)
μ	liquid viscosity (centipoise)
ρ	liquid density (gm/cm^3)
σ	liquid surface tension (dynes/cm)
θ	t / \bar{t}

REFERENCES

1. Shulman H.L., Ullrich C.F. and Wells H., *AICHE JI.* 1, 247 (1955)
 2. Hochman J.M. and Efron E., *I&EC Fundm.* 8, 63 (1969)
 3. Hoogendoorn C.J. and Lipps J., *Can. J. Chem. Eng.* 43, 125 (1965)
 4. Schwartz J.G. and Roberts G.W., *I&EC Proc. Des. Dev.* 12, 262 (1973)
 5. Villermaux J. and Van Swaaij W.P.M., *Chem. Eng. Sci.*, 18, 63 (1969)
 6. Bennett A. and Goodridge F., *Trans. Inst. Chem. Engr.* 48, T 232 (1970)
 7. Matsuura A., Akehata T. and Shiraj T., *J. Chem. Eng. Jap.* 9, 294 (1976)
 8. Stepanek J.B. and Shilimkan R.V., *Trans. Inst. Chem. Eng.* 51, 112 (1973)
 9. Gianetto A., Baldi G., Specchia V. and Sicardi S., *AICHE JI.* 24, 1087 (1978)
 10. Popovic M. and Deckwer W.D., *Chem. Eng. JI.* 11, 67 (1976)
 11. Rao V.G. and Varma Y.B.C., *AICHE JI.* 22, 612 (1976)
 12. Schulman H.L., Mellish W.G. and Lyman W.H., *AICHE JI.* 17, 631 (1971)
 13. Joosten G.E.H. and Dankwerts P.V., *Chem. Eng. Sci.*, 28, 453 (1973)
 14. Puranik S.S. and Vogelwohl A., *Chem. Eng. Sci.* 29, 501 (1974)
 15. Patwardhan V.S., *Can. JI. Chem. Eng.*, 56, 56 (1978)
-

TABLE

CONTENTS

TABLE I

TABLE 3.1RANGES OF PARAMETERS USED

<u>Parameter</u>	<u>Range</u>
Liquid flow rate	0.1 - 1.66 lit/min
Liquid viscosity	1.0 - 14.0 cp
Surface tension	20.0 - 72.0 dynes/ cm

TABLE 3.2
EXPERIMENTAL DATA FOR
WETTABLE PACKINGS

No.	Liquid flow rate (c.c./min)	Viscosity (centi poise)	Surface tension (-dynes/ cm)	Slope
1	2	3	4	5
PACKING TYPE - 1.27 C.M. WETTABLE RASCHIG RINGS				
1.	250	1	72	2.81
2.	310	1	72	2.94
3.	430	1	72	3.21
4.	550	1	72	3.62
5.	720	1	72	4.01
6.	900	1	72	5.15
7.	1010	1	72	5.40
8.	1320	1	72	7.21
9.	240	11.2	21	3.41
10.	300	11.2	21	3.52
11.	410	11.2	21	3.81
12.	600	11.2	21	4.33
13.	930	11.2	21	6.82
14.	1100	11.2	21	7.22
15.	400	14	20	5.1
16.	560	14	20	6.22
17.	720	14	20	6.81
18.	890	14	20	7.38
19.	990	14	20	7.62
20.	1400	14	20	10.13
21.	100	1	47	1.90
22.	230	1	47	2.51
23.	460	1	47	3.11
24.	770	1	47	5.23
25.	880	1	47	6.12
26.	1010	1	47	7.81
27.	1310	1	47	9.27

.....

1	2	3	4	5
28.	150	1	30	2.00
29.	190	1	30	2.15
30.	330	1	30	2.87
31.	420	1	30	3.41
32.	570	1	30	4.28
33.	870	1	30	7.21
34.	1250	1	30	9.28
35.	190	1	20	2.51
36.	220	1	20	2.84
37.	390	1	20	3.29
38.	570	1	20	4.22
39.	850	1	20	6.99
40.	1210	1	20	8.21

PACKING TYPE-0.635 C.M. WETTABLE RASCHIG RINGS

41.	340	1	72	3.01
42.	410	1	72	3.56
43.	510	1	72	4.01
44.	650	1	72	4.82
45.	770	1	72	5.98
46.	800	1	72	6.28
47.	960	1	72	7.01
48.	1080	1	72	7.51
49.	1210	1	72	8.02
50.	1400	1	72	9.92
51.	300	4.5	35	3.48
52.	400	4.5	35	4.21
53.	550	4.5	35	4.87
54.	705	4.5	35	6.63
55.	910	4.5	35	8.98
56.	1050	4.5	35	9.02
57.	1120	4.5	35	9.77

.....

1	2	3	4	5
	1080			
58.	150	6.8	31	2.27
59.	240	6.8	31	2.82
60.	370	6.8	31	3.91
61.	590	6.8	31	5.11
62.	640	6.8	31	5.34
63.	770	6.8	31	6.93
64.	870	6.8	31	7.05
65.	500	14	20	7.85
66.	710	14	20	9.28
67.	1000	14	20	10.88
68.	1220	14	20	11.27
69.	1400	14	20	12.77
70.	300	1	48	4.00
71.	420	1	48	4.77
72.	550	1	48	5.27
73.	600	1	48	5.58
74.	740	1	48	6.21
75.	790	1	48	6.43
76.	1000	1	48	7.55
77.	240	1	30	4.21
78.	280	1	30	4.44
79.	350	1	30	4.78
80.	570	1	30	5.38
81.	800	1	30	6.82
82.	990	1	30	7.98
83.	1100	1	30	9.50

PACKING TYPE - 0.937 C.M. WETTABLE RASCHIG RINGS

84.	960	1	72	6.87
85.	350	1	72	2.96
86.	360	1	72	3.16
87.	650	1	72	6.38
88.	380	1	72	3.38

.....

27 C.M. 1977

1	2	3	4	5
89.	1060	1	72	7.82
90.	390	1	72	4.00
91.	500	1	72	5.03
92.	700	1	72	7.41
93.	675	1	72	6.79
94.	575	1	72	6.63
95.	560	1	72	5.86
96.	800	1	72	7.67
97.	640	1	72	6.25
98.	400	3	42	5.28
99.	540	3	42	5.81
100.	740	3	42	6.99
101.	880	3	42	7.25
102.	990	3	42	8.28
103.	1310	3	42	9.17
104.	410	8	26	5.31
105.	530	8	26	5.91
106.	660	8	26	7.00
107.	890	8	26	7.89
108.	1000	8	26	8.40
109.	1100	8	26	8.61
110.	1370	8	26	9.81
111.	100	1	55	2.01
112.	210	1	55	2.48
113.	330	1	55	3.15
114.	490	1	55	3.81
115.	600	1	55	4.98
116.	1000	1	55	7.89
117.	140	1	30	2.50
118.	190	1	30	2.67
119.	400	1	30	4.21
120.	870	1	30	6.56
121.	1000	1	30	7.92
122.	1400	1	30	9.93
123.	1500	1	30	10.01

.....

PACKING TYPE - 1.27 C.M. WETTABLE PARTITION RASCHIG RINGS

1	2	3	4	5
124.	200	1	72	3.00
125.	400	1	72	3.51
126.	450	1	72	3.62
127.	540	1	72	4.00
128.	610	1	72	4.38
129.	880	1	72	6.43
130.	920	1	72	6.64
131.	1300	1	72	8.13
132.	1400	1	72	8.38
133.	240	10	22	3.63
134.	340	10	22	3.90
135.	520	10	22	4.33
136.	630	10	22	4.79
137.	850	10	22	6.88
138.	900	10	22	7.23
139.	1090	10	22	8.00
140.	500	13	20	5.68
141.	770	13	20	6.77
142.	900	13	20	8.01
143.	1310	13	20	9.87
144.	1400	13	20	9.91
145.	1600	13	20	10.7
146.	300	1	40	2.80
147.	410	1	40	3.17
148.	510	1	40	3.81
149.	760	1	40	5.83
150.	810	1	40	6.78
151.	1000	1	40	8.92

.....

1	2	3	4	5
152.	200	1	24	2.91
153.	280	1	24	3.32
154.	400	1	24	4.12
155.	600	1	24	6.78
156.	850	1	24	7.36
157.	900	1	24	7.63
158.	1000	1	24	8.97

TABLE 3.3

EXPERIMENTAL DATA FOR
NON-WETTABLE PACKINGS

No.	Liquid flow rate (c.c./min)	Viscosity (centi poise)	Surface tension (-dynes/ cm)	Slope
1	2	3	4	5
PACKING TYPE-0.635 C.M. NON-WETTABLE RASCHIG RINGS				
1.	720	1	72	6.18
2.	830	1	72	6.99
3.	450	1	72	4.69
4.	500	1	72	3.85
5.	640	1	72	6.40
6.	750	1	72	5.46
7.	870	1	72	4.22
8.	510	4	38	5.13
9.	600	4	38	5.81
10.	700	4	38	6.33
11.	750	4	38	6.38
12.	820	4	38	6.42
13.	890	4	38	6.50
14.	1010	4	38	7.92
15.	1400	4	38	9.02
16.	300	7.2	30	3.48
17.	420	7.2	30	3.97
18.	500	7.2		
19.	580	7.2	30	4.82
20.	700	7.2	30	5.81
21.	900	7.2	30	6.18
22.	950	7.2	30	6.29
23.	270	9	24	3.53
24.	340	9	24	3.82
25.	460	9	24	4.44
26.	560	9	24	5.18
27.	770	9	24	6.82
28.	1000	9	24	9.88

.....

1	2	3	4	5
29.	310	1	45	5.82
30.	400	1	45	6.11
31.	520	1	45	6.89
32.	740	1	45	9.8
33.	950	1	45	10.7
34.	800	1	45	10.0
35.	1200	1	45	12.33
36.	250	1	22	5.43
37.	330	1	22	6.12
38.	420	1	22	6.85
39.	550	1	22	7.25
40.	705	1	22	8.5
41.	900	1	22	9.38

PACKING TYPE - 1.27 C.M. NON-WETTABLE RASCHIG RINGS

42.	740	1	72	9.32
43.	540	1	72	10.15
44.	825	1	72	6.96
45.	550	1	72	4.06
46.	575	1	72	9.06
47.	700	1	72	6.21
48.	840	1	72	9.60
49.	390	1	72	3.93
50.	970	1	72	10.00
51.	810	1	72	9.37
52.	500	5	35	5.13
53.	590	5	35	5.89
54.	300	5	35	4.07
55.	640	5	35	6.00
56.	810	5	35	7.1
57.	1230	5	35	9.21
58.	1110	5	35	9.08

.....

1	2	3	4	5
59.	330	13	20	4.27
60.	440	13	20	4.73
61.	505	13	20	4.91
62.	730	13	20	6.73
63.	770	13	20	6.80
64.	920	13	20	7.98
65.	600	1	50	6.17
66.	810	1	50	8.21
67.	890	1	50	8.71
68.	1050	1	50	9.01
69.	1400	1	50	10.11
70.	1660	1	50	12.38
71.	210	1	40	2.18
72.	340	1	40	2.92
73.	410	1	40	3.21
74.	730	1	40	5.80
75.	800	1	40	6.21
76.	920	1	40	6.62

PACKING TYPE - 1.27 C.M. NON-WETTABLE PALL RINGS

77.	440	1	72	2.94
78.	570	1	72	3.14
79.	400	1	72	2.03
80.	520	1	72	3.97
81.	710	1	72	6.40
82.	940	1	72	5.72
83.	870	1	72	5.07
84.	910	1	72	4.49
85.	760	1	72	5.78
86.	400	6	33	3.21
87.	550	6	33	3.62
88.	580	6	33	4.85
89.	680	6	33	5.77
90.	700	6	33	6.37
91.	900	6	33	6.66
92.	1400	6	33	9.8

.....

1	2	3	4	5
93.	300	11.5	21	3.05
94.	480	11.5	21	3.88
95.	550	11.5	21	4.12
96.	610	11.5	21	4.5
97.	700	11.5	21	5.0
98.	1000	11.5	21	7.1
99.	1550	11.5	21	9.95
100.	150	1	40	2.22
101.	270	1	40	3.13
102.	500	1	40	4.28
103.	690	1	40	5.71
104.	1000	1	40	7.89
105.	800	1	40	6.82
106.	200	1	25	2.8
107.	310	1	25	3.05
108.	370	1	25	3.12
109.	420	1	25	3.47
110.	530	1	25	3.91
111.	600	1	25	5.13
112.	710	1	25	5.81
113.	900	1	25	7.72
114.	990	1	25	8.12
115.	1200	1	25	10.12

TABLE 3.4

STATISTICAL ANALYSIS OF EXPERIMENTAL DATA USING $\frac{K_d \mu}{\sigma} = k_1 Re^{\alpha_1} We^{\beta_1}$

Packing material	Wettable				Non-wettable			
	1/4" R.R.	3/8" R.R.	1/2" R.R.	1/2" Partion RR	1/4" R.R.	1/2" R.R.	1/2" Pall R.R.	
$k_1 (\times 10^2)$	10.64	6.78	4.73	4.43	1.38	2.47	1.59	
α_1	-1.17	-1.24	-1.23	-1.18	-0.945	-1.07	-1.035	
β_1	1.70	1.28	1.39	1.41	1.39	1.11	1.395	
Multiple correlation coefficient	0.975	0.943	0.969	0.975	0.982	0.948	0.985	
Sum of sqrs	Total corr	95.46	74.02	115.9	100.7	52.5	74.42	78.13
	Reg.	93.04	69.82	112.3	98.13	51.4	70.59	76.9
	Res.	2.42	4.20	3.52	2.52	0.945	3.82	1.209
Deg. of freedom	Reg.	2.0	2.0	2.0	2.0	2.0	2.0	2.0
	Res.	40.0	37.0	34.0	31.0	39.0	32.0	34.0
Mean sqrs	Reg.	46.52	34.9	56.17	49.07	25.7	35.3	38.5
	Res.	0.060	0.113	0.104	0.081	0.024	0.119	0.035
F reg.	775.3	308.8	540.1	605.8	1070.8	296.6	1100.0	

TABLE 3.5

STATISTICAL ANALYSIS OF EXPERIMENTAL DATA USING $\frac{K d_p \mu}{\sigma} = k_2 Re^{\alpha_2} Ga^{\beta_2}$

Packing material	Wettable				Non-wettable																											
	1/4" R.R.	3/8" R.R.	1/2" R.R.	1/2" partition R.R.	1/4" R.R.	1/2" R.R.	1/2" Pall R.R.																									
k_2	1.6×10^8	1.8×10^8	3.8×10^8	2.6×10^8	6.65×10^2	4.8×10^5	2.1×10^5																									
α_2	3.78	3.26	3.36	3.22	0.589	1.27	1.47																									
β_2	-2.84	-2.58	-2.58	-2.50	-0.815	-1.39	-1.41																									
Multiple correlation coefficient	0.930	0.934	0.925	0.931	0.769	0.95	0.896																									
Sum of sqrs	<table border="0"> <tr> <td rowspan="3" style="vertical-align: middle;"> <div style="font-size: 2em;">{</div> </td> <td>Total corr.</td> <td>95.46</td> <td>74.02</td> <td>115.9</td> <td>100.7</td> <td>52.5</td> <td>74.42</td> <td>78.13</td> </tr> <tr> <td>Reg.</td> <td>88.83</td> <td>69.14</td> <td>107.1</td> <td>93.7</td> <td>40.2</td> <td>70.7</td> <td>70.0</td> </tr> <tr> <td>Res.</td> <td>6.63</td> <td>4.88</td> <td>8.71</td> <td>6.95</td> <td>12.0</td> <td>3.69</td> <td>8.13</td> </tr> </table>							<div style="font-size: 2em;">{</div>	Total corr.	95.46	74.02	115.9	100.7	52.5	74.42	78.13	Reg.	88.83	69.14	107.1	93.7	40.2	70.7	70.0	Res.	6.63	4.88	8.71	6.95	12.0	3.69	8.13
<div style="font-size: 2em;">{</div>	Total corr.	95.46	74.02	115.9	100.7	52.5	74.42		78.13																							
	Reg.	88.83	69.14	107.1	93.7	40.2	70.7		70.0																							
	Res.	6.63	4.88	8.71	6.95	12.0	3.69	8.13																								
Deg. of freedom	<table border="0"> <tr> <td rowspan="2" style="vertical-align: middle;"> <div style="font-size: 2em;">{</div> </td> <td>Reg.</td> <td>2.0</td> <td>2.0</td> <td>2.0</td> <td>2.0</td> <td>2.0</td> <td>2.0</td> <td>2.0</td> </tr> <tr> <td>Res.</td> <td>40.0</td> <td>37.0</td> <td>34.0</td> <td>31.0</td> <td>39.0</td> <td>32.0</td> <td>34.0</td> </tr> </table>							<div style="font-size: 2em;">{</div>	Reg.	2.0	2.0	2.0	2.0	2.0	2.0	2.0	Res.	40.0	37.0	34.0	31.0	39.0	32.0	34.0								
<div style="font-size: 2em;">{</div>	Reg.	2.0	2.0	2.0	2.0	2.0	2.0		2.0																							
	Res.	40.0	37.0	34.0	31.0	39.0	32.0	34.0																								
Mean sqrs	<table border="0"> <tr> <td rowspan="2" style="vertical-align: middle;"> <div style="font-size: 2em;">{</div> </td> <td>Reg.</td> <td>44.4</td> <td>34.5</td> <td>53.5</td> <td>46.85</td> <td>20.13</td> <td>35.4</td> <td>35.0</td> </tr> <tr> <td>Res.</td> <td>0.165</td> <td>0.132</td> <td>0.256</td> <td>0.224</td> <td>0.309</td> <td>0.116</td> <td>0.238</td> </tr> </table>							<div style="font-size: 2em;">{</div>	Reg.	44.4	34.5	53.5	46.85	20.13	35.4	35.0	Res.	0.165	0.132	0.256	0.224	0.309	0.116	0.238								
<div style="font-size: 2em;">{</div>	Reg.	44.4	34.5	53.5	46.85	20.13	35.4		35.0																							
	Res.	0.165	0.132	0.256	0.224	0.309	0.116	0.238																								
$F_{reg.}$	269.1	261.4	208.9	209.15	65.15	305.2	147.1																									

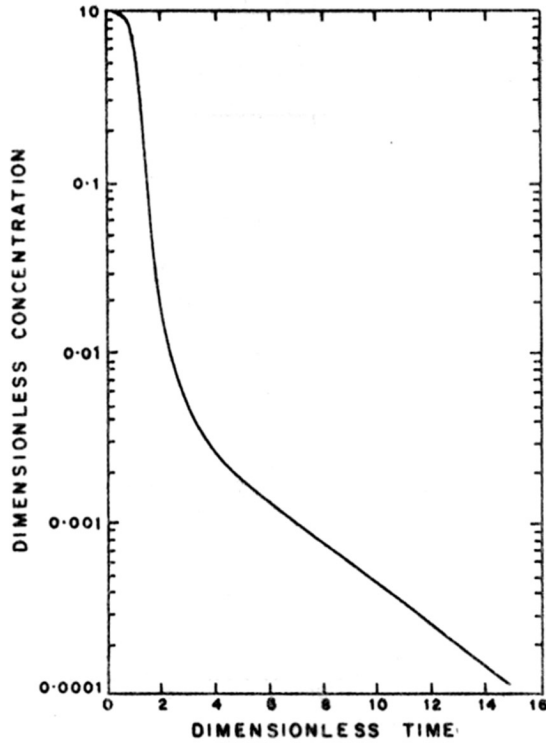


FIG. 3-1: A TYPICAL OUTLET RESPONSE CURVE FOR A STEP DECREASE INPUT.

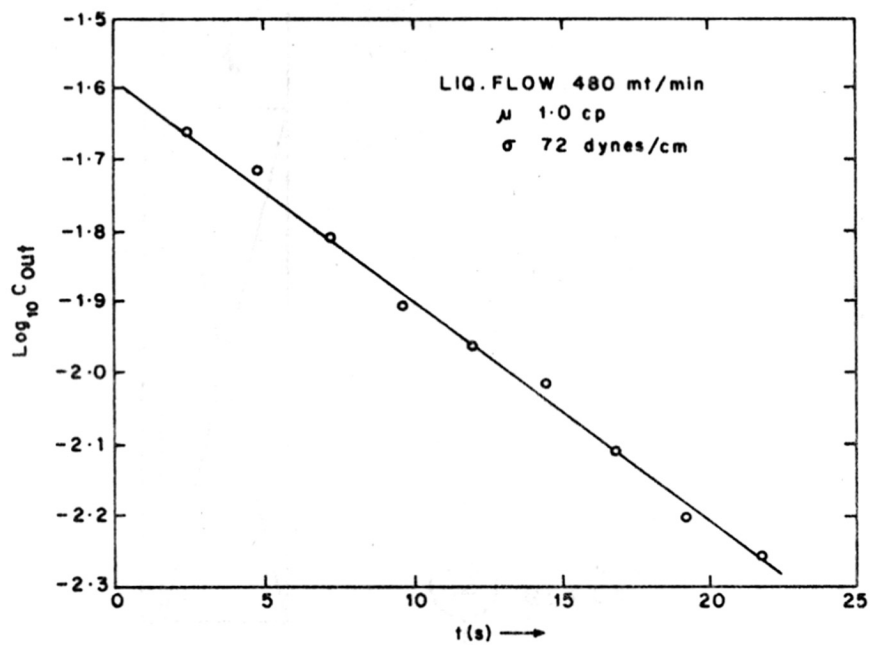


FIG. 3-2 : A TYPICAL PLOT OF Log C_{out} vs t.

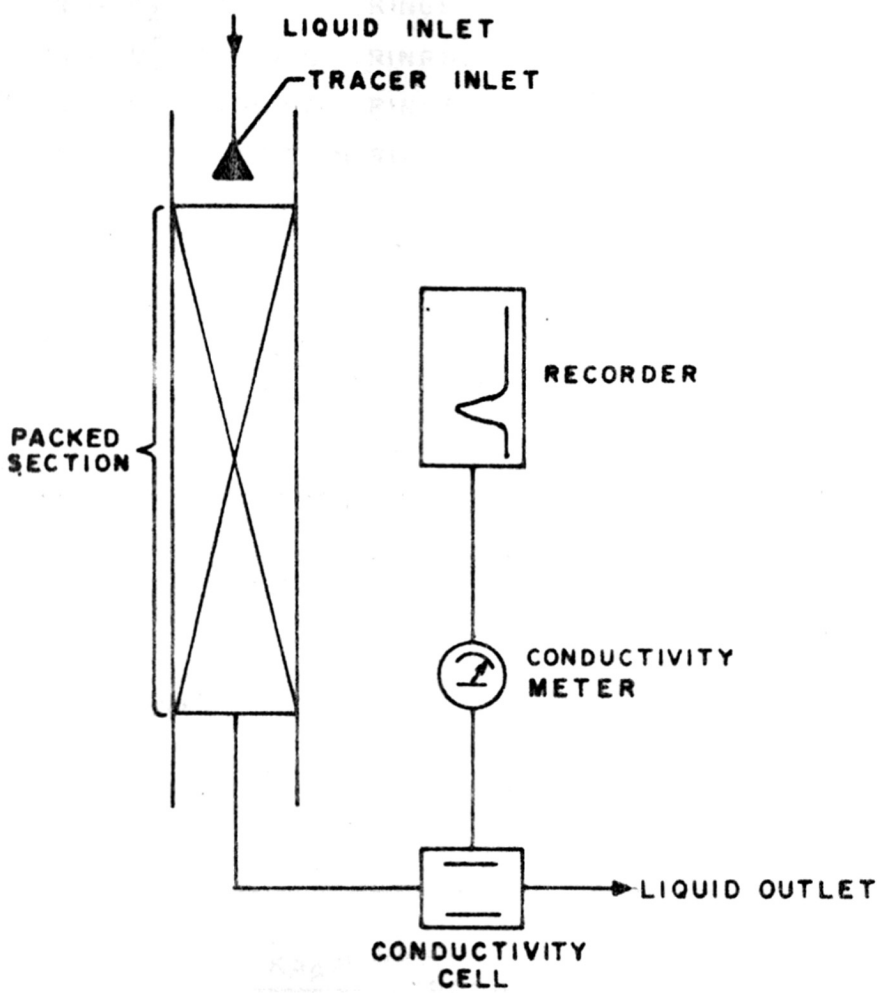


FIG.3.3: SCHEMATIC REPRESENTATION OF EXPERIMENTAL SET UP.

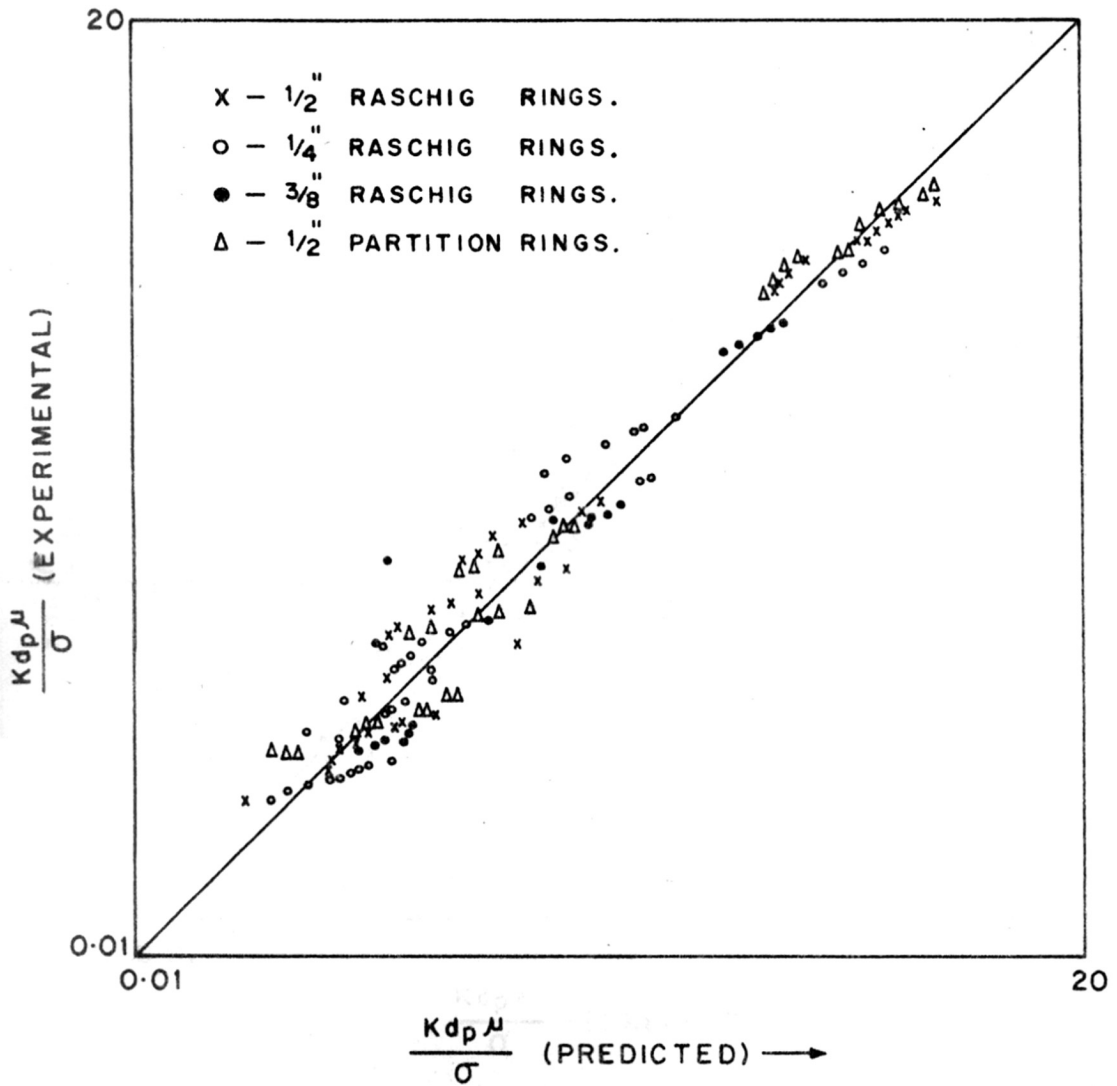


FIG. 3.4: EXPERIMENTAL AND PREDICTED [Equn. (3.11)]

VALUES OF $\frac{K_d \mu}{\sigma}$ FOR WETTABLE PACKINGS.

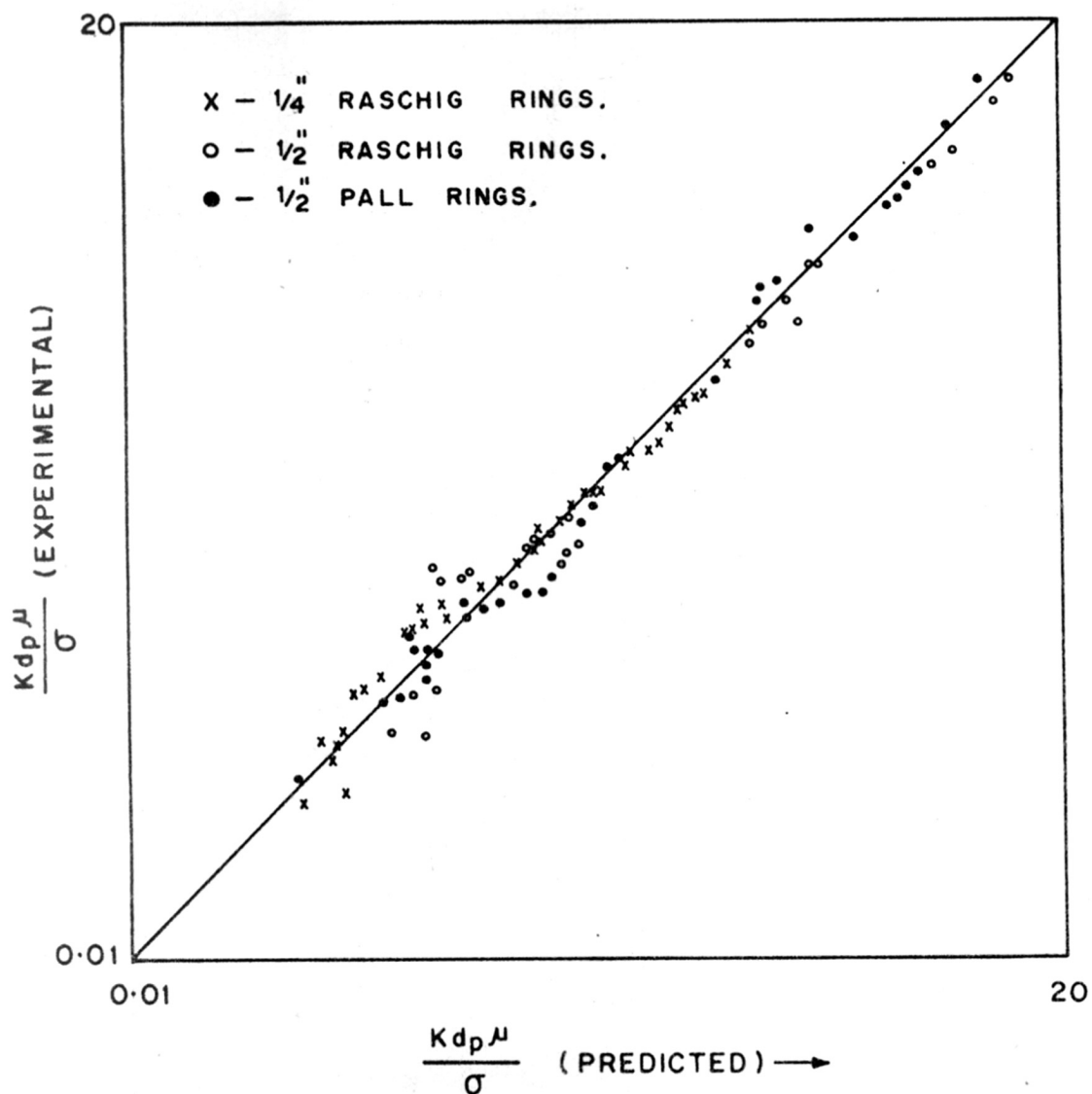
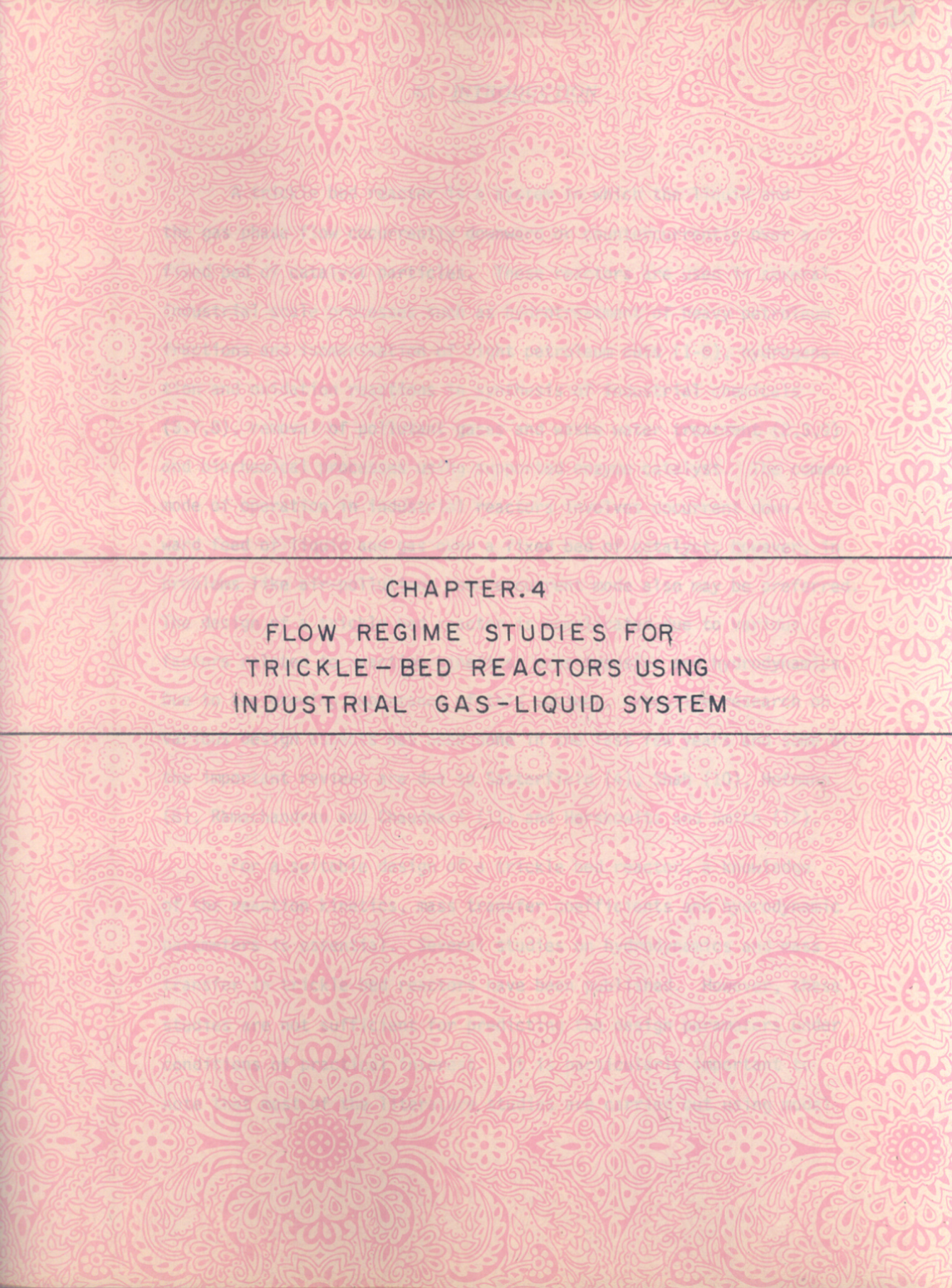


FIG. 3.5: EXPERIMENTAL AND PREDICTED [Equn. (3.11)]
 VALUES OF $\frac{Kdp\mu}{\sigma}$ FOR NON-WETTABLE
 PACKINGS.



CHAPTER.4
FLOW REGIME STUDIES FOR
TRICKLE-BED REACTORS USING
INDUSTRIAL GAS-LIQUID SYSTEM

4.1 INTRODUCTION

A trickle bed reactor is a system in which the liquid and the gas phase flow cocurrently downward or countercurrently over a fixed bed of catalyst particles. These reactors are used in several industrial scale processes such as hydrotreatment of heavy petroleum fractions and isomerisation of light petroleum cuts (1-6), hydrogenation and oxidation reactions in synthesis of industrial chemicals (3,7,8), removal of pollutant gases and waste water treatment (2,3,9) and biochemical processes using supported enzyme catalyst. The common mode of operation in industrial reactors involves cocurrent downward feed of liquid and gas over a fixed bed of catalyst, however, in problems like air-pollution, countercurrent mode also may be preferred. The design of a trickle bed reactor is complicated due to various factors related to reaction kinetics, mass transfer and hydrodynamics. Due to the growing importance of this subject, extensive research on various design aspects has been done in the last few years and some of the important reviews are due to Satterfield (4), Shah (10), Hofmann (8), Ramachandran and Chaudhari (11) and Herskowitz and Smith (12).

For a suitable design of a trickle bed reactor, a knowledge of the reaction kinetics, mass transfer coefficients and hydrodynamic parameters is essential. Several studies on hydrodynamics and mass transfer in trickle bed reactors have been published. However, these studies are not sufficient for predicting the design parameters under conditions of practical interest. It is particularly important to note that most of the literature studies are carried out using model

systems such as air-water-sand or glass beads and ambient conditions. There is hardly any information on hydrodynamic and mass transfer parameters for practical systems. The first important aspect in the design of trickle bed reactor is the prevailing flow regime for a given gas and liquid velocity. The mass transfer coefficient and other design parameters like hold-up, pressure drop, dispersion coefficient, largely depend on the flow regime. In this work, the main objective was to investigate the transition in flow regimes under different operating conditions and assess the predictability of literature correlations for systems of practical interest. The literature survey on flow regimes and a detailed scope of the present work are discussed in the following sections.

4.2 PREVIOUS WORK

Different flow regimes in trickle bed reactors have been observed depending on gas and liquid flow rates and physical properties of gases and liquids. The various investigations on this subject are summarised in Table 4.1. The flow regimes have been generally classified as follows.

(1) Trickle flow regime - At low liquid velocity, the flow pattern is referred to as a trickle flow or a gas continuous flow regime. In this case, the liquid phase trickles over the packing essentially in a laminar flow. Since the flow in one phase is not significantly affected by the flow in other phase, it is also known as a low interaction regime.

(2) Pulse flow regime - At higher gas and liquid rates, a pulsing or rippling flow behaviour is generally observed. In this regime the interaction between gas and liquid phases is high and therefore is also referred to as a high interaction regime.

(3) Dispersed bubble flow regime - At very high liquid rates and low gas rates, the liquid tends to become a continuous phase with gas in a dispersed bubble flow. This regime is called as dispersed bubble flow regime.

Most of the laboratory and commercial reactors are operated either in a trickle or pulse flow regime. The transition between the flow regime becomes an important design aspect and has been the subject of several investigations. Weekman and Myers (14) were the first to observe the transition between trickle and pulse flow regimes. The different methods used for determining the flow regime transitions are: (a) visual observation [Talmor, (26)], (b) sharp increase in pressure fluctuations [Chou et al. (15), Sicardi et al. (16)], (c) sudden change in gas-liquid mass transfer coefficient [Fukushima and Kusaka, (13)] and (d) variations in apparent electric conductivity [Matsuura et al. (17)]. The parameters affecting the flow regime transitions are gas to liquid velocity ratio, physical properties of the liquid phase and the shape and the size of the catalyst particles. The investigations by Chou et al. (15), Kobayashi et al. (18), Morsi et al. (19) and Sicardi et al. (16) have shown that the effect of the physical properties of fluids on the transition from trickle flow to the pulsing flow regime is very significant. Chou et al. (15) have observed a major

effect of particle wettability. The studies on nonfoaming systems for a cocurrently operated trickle bed have been reported by Larkins et al. (20), Weekman and Meyers (14), Sato et al. (21), Charpentier and Favier (22), Midoux et al. (23), Specchia and Baldi (24). Charpentier and Favier (22) obtained data for systems such as air-water, air-cyclohexane, CO₂-cyclohexane or gasoline or petroleum ether and 3 mm particles. They correlated the transition conditions between low and high interaction regimes by a single curve valid for foaming and nonfoaming systems. The results of a later experimental study by Specchia and Baldi (24) with glass spheres and air-water or aqueous glycerol systems agreed with the results of Charpentier and Favier (22) for nonfoaming systems. For foaming systems, the transition was observed at lower liquid flow rate than for nonfoaming systems by Specchia and Baldi (24).

Charpentier and Favier presented the flow map transition in terms of the Baker coordinates (25) in which $u_l \rho_l \lambda \psi / u_g \rho_g$ vs. $u_g \rho_g / \lambda \epsilon_B$ is plotted. In a later study, Chou et al. (15) have shown that the use of the Baker coordinate may not be sufficient to distinguish the flow regimes, particularly if the effect of wetting characteristics of the packing have to be considered. Talmor (26) proposed u_g / u_l and $(1 + 1 / Fr_{lg}) / (We_{lg} + 1 / Re_{lg})$ as coordinates for the flow map to account for the effects of particle shape and size and reactor to particle diameter ratio. This approach accounts for inertia, gravity, interface and viscous resistances.

Gianetto et al. (27) and Sicardi et al. (16) have also proposed approximate criteria for predicting the transition to pulse flow regime.

While extensive studies on air-water-solid systems have been published, there is little information on systems of practical interest. Also, the generalized approaches of Talmor (26) and Charpentier and Favier (22) need to be further confirmed with data on real systems.

The present work was therefore undertaken with the following objectives:

(1) Experimental determination of flow regime transitions for several systems of practical interests. The systems chosen were:

- (a) Air-water-glass spheres
- (b) Acetylene-aqueous formaldehyde-alumina
- (c) Chlorine-toluene-ceramic cylinders
- (d) Hydrogen-benzaldehyde-alumina
- (e) Ethylene-water-alumina

(2) Effect of particle size on flow regime- transitions.

(3) Comparison of the results with earlier work.

4.3 EXPERIMENTAL

A schematic diagram of the experimental set-up is shown in Fig. 4.1. The system consisted of a 5.6 cm ID glass column which was 100 cm long, a circulation pump and gas and liquid flow meters. The column was packed up to 85 cm length and was operated in a cocurrent down-flow manner. The liquid and gas phases were distributed over the column cross-section using a 12 point glass tube distributor. The

packing types consisted of glass spheres, Norton-alumina supports and ceramic cylinders. The physical properties of the systems used are listed in Table 4.2.

In order to observe the flow regime transition, a desired liquid flow was set and after a constant liquid flow rate was established, the gas flow was introduced. Keeping the liquid flow rate constant, gas rates were progressively increased and the corresponding flow regime was observed. The region of flow rates at which the transition from trickle flow to pulse flow occurred, was visually observed in a series of experiments. The liquid and gas velocity ranges covered were 0.1-1.1 and 0.5-100 cm/sec respectively. The packing diameter was varied between 1-5 mm.

For each system, depending on a flow rate, the starting flow regime at low gas rates was trickle flow. The starting point of the pulse flow regime was quite distinct in most cases. The following systems were investigated: (a) Air-water-glass spheres, (b) Acetylene-aqueous formaldehyde-alumina, (c) Chlorine-toluene-ceramic cylinders, (d) Hydrogen-benzaldehyde-alumina, (e) Ethylene-water-alumina.

4.4 RESULTS AND DISCUSSION

The flow regime transitions were observed for the various systems mentioned earlier. Four distinct patterns were observed experimentally. These are: (1) Spray flow (2) Trickle flow (3) Pulsing

flow and (4) Dispersed bubble flow. The relative location of each of these flow patterns with respect to gas and liquid superficial velocity is shown in Figs. 4.2 to 4.6. for each of the systems studied. The results for the air-water-glass spheres system are shown in Fig. 4.2 along with the results of Chou et al. (15). The results of this work have been found to agree well with those of Chou et al.(15). Thus indicating that the experimental method used in this work is satisfactory.

In the visual observations of the flow regime transition, the gas velocity was increased in each successive experiments keeping the liquid rate constant. At lower liquid rates, gas continuous or trickle flow pattern was observed. Also at low liquid rate and higher gas flow rate, spray flow regime was observed. This is gas continuous flow regime in which liquid phase is distributed as a heavy mist in gas stream. This is because the liquid drops are finely broken by a large stream of gas flow in these conditions. As the gas velocity is increased further at a given liquid rate, a non-homogeneous flow regime called as pulse flow regime is observed. This regime is characterised by alternate portions of more dense and less dense mixtures of two phases through the column. The transition from trickle flow to pulse flow was found to be very sharp in general, however, the transition occurred for different gas and liquid rates for each case. In the case of chlorine-toluene-ceramic cylinders system, the transition point is in close agreement with that in air-water-glass sphere system. In the case of hydrogen-benzaldehyde-alumina, ethylene-water-alumina

systems, (Figs. 4.5 and 4.6), the transition to pulse flow has been observed at lower gas velocities than the air-water-glass sphere system.

As the gas flow rate was increased further, the pulse frequency was found to increase and with still further increase in the gas velocity, these pulses merged into each other and a dispersed bubble flow regime was observed. This regime is characterised by fast moving liquid with formation of gas bubbles. Except for chlorine-toluene-ceramic cylinders system, the transition from pulse flow to dispersed bubble flow was found to occur at higher gas and liquid rates compared to that of air-water-glass sphere system. For acetylene-formaldehyde-alumina system, the transition occurred at very high gas and liquid flow rates. This is likely to be due to the fact that the density of acetylene is lower compared to air or chlorine. Also, for this system, foaming was observed to a certain extent.

The effect of packing diameter on the flow regime transition was not found to be significant as far as the transition points are concerned. The main observation of this work was that the flow regime transition observed for systems with different physical properties are widely different from that of air-water-glass spheres system.

The results of this work were also compared with the literature correlations of Fukushima and Kusaka (13) and Talmor (26). Fukushima and Kusaka (13) proposed following correlations for transition between pulse to trickle and pulse to dispersed bubble flow regime.

Trickle-pulse

$$\phi_c^{-0.2} \text{Re}_L^* 0.27 \text{Re}_G^* 0.27 \left(\frac{d_p}{d_T} \right)^{-0.5} = 18 \quad (1)$$

Pulse-dispersed bubble flow

$$\phi_c^{-0.6} \text{Re}_L^* 1.13 \text{Re}_G^*^{-0.2} \left(\frac{d_p}{d_T} \right)^{-0.8} = 790 \quad (2)$$

where, ϕ_c is the shape factor of the packing defined as the ratio of the geometric surface area of the packing to the square of the packing diameter. The Reynold's number Re_L^* and Re_G^* are defined as:

$$\text{Re}_L^* = \frac{d_{pe} u_l \rho_L}{\mu_L} \quad (3)$$

$$\text{Re}_G^* = \frac{d_{pe} u_g \rho_g}{\mu_G} \quad (4)$$

The predicted results of eqn. (1) for trickle to pulse transition of the flow regime are shown in Figure (4.7) along with experimental data obtained in this work. It can be seen that for most cases the correlations of Fukushima and Kusaka (13) does not agree with the experiments. The results for pulse to dispersed bubble flow, when compared with predictions of equation (2) also showed disagreement. This indicates that the correlation of Fukushima and Kusaka (13) is not suitable to represent data for a wide variety of systems.

The results of this work have also been compared with the flow map proposed by Talmor (26) in Figure (4.8). In this case the flow map is presented as u_g/u_l vs. $(1 + 1/Fr_{lg})/(We_{lg} + (1/Re_{lg}))$. The parameters Fr_{lg} , We_{lg} and Re_{lg} are defined in Table (4.3). In certain range of conditions, the results of this work agree with the flow map of Talmor (26) for transition from trickle to pulse flow regimes. However, in the lower range of the effective parameter $(1 + \frac{1}{Fr_{lg}}) / (We_{lg} + \frac{1}{Re_{lg}})$, the results were not found to agree well. This indicates that, more work is essential to develop a generalized flow map for trickle bed reactors. The present study clearly indicates that the data obtained for systems with different physical properties cannot be explained based on correlations developed from air-water system data.

4.5 CONCLUSIONS

The transition of flow regimes in a trickle bed has been studied using systems of widely different physical properties. The experimental data have been obtained over a wide range of gas and liquid velocity. On comparison of the results with data on air-water-glass sphere system, it was found that our results agreed with earlier work only for air-water system. For other systems such as chlorine-toluene, hydrogen-benzaldehyde, ethylene-water and acetylene-formaldehyde, the flow regime transition points were observed to be widely different from that of air-water system. The present data were also compared with literature correlations and it was found that the data agreed with the

flow map of Talmor (26) only in certain range of conditions. For trickle to pulse flow regime transition. The present data disagreed with the correlation of Fukushima and Kusaka (13). This concludes, that the earlier flow maps developed based on systems such as air-water and limited range of parameters are not suitable to explain behaviour of a wide variety of systems. Further work is recommended on this subject to evolve a generalized flow map of a trickle bed.

.....

NOTATION

d_h	equivalent diameter defined as $\epsilon_1 d_p / 1.5 (1 - \epsilon_1)$
d_p	diameter of the particle, cm
d_{pe}	equivalent diameter of particle defined as $2/3 \frac{d_p \epsilon_B}{1 - \epsilon_B}$
d_T	diameter of the column
Fr_{1g}	Froud number as defined in Table (4.3)
g	acceleration due to gravity, cm/s^2
Re_G^*	gas-phase Reynolds number based on $d_{pe} u_g \rho_g / \mu_g$
Re_L^*	liquid-phase Reynolds number based on d_{pe}
Re_{1g}	Reynolds number as defined in Table (4.3)
S_T	surface tension of liquid, dyne/cm
u_g	superficial velocity of the gas phase in the column, cm/s
u_l	superficial velocity of the liquid in the column, cm/s
We_{1g}	Weber number as defined in Table (4.3)
Greek letters	
ϵ_B	bed voidage
ϵ_1	external liquid hold-up
λ	a parameter defined as $(\rho_g \rho_l / \rho_{air} \rho_{water})^{0.5}$
μ_g	viscosity of gas-phase, poise
μ_l	viscosity of liquid, poise

.....

μ_{1g}	Parameter defined in Table (4.3)
ν_{1g}	parameter defined in Table (4.3)
ρ_g	gas density, g/cm ³
ρ_l	density of liquid, g/cm ³
θ_c	shape factor
γ	a parameter defined as $\frac{S_{Tw}}{S_T} \left[\frac{\mu_L}{\mu_w} (\rho_w/\rho_l)^2 \right]^{1/3}$

REFERENCES

1. Satterfield, C.N. and Way, P.F., *AIChE J.* 18, 305 (1972)
2. Charpentier, J.C., *Chem. Eng. J.* 11, 161 (1976)
3. Charpentier, J.C., *Chemical Reaction Engineering Reviews*, Houston (1978)
4. Satterfield, C.N., *AIChE J.* 21, 909 (1975)
5. Urazaer, F. Kh., Akhmetov, I.G. and Varfolomev, D., *Intern. Chem. Eng.* 18, 102 (1978)
6. Paraskos, J.A., Frayer, J.A. and Shah, Y.T., *Ind. Eng. Chem. Proc. Des. Dev.* 14, 315 (1975)
7. Hofmann, H., *Intern. Chem. Eng.* 17, 1 (1977)
8. Hofmann, H., *Catal. Rev. Sci. Eng.* 17, 71 (1978)
9. Germain, A., *Kinetic Study of a catalytic reaction in a gas-liquid-solid system*, 40 (1970).
10. Shah, Y.T., *Gas-liquid-solid reactor design*, McGraw-Hill, New York (1979)
11. Ramachandran, P.A. and Chaudhari, R.V., 'Three phase catalytic reactor,' Gordon and Breach Science Publishers, New York (1983)
12. Herskowitz, M. and Smith, J.M., *AIChE J.* 1, 1 (1983)
13. Fukushima, S., and Kusaka, K., 'Interfacial area and boundary of hydrodynamic flow region in packed column with cocurrent downward flow,' *J. Chem. Eng. Japan*, 10, 461 (1977a)
14. Weekman, V.W., and Myers, J.E. 'Fluid flow characteristics of cocurrent gas-liquid flow in packed beds', *AIChE J.* 10, 951 (1964)
15. Chou, T.S. Worley, F.L. and Luss, D., *Ind. Eng. Chem. Proc. Des. Dev.* 16, 424 (1977).

.....

16. Sicardi, S., Gerhard, H. and Hofman, H., Chem. Eng. J. 18, 173 (1979)
17. Matsuura, A., Akehata, T., and Shirai, T., J. Chem. Eng. Japan
18. Kobayashi, T. and Saito, H., Kagaku Kogaku, 3, 210 (1965)
19. Morsi, B.I., Midoux, N. and Charpentier, J.C., AIChE J. 24, 357 (1978)
20. Larkins, R.P., White, R.R. and Jeffrey, D.W., AIChE J. 7, 231 (1961)
21. Sato, Y., Hirose, T., Takahashi, F., Toda, M., and Hashiguchi, Y., J. Chem. Eng. Japan 6, 315 (1973b)
22. Charpentier, J.C. and Favier, M., AIChE J. 21, 1113 (1975)
23. Midoux, N., Favier, M. and Charpentier, J.C., J. Chem. Eng. Japan, 9, 350 (1976)
24. Specchia, V. and Baldi, G., Chem. Eng. Sci. 32, 515 (1977)
25. Baker, O., Oil Gas J. 53, 185 (1954)
26. Talmor, E. Part I. Flow Maps. AIChE J. 23, 868 (1977)
27. Gianetto, A., Baldi, G. and Specchia, V., Ing. Chim. 6, 125 (1970)
28. Charpentier, J.C. and Favier, M., AIChE J. 21, 1213 (1975)
29. Charpentier, J.C., Bakos, M. and LeGoff., Proc. 2nd Int. Congr. Vesprem, Hungary (1971)
30. Beimesch, W.E. and Kessler, D.P., AIChE J. 17, 1160 (1971)

TABLE 4.1 : A SUMMARY OF LITERATURE ON FLOW REGIMES IN TRICKLE BED REACTOR

Reference	Column diameter D(m)	Packing type and shape	dp (mm)	Gas and liquid systems
(28,23)	0.05	Catalyst spheres	3	Air, CO ₂ water, cyclohexane
		Catalyst cylinders (I)	1.8x6	He, N ₂ petroleum, ether, gasoline
		Catalyst cylinders (II)	1.4x5	
		Catalyst spheres	3	Air-water
		Catalyst cylinders (I)	1.8x6	Air-water
		Catalyst cylinder (II)	1.4.x5	N ₂ - cyclohexane
(15)	0.0635	Beads	2.9	Air-water, water+alcohol, etc.
(27)	0.08	Glass spheres	6	Air-water
		Raschig rings	6	
		Berl saddles	6	
(21)	0.066	Glass beads	2.59-16.5	Air-water
	0.122			
(24)	0.066	Glass beads	2.59	Air-water
		Glass beads	8.01	Air-water

(ii)

Table 4.1 contd.

Reference	Column diameter $D(m)$	Packing type and shape	d_p (mm)	Gas and liquid systems
(30,14)	0.08	Glass spheres	6	Air-water
		Glass cylinders	2.7	Air-water + glycerol
		Glass cylinders	5.4	
		Glass spheres	6	Air-water
		Glass cylinders	2.7	
(29)	0.10	Glass cylinders	5.4	
		Glass spheres	6	Air-water
(26)	0.0762	Glass spheres	4.7	Air-water
		TCC beads	3.8	
		Alumina beads	6.5	
		Raschig rings	6.4	Air-water
		Raschig rings	10.3	
(26)	0.20	Raschig rings	22	
		Raschig rings	22	
(26)	0.292	Cylinders	3.5	Air-water

TABLE 4.2

PHYSICAL PROPERTIES OF THE SYSTEMS INVESTIGATED

Gas phase	Gas phase properties μ_g poise	Gas phase properties ρ_g g/cm ³	Liquid phase	Liquid phase properties μ_l poise	Liquid phase properties σ_T dyne/cm	Liquid phase properties ρ_l g/cm ³	Particle diameter dp in cm
Air	1.8×10^{-4}	1.3×10^{-3}	Water	8.0×10^{-3}	72	1.0	0.3, glass spheres
Acetylene	9.7×10^{-5}	1.171×10^{-3}	Formaldehyde 20% solution	1.0	72	1.11	0.18, 0.3, and 0.4 alumina particles
Chlorine	1.4×10^{-4}	3.224×10^{-3}	Toluene	5.5×10^{-3}	27.4	0.867	0.18, 0.2 and 0.5 ceramic cylinders
Hydrogen	9×10^{-5}	8.98×10^{-5}	Benzaldehyde	1.39×10^{-2}	40	1.04	0.15, 0.2, and 0.3 alumina particles
Ethylene	1×10^{-4}	1.26×10^{-3}	Water	8.0×10^{-3}	72	1.0	0.15, 0.38, and 0.21 alumina particles

TABLE 4.3

DEFINITION OF PARAMETERS FOR PREDICTION OF FLOW MAPS GIVEN BY
TALMOR (26)

Parameter	Definition
Fr_{1g}	$\frac{[(u_1 \rho_1 + u_g \rho_g) v_{1g}]^2}{g/d_h}$
We_{1g}	$\frac{d_h v_{1g} (u_1 \rho_1 + u_g \rho_g)^2}{S_T}$
Re_{1g}	$\frac{d_h (u_1 \rho_1 + u_g \rho_g)}{\mu_{1g}}$
γ_{1g}	$\frac{1/\rho_1 (u_1 \rho_1 / u_g \rho_g) + (1/\rho_g)}{1 + (u_1 \rho_1 / u_g \rho_g)}$
μ_{1g}	$\frac{\mu_1 (u_1 \rho_1 / u_g \rho_g) + \mu_g}{1 + (u_1 \rho_1 / u_g \rho_g)}$
d_h	$\frac{2 \epsilon_B d_T}{2+3 (1-\epsilon_B) d_T / d_p}$

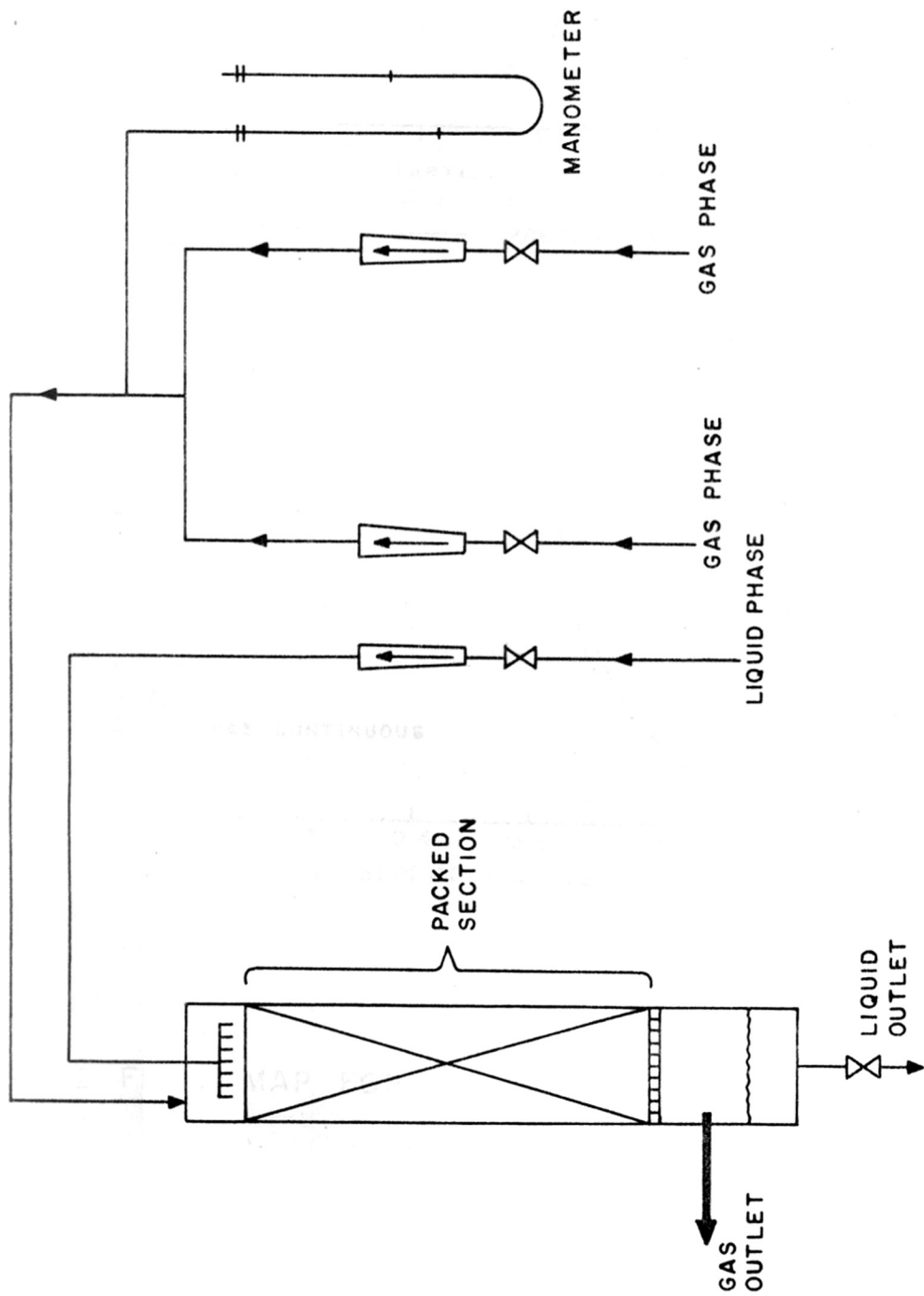


FIG. 4-1: A SCHEMATIC DIAGRAM OF THE EXPERIMENTAL SET UP

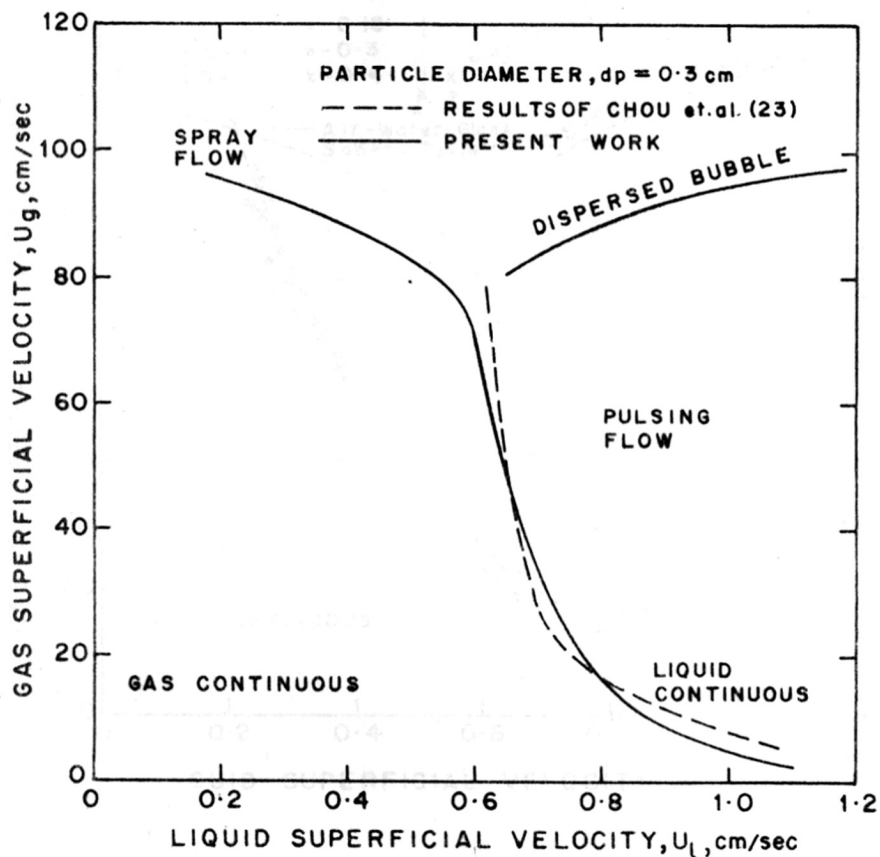


FIG 4-2: FLOW MAP FOR AIR-WATER-GLASS SPHERES SYSTEM

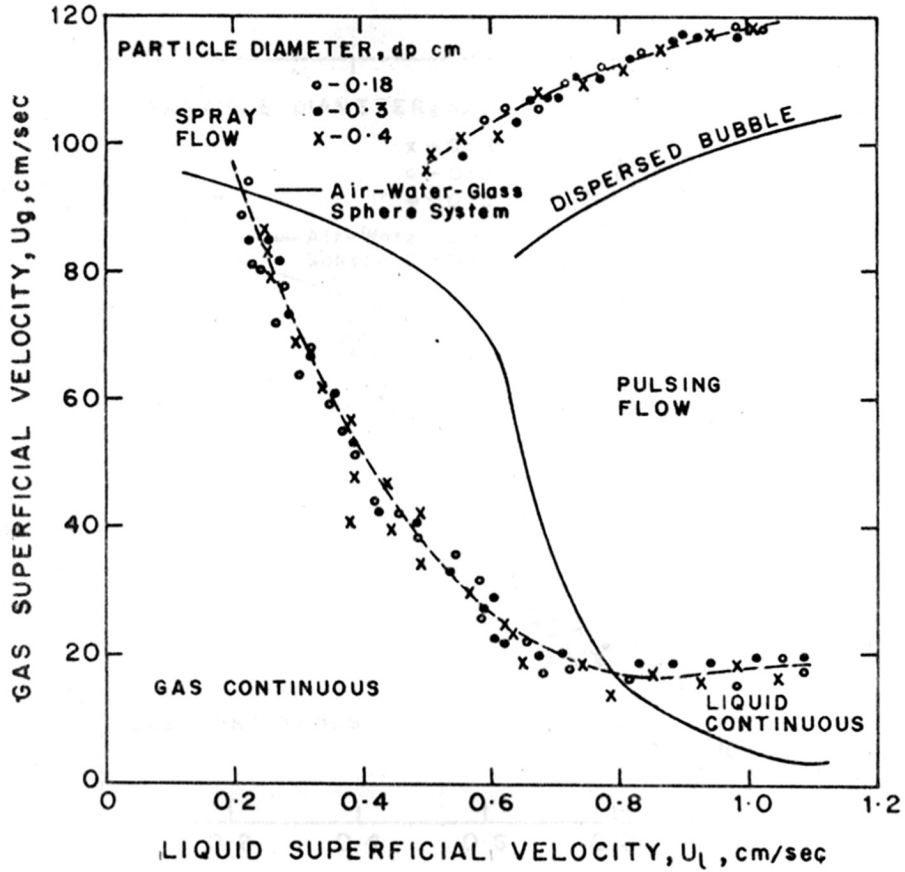


FIG.4-3: FLOW MAP FOR ACETYLENE FORMALDEHYDE ALUMINA SYSTEM

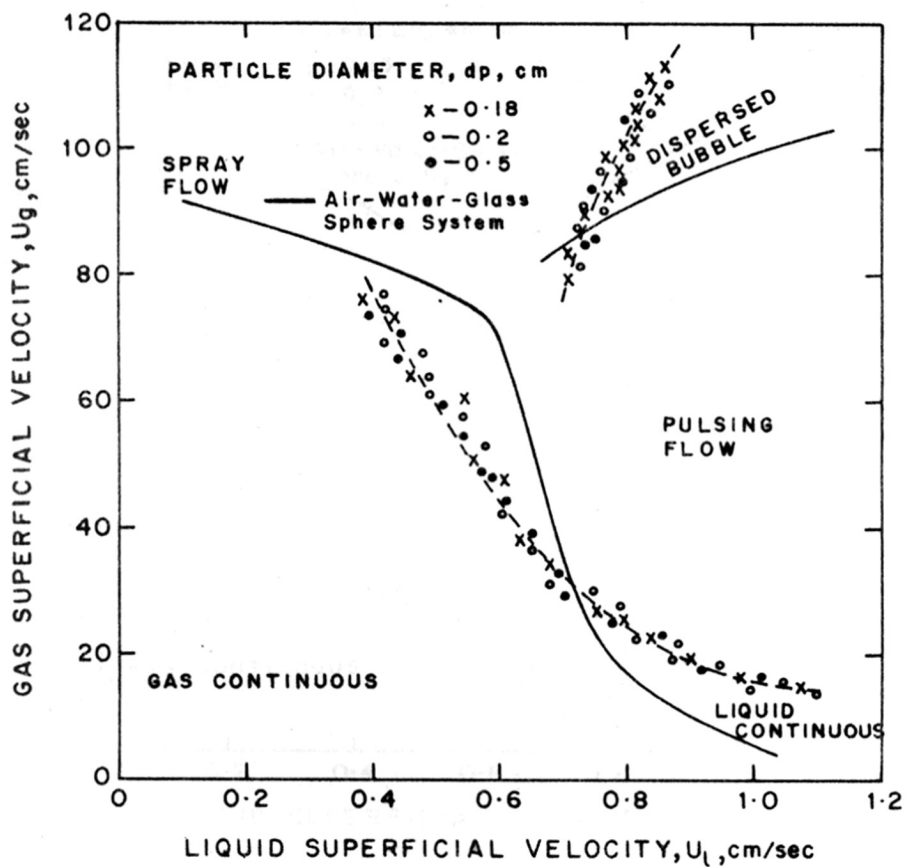


FIG. 4.4: FLOW MAP FOR TOULENE - CHLORINE CERAMIC CYLINDER SYSTEM.

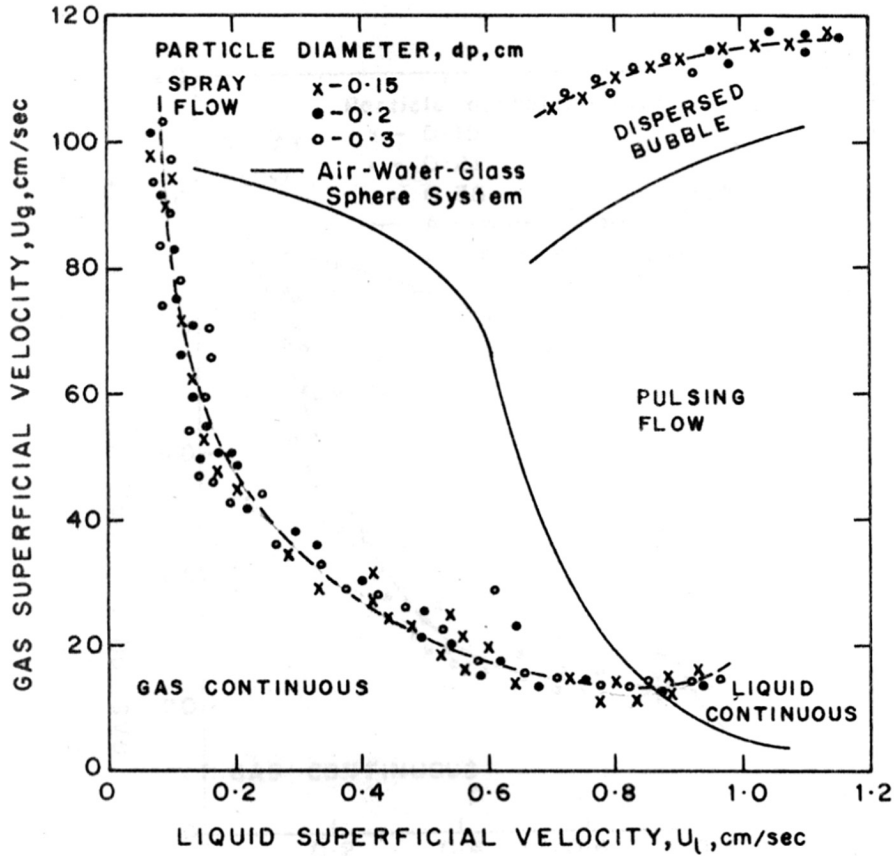


FIG. 4.5 : FLOW MAP FOR HYDROGEN-BENZALDEHYDE ALUMINA SYSTEM.

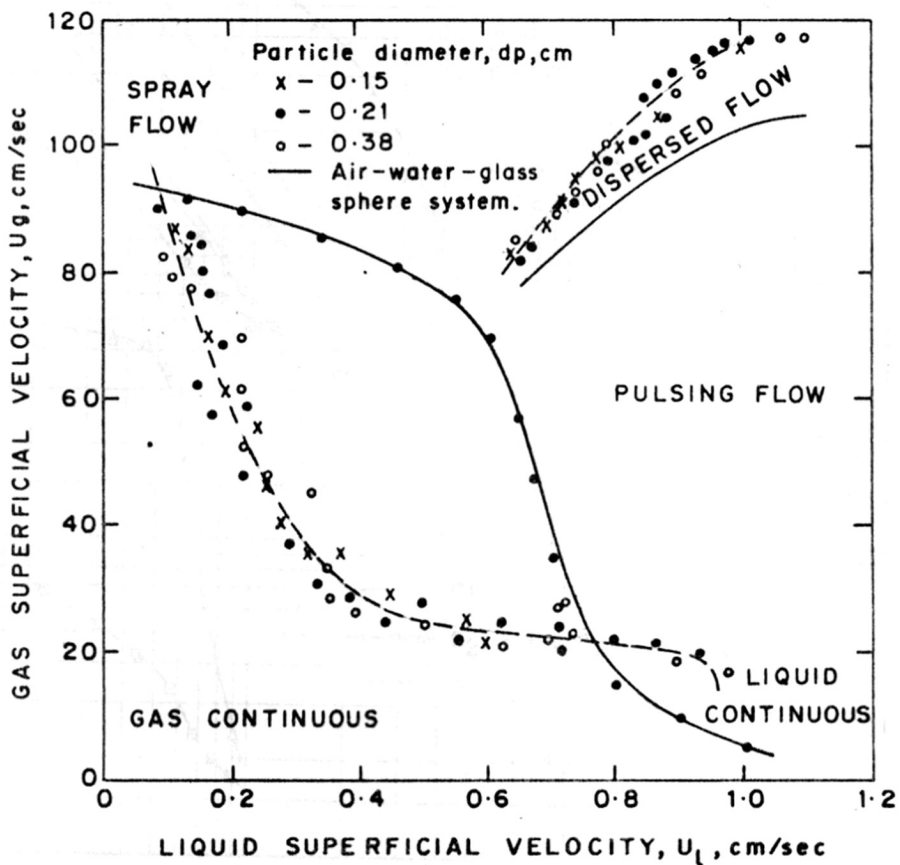


FIG. 4-6: FLOW MAP FOR ETHYLENE-WATER-ALUMINA SYSTEM

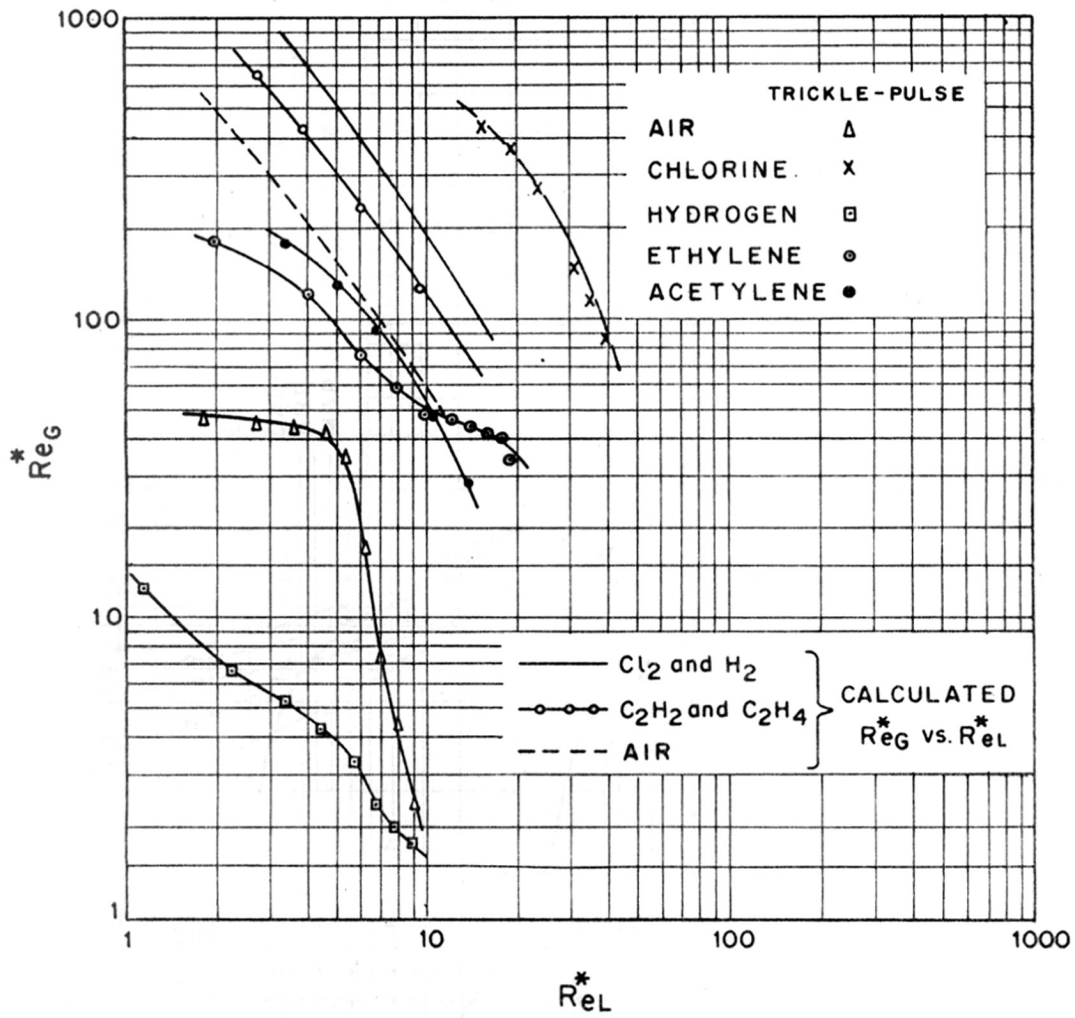


FIG 4-7 : COMPARISON OF FLOW REGIME TRANSITION WITH THE CORRELATION OF FUKUSHIMA AND KUSAKA (13)

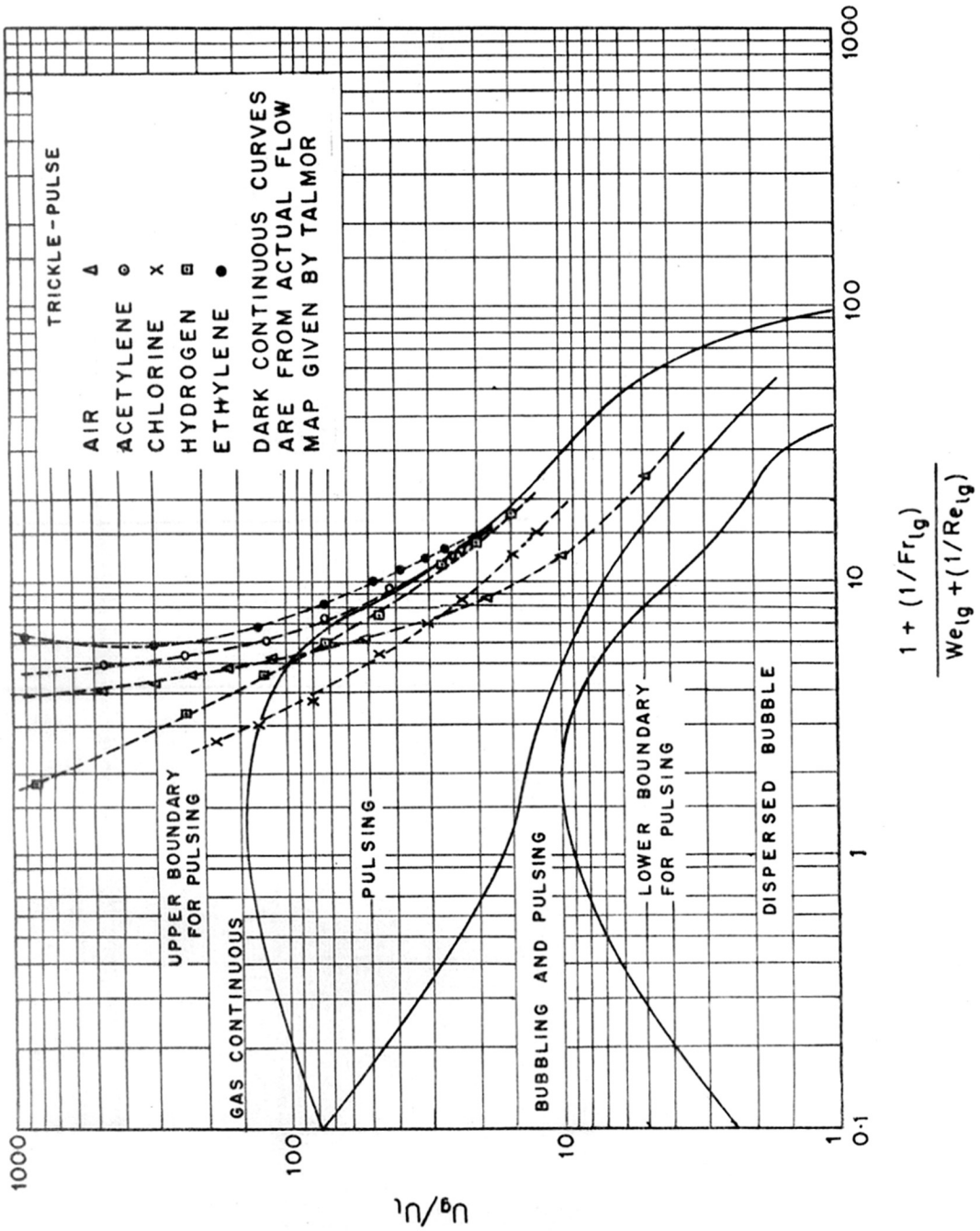


FIG. 4-8: COMPARISON OF FLOW REGIME TRANSITION WITH TALMOR'S FLOW MAP (2C)



LIST OF PUBLICATIONS

LIST OF PUBLICATIONS

1. Patwardhan V.S. and Shrotri V.R., Mass Transfer Coefficient Between the Static and Dynamic Hold-ups in a Packed Column, Chem. Engg. Commun. 1981,10, 349
2. Patwardhan V.S. and Shrotri V.R., Dynamic Hold-up in Non-Wettable Packings, Presented at the 34th Annual Session of the Indian Institute of Chemical Engineers, held in Madras, India (1981)
3. Shrotri V.R. and Patwardhan V.S., The Effect of Wettability on Dynamic Hold-up in Packed-Trickle Columns, in Frontiers in Chemical Reaction Engineering, Vol. 1, Ed. L.K. Doraiswamy and R.A. Mashelkar, p. 359, pub. Wiley Eastern Ltd., New Delhi, India (1984)

Under Preparation

4. Shrotri V.R. and Patwardhan V.S., Mass Transfer Between Static and Dynamic Hold-ups in Packed Columns for Wettable and Non-Wettable Packings
5. Shrotri V.R. and Patwardhan V.S., Mass Transfer in Packed Columns Under the Condition of Developing Wall Flow
6. Shrotri V.R., Patwardhan V.S. and Chaudhari R.V., Flow Regime Behaviour of Packed Columns with Industrial Gas-Liquid Systems

.....